

# Connected and Autonomous Technology Applications and Modeling Analysis for Commercial and Shared Vehicle Operations

Lead Guest Editor: Xumei Chen

Guest Editors: Haneen Farah, Xiaoyue Liu, Hyoungsoo Kim, and Peter  
Chen





---

**Connected and Autonomous Technology  
Applications and Modeling Analysis for  
Commercial and Shared Vehicle Operations**

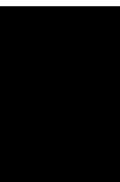
Journal of Advanced Transportation

---

**Connected and Autonomous  
Technology Applications and Modeling  
Analysis for Commercial and Shared  
Vehicle Operations**

Lead Guest Editor: Xumei Chen

Guest Editors: Haneen Farah, Xiaoyue Liu,  
Hyoungsoo Kim, and Peter Chen







---

Copyright © 2021 Hindawi Limited. All rights reserved.

This is a special issue published in "Journal of Advanced Transportation." All articles are open access articles distributed under the Creative Commons Attribution License, which permits unrestricted use, distribution, and reproduction in any medium, provided the original work is properly cited.














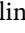




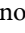



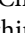
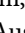


## Associate Editors

Juan C. Cano , Spain  
Steven I. Chien , USA  
Antonio Comi , Italy  
Zhi-Chun Li, China  
Jinjun Tang , China

## Academic Editors

Kun An, China  
Shriniwas Arkatkar, India  
José M. Armingol , Spain  
Socrates Basbas , Greece  
Francesco Bella , Italy  
Abdelaziz Bensrhair, France  
Hui Bi, China  
María Calderon, Spain  
Tiziana Campisi , Italy  
Giulio E. Cantarella , Italy  
Maria Castro , Spain  
Mei Chen , USA  
Maria Vittoria Corazza , Italy  
Andrea D'Ariano, Italy  
Stefano De Luca , Italy  
Rocío De Oña , Spain  
Luigi Dell'Olio , Spain  
Cédric Demonceaux , France  
Sunder Lall Dhingra, India  
Roberta Di Pace , Italy  
Dilum Dissanayake , United Kingdom  
Jing Dong , USA  
Yuchuan Du , China  
Juan-Antonio Escareno, France  
Domokos Esztergár-Kiss , Hungary  
Saber Fallah , United Kingdom  
Gianfranco Fancello , Italy  
Zhixiang Fang , China  
Francesco Galante , Italy  
Yuan Gao , China  
Laura Garach, Spain  
Indrajit Ghosh , India  
Rosa G. González-Ramírez, Chile  
Ren-Yong Guo , China

Yanyong Guo , China  
Jérôme Ha#rri, France  
Hocine Imine, France  
Umar Iqbal , Canada  
Rui Jiang , China  
Peter J. Jin, USA  
Sheng Jin , China  
Victor L. Knoop , The Netherlands  
Eduardo Lalla , The Netherlands  
Michela Le Pira , Italy  
Jaeyoung Lee , USA  
Seungjae Lee, Republic of Korea  
Ruimin Li , China  
Zhenning Li , China  
Christian Liebchen , Germany  
Tao Liu, China  
Chung-Cheng Lu , Taiwan  
Filomena Mauriello , Italy  
Luis Miranda-Moreno, Canada  
Rakesh Mishra, United Kingdom  
Tomio Miwa , Japan  
Andrea Monteriù , Italy  
Sara Moridpour , Australia  
Giuseppe Musolino , Italy  
Jose E. Naranjo , Spain  
Mehdi Nourinejad , Canada  
Eneko Osaba , Spain  
Dongjoo Park , Republic of Korea  
Luca Pugi , Italy  
Alessandro Severino , Italy  
Nirajan Shiwakoti , Australia  
Michele D. Simoni, Sweden  
Ziqi Song , USA  
Amanda Stathopoulos , USA  
Daxin Tian , China  
Alejandro Tirachini, Chile  
Long Truong , Australia  
Avinash Unnikrishnan , USA  
Pascal Vasseur , France  
Antonino Vitetta , Italy  
S. Travis Waller, Australia  
Bohui Wang, China  
Jianbin Xin , China







---

Hongtai Yang , China  
Vincent F. Yu , Taiwan  
Mustafa Zeybek, Turkey  
Jing Zhao, China  
Ming Zhong , China  
Yajie Zou , China

## Contents






---

### **Investigation of Control Method for Connected-Automated Vehicle to Multiplex Dedicated Bus Lane**

Wei-Jie Xiu , Li Wang , Meng-Yang Guo , Li-Li Zhang , and Qi Zhao

Research Article (11 pages), Article ID 2470738, Volume 2021 (2021)

### **The Impact of Automated Vehicles on Traffic Flow and Road Capacity on Urban Road Networks**

Ji Eun Park , Wanhee Byun , Youngchan Kim , Hyeonjun Ahn , and Doh Kyoum Shin 







Research Article (10 pages), Article ID 8404951, Volume 2021 (2021)

### **An Algorithm for Detecting Collision Risk between Trucks and Pedestrians in the Connected Environment**

Seung-oh Son , Juneyoung Park , Cheol Oh , and Chunho Yeom 





Research Article (9 pages), Article ID 9907698, Volume 2021 (2021)

### **Exploring the Potential of Using Privately-Owned, Self-Driving Autonomous Vehicles for Evacuation Assistance**

Thomas Shirley , Bhavya Padmanabha , Pamela Murray-Tuite , Nathan Huynh , Gurcan Comert , and Jiayun Shen 

Research Article (11 pages), Article ID 2156964, Volume 2021 (2021)

### **Multi-Depot Pickup and Delivery Problem with Resource Sharing**

Yong Wang , Lingyu Ran , Xiangyang Guan , and Yajie Zou 

Research Article (22 pages), Article ID 5182989, Volume 2021 (2021)

## Research Article

# Investigation of Control Method for Connected-Automated Vehicle to Multiplex Dedicated Bus Lane

Wei-Jie Xiu <sup>1</sup>, Li Wang <sup>1</sup>, Meng-Yang Guo <sup>1</sup>, Li-Li Zhang <sup>2</sup> and Qi Zhao<sup>1</sup>

<sup>1</sup>Beijing Key Laboratory of Urban Intelligent Traffic Control Technology, North China University of Technology, Beijing 100144, China

<sup>2</sup>College of Information Engineering, Beijing Institute of Petrochemical Technology, Beijing 102617, China

Correspondence should be addressed to Li Wang; [li.wang@ncut.edu.cn](mailto:li.wang@ncut.edu.cn) and Li-Li Zhang; [zhanglili@bipt.edu.cn](mailto:zhanglili@bipt.edu.cn)

Received 27 August 2021; Revised 28 October 2021; Accepted 7 December 2021; Published 28 December 2021

Academic Editor: Peter Chen

Copyright © 2021 Wei-Jie Xiu et al. This is an open access article distributed under the Creative Commons Attribution License, which permits unrestricted use, distribution, and reproduction in any medium, provided the original work is properly cited.

Dedicated bus lanes (DBLs) have been widely utilized to ensure public transport priority. To improve overall road efficiency, various control methods of multiplexing DBL are developed and discussed. In this study, we focus on the control method which is based on the connected-automated vehicle (CAV) technology, and the proposed method is validated by using microscopic traffic simulation. The simulation results show that two proposed control methods of multiplexing DBL can reduce the average delay and the average number of stops and increase the travel speed. In comparison, the real-time control method based on the CAV technology offers better effects than the improved signal light control method.

## 1. Introduction

Under the conditions of the shortage of urban road resources and the high cost of infrastructure construction, one or more lanes have been set up on existing urban roads with traffic signs and markings as DBL for public buses, which has become one of the effective measures to ensure public transport priority in many big cities [1]. 89% of cities in Europe, including cities which have smaller numbers of DBL, own DBL. Some large cities in China, including Beijing, Shanghai, Guangzhou, Shenzhen, Qingdao, Kunming, Hangzhou, Wuhan, Xi'an, Shijiazhuang, and so on, have also built a large number of DBLs [2].

Although DBL can improve bus operation efficiency, there are two main problems: one is the reduction of total road capacity and the other is the low utilization rate of DBL, leading to a waste of road resources. Numerous research studies have attempted to multiplex these road resources, which might be potentially wasted. A commonly used method is to restrict the time for DBL so that only buses can use them during certain periods of the day (morning and evening peak hours), and other vehicles are

not allowed to enter during these periods, and during the rest of the time, the DBL is used as a general lane for all vehicles. However, this solution does not take into account dynamic traffic demands of road resources for various types of vehicles. When other vehicles are prohibited from entering the DBL, there are still some spare road resources that could be utilized; during the period of mixed use of buses and other types of vehicles on DBL, the lack of effective control measures for other types of vehicles is easy to affect the efficiency of bus system, and the public transport priority cannot be guaranteed. Viegas first proposed the concept of intermittent bus lanes (IBLs), which determine whether a certain section of the lane becomes a DBL according to whether the bus presents or not: when the bus approaches a certain section of the lane, this lane becomes a DBL; when the bus leaves this section, the lane becomes a normal lane and is open to all types of vehicles [3, 4]. Eichler et al. found that bus lanes with intermittent priority (BLIPs), unlike dedicated ones, do not significantly reduce street capacity [5].

With the advanced technologies of vehicle to everything (V2X), Internet of vehicle (IOV), and CAV, the control method and the logic of designing DBL can be improved

dramatically. For instance, the roadside units can be set up near the bus lane to collect and upload the real-time bus positioning data and traffic operation data to the central control platform and then the dynamic control strategy for different vehicles could be implemented by combining the real-time data and the control algorithm [6].

In practical situations, CAV technology will firstly be used in commercial vehicles [7], which include buses, freight vehicles (logistic, express delivery, and so on), etc. What is strikingly noticeable is that the operation characteristics (speed and acceleration) of these vehicles are relatively similar. The mixed use by slow-moving vehicles and fast-moving vehicles is one of the most important reasons that limit the road capacity to reach the designed level [8], and slow-moving vehicles, such as buses or trucks, will cause “movement bottleneck” phenomenon [9, 10]. A possible scenario in the near future is that the commercial vehicles have already popularized CAV technologies, while other types of vehicles are still in a state of human driving. In this case, considering to multiplex the DBL for these slow-moving vehicles would have the following three advantages: the first is that multiplexing DBL will reduce the occurrence of moving bottleneck [11]; the second is that the efficiency of the DBL under the premise of ensuring public transport priority will be improved; the third is that the CAV freight vehicles can be investigated as the basis of DBL multiplexing technology, which is favourable for the efficiency of DBL.

Zhu [12] compared DBL with IBL by using a cellular automaton traffic flow model, and the results proved that when the traffic flow was low, opening the DBL to general vehicles significantly improved the efficiency of road traffic. Zyryanov and Mironchuk [13] used the microscopic traffic simulation model to evaluate the effects of different traffic volume and bus priority signals on the IBL and found that the IBL can increase the travel speed of public buses and other vehicles even when the traffic volume increased. Wu et al. [14] explored the benefits of BLIP. Yang and Wang [15] compared the influences of DBL and IBL on the buses and adjacent traffic, and the results showed that IBL performs better than DBL because it has less negative impact on other vehicles. Joskowicz [16] studied the following issues: the configuration method of dynamic traffic signs on the IBL, the data collection, the queuing time of public buses on the IBL, and the effect of IBL on road capacity. Dong and Zhao [17] developed a “time division multiple” method of DBL which can calculate the appropriate time period for other vehicles to “borrow” the bus lane. Chiabaut and Barcet [18] assessed the impact of IBL on the public traffic and suggested that the IBL system could be a promising strategy; when it is combined with the traffic signal priority, the average bus travel time is significantly reduced. Song et al. [19] suggested a shared lane of DBL and right-turn-exclusive lane to reduce the impact of DBL on traffic conditions.

The studies mentioned above have focused on the impact of multiplexing DBL on the traffic flow, and the effect of different types of vehicles as the main

multiplexing subject was neglected; moreover, the control device such as traffic signal is the main DBL multiplexing control device, and the limitations of such device and method also affect the performance of DBL multiplexing. If CAV and other advanced technology can be applied to DBL multiplexing, the application effect of IBL can be enhanced at a lower cost while ensuring bus priority.

Regarding the highly controllable and self-control achievable character of CAVs, which are similar to buses, this study takes the CAVs as the DBL utilization subject. On the basis of the existing multiplexing control method, the new method which combines signal light and CAV technology is proposed. Then, the traffic simulation will be used to evaluate and compare the impact of the two implementation methods on the road traffic [20]. Considering the need of secondary development and research conditions in this study, we select PTV Vissim and Python as the traffic simulation tools.

## 2. Control Methods of DBL Multiplexing

*2.1. Method 1: Improved Signal Light Control Method.* In this method, as the signal detection and control device, the roadside units were set from the upstream intersection beside the DBL at intervals of distance  $L$ , the position and speed of CAVs and buses were collected in real time, and they were uploaded to the central control platform. The platform returned the control signal to the roadside units according to the control strategy. The CAVs thus followed the instruction of roadside units to enter or exit the DBL. Figure 1 shows the sketch map of this method. The control strategy was divided into flowing five steps [17].

- (1) Taking the  $i$ -th roadside unit as the center of a circle and using  $R$  as the radius to search for the closest bus to the upstream of the unit, which is called the approaching bus, the distance to the  $i$ -th roadside unit is  $D_{\text{bus}}(i)$  (according to the distance to the upstream intersection, from near to far,  $i = 1, 2, \dots, n$ , where  $n$  is the total number of roadside units on the utilizing road section).
- (2) Assuming that the CAV is allowed to travel on the DBL between the  $i$ -th and the  $(i+1)$ -th roadside unit at the moment  $t$ , the roadside unit  $i$ -th will broadcast the signal “CAVs are allowed to enter,” and the holding time of this signal is the DBL multiplexing time; at the end time, the roadside unit  $i$ -th will broadcast the signal “CAVs are prohibited from entering,” at the same time, CAVs on the DBL must exit.
- (3) The travel time of the CAV between  $i$ -th and  $(i+1)$ -th units is calculated as

$$T_{\text{cav}} = \frac{L}{v_{\text{cav}}} + T_{\text{borrow}} + \lambda_1 T_{\text{light}} + T_{\text{return}}, \quad (1)$$

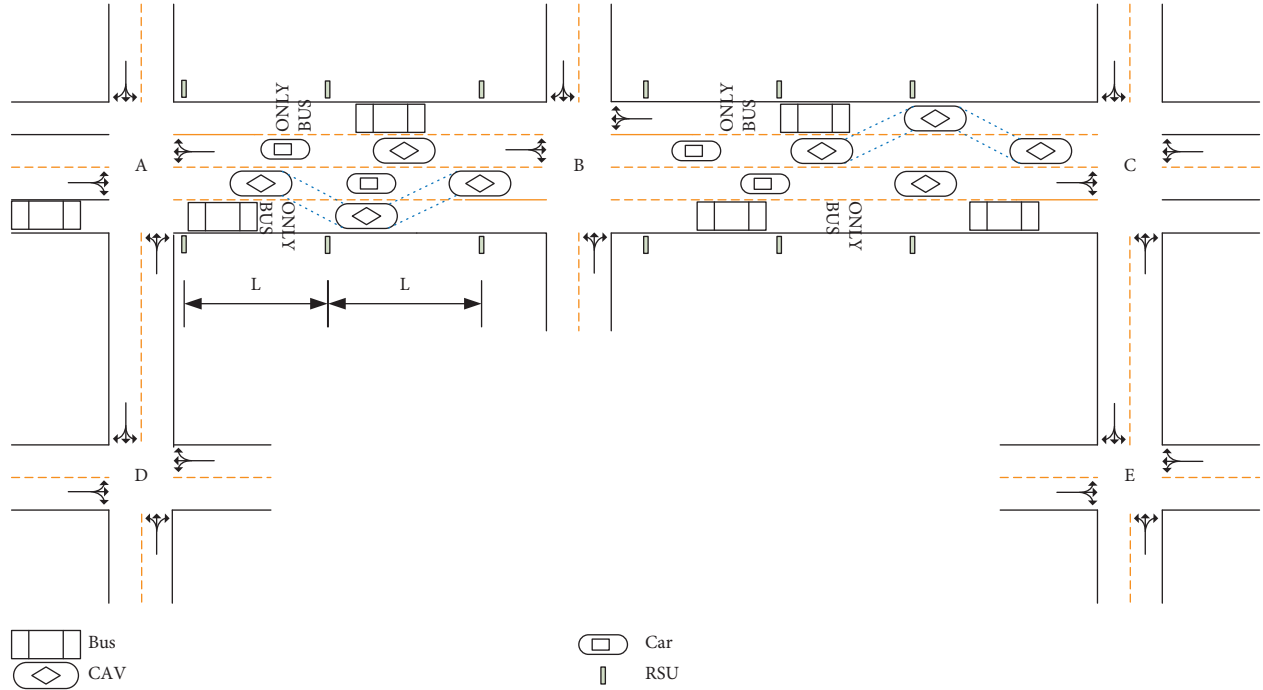


FIGURE 1: The sketch map of method 1.

where  $T_{light}$  is the predicted waiting time for the signal lights at the downstream intersection;  $v_{cav}$  is the speed of the CAV;  $T_{borrow}$  is the minimum time required for the CAV to enter the DBL;  $T_{return}$  is the minimum time required for the CAV to exit the DBL;  $T_{borrow}$  and  $T_{return}$  are affected by many factors such as individual driver differences, roads, and weather; and  $\lambda_1$  indicates the introduced coefficient, assuming that there are two following scenarios : when there is no intersection between  $i$ -th and  $(i+1)$ -th units,  $\lambda_1 = 0$ ; when there is an intersection,  $\lambda_1 = 1$ .

- (4) The travel time of the approaching bus from the current position to the  $(i+1)$ -th unit searched at the  $i$ -th unit is calculated as

$$T_{bus} = \frac{D_{bus}(i) + L}{v_{bus}} + \lambda_2 T_{light}, \quad (2)$$

where  $v_{bus}$  is the speed of the approaching bus;  $\lambda_1$  indicates the introduced coefficient, assuming that there are two following scenarios : when there is no intersection between  $i$ -th and  $(i+1)$ -th units,  $\lambda_1 = 0$ ; when there is an intersection,  $\lambda_1 = 1$ .

- (5) Determine whether to allow CAVs to multiplex DBL.

The methodology is further illustrated through the use of two scenarios.

The first scenario is to take the  $i$ -th roadside unit as the center of a circle and use  $R$  as the radius to search for the closest bus to the upstream of the unit. If no approaching bus is found, the CAV will be allowed to enter the DBL between units  $i$ -th and  $(i+1)$ -th, the roadside unit  $i$ -th will broadcast the signal "CAVs are allowed to enter DBL."

The second scenario is to take the  $i$ -th roadside unit as the center of a circle and use  $R$  as the radius to search for the closest bus to the upstream of the unit. If the approaching bus is located, the formula is

$$T_{bus} \geq T_{cav} + T_{min} + T_{head}, \quad (3)$$

where  $T_{head}$  is the minimum headway between the CAV and the bus on DBL (specified as 1.5 seconds to 2 seconds) (defined by numerous studies) and  $T_{min}$  is the minimum time for the CAV using the DBL (too short will cause frequent lane changing, whereas too long will affect the bus priority). Figure 2 shows the flowchart of this method.

**2.2. Method 2: Real-Time Control Method Based on CAV Technology.** In this method, the real-time position and speed data of CAVs is known, taking the CAV as the center of a circle,  $R$  as the radius, according to whether there is an approaching bus within the search radius, comparing the moving characteristics of the approaching bus with the CAV to decide whether the CAV is allowed to enter the DBL, the steps are as follows. Figure 3 shows the sketch map of this method.

- (1) If there is no approaching bus in the searching area, the CAV is allowed to enter the DBL.
- (2) If there is one and only bus in the searching area, it is necessary to judge whether the CAV is allowed to enter or is forced to leave. The judgment method is as follows:

$$T_{borrow} \leq T_{bus} - T_{head} = \frac{D_{bus}}{v_{bus}} - T_{head}, \quad (4)$$

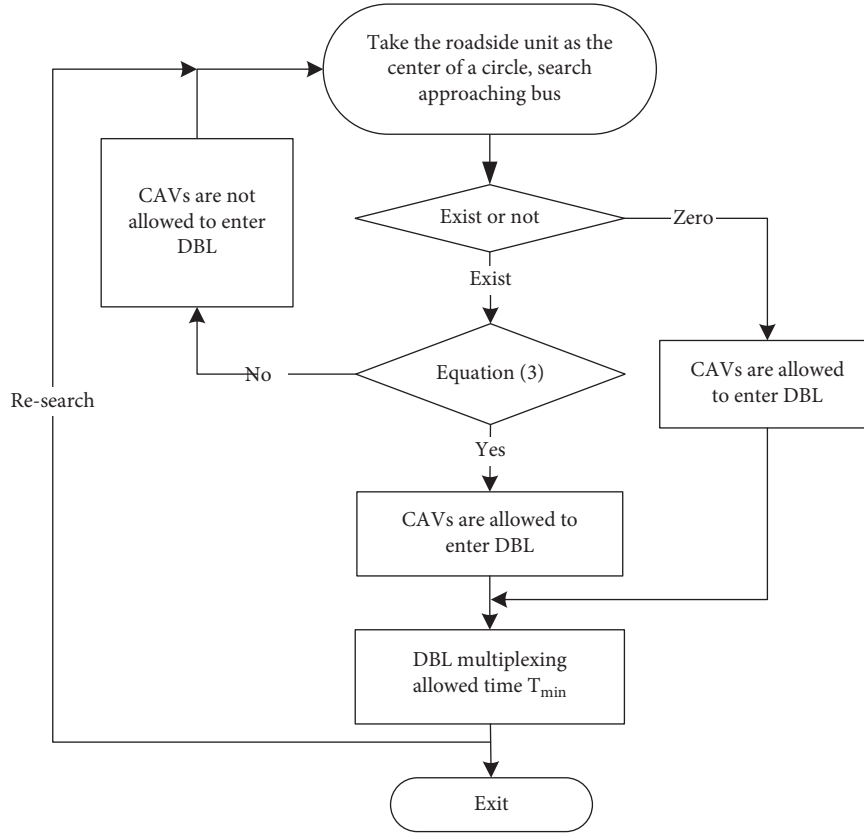


FIGURE 2: The flowchart of method 1.

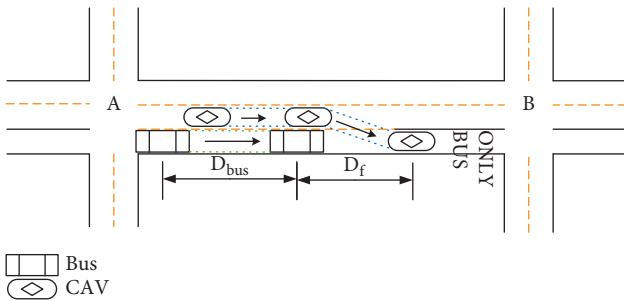


FIGURE 3: The sketch map of method 2.

where  $T_{\text{borrow}}$  is the minimum time required for the CAV to enter the DBL;  $T_{\text{bus}}$  is the time required for the bus to travel from the current position to the safe headway with the smallest distance from the CAV on the DBL;  $T_{\text{head}}$  is the minimum headway safety time when the vehicle changes lanes;  $D_{\text{bus}}$  is the distance from the bus's current position to the headway safety position of the CAV on the DBL; and  $v_{\text{bus}}$  is the speed of the bus.

- (3) If there are multiple buses in the searching area, the closest bus is determined as an approaching bus. Since the premise of multiplexing DBL is to ensure the bus priority and not cause interference to the buses, if there are multiple buses within the search radius, it is considered that the duration of

multiplexing the DBL must exceed all the buses within the search radius. The judgment method is as follows:

$$T_{\text{borrow}} \leq T_{\text{dsbus}} - T_{\text{head}} = \frac{D_{\text{dsbus}}}{v_{\text{dsbus}}} - T_{\text{head}}, \quad (5)$$

where  $T_{\text{dsbus}}$  is the time required for the closest bus to travel from the current position to the safe headway with the smallest distance from the CAV on the DBL;  $T_{\text{head}}$  is the minimum headway safety time when the vehicle changes lanes;  $v_{\text{dsbus}}$  is the speed of the bus; and  $D_{\text{dsbus}}$  is the distance from the bus's current position to the headway safety position of the CAV on the DBL. Figure 4 shows the flowchart of this method.

### 3. Simulation Experiment Design

In this study, Vissim and Python were used to verify and compare the impact of the two DBL multiplexing control methods mentioned above on traffic flow.

**3.1. Objective Function.** The travel speed and road capacity are important indices of road performance evaluation. This study takes the travel speed of the CAV  $\bar{V}_{\text{cav}}$  as the optimization goal.

$$F(R, T_{\text{min}}) = \text{Min}(\bar{V}_{\text{cav}}). \quad (6)$$



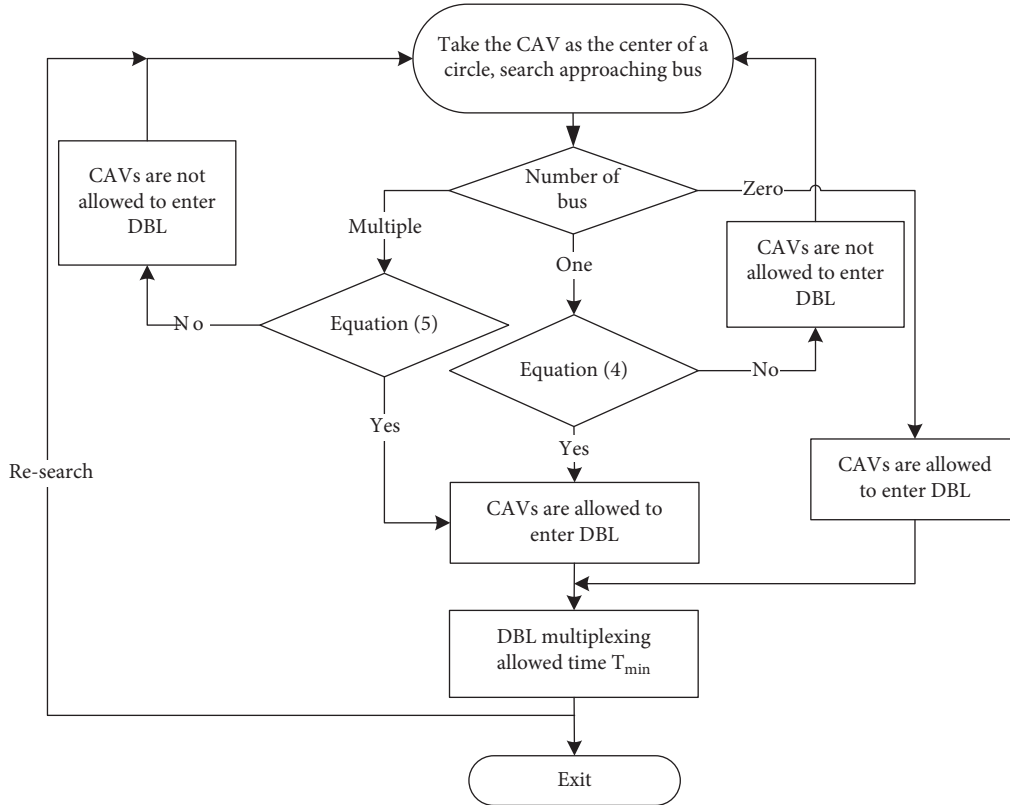


FIGURE 4: The flowchart of method 2.

### 3.2. Constraints

**3.2.1. Bus Volume.** The purpose of setting up DBL is to ensure bus priority. Compared with normal lanes, buses can get a better driving environment with DBL. When the bus traffic volume on the bus lane is greater than the volume on the adjacent normal lane, the driving environment of the bus on the DBL is actually inferior to that of the normal lane, and the bus lane loses its multiplexing significance. The following constraints must be met between the bus flow and other vehicles' flow:

$$Q_{\text{bus}} < \frac{Q_{\text{lane}}}{n_1}, \quad (7)$$

where  $Q_{\text{bus}}$  is the bus volume of the DBL;  $Q_{\text{lane}}$  is other vehicles volume; and  $n_1$  is the quantity of normal lanes in the road section.

**3.2.2. Saturation of DBL.** According to the U.S. "Highway Capacity Manual" and the literature research summary [21], when the saturation on the DBL is greater than 0.7, the lane will be congested, the effect of multiplexing DBL will decrease sharply, and the bus delay will significantly increase. In this research, the following saturation constraint was set:

$$\frac{Q_{\text{bus}} + Q_{\text{cav}}}{C_{\text{bus}}} < 0.7, \quad (8)$$

where  $Q_{\text{bus}}$  is the bus volume of the DBL;  $Q_{\text{car}}$  is the CAV volume of multiplexing DBL; and  $C_{\text{bus}}$  is the capacity of the DBL.

## 4. Simulation Results and Analysis

A road network in Shijingshan District, Beijing, is established in the Vissim, as shown in Figure 5. The chosen experimental road section is 2,300 m long from east to west, and the nearside lane is the DBL. The experimental road section is a long-distance road with four intersections. Seven roadside units are set next to the DBL: three roadside units are set on the east of intersection 1, with distance of 100 m, 400 m, and 700 m, respectively; two roadside units are set on the east of intersection 2, with distance of 50 m and 300 m; one roadside unit is set on the east of intersection 3, with distance of 80 m; and one roadside unit is set on the south of intersection 4, with distance of 50 m.

Figures 6–8 show the phase and time of the four intersections on the experimental road; the simulation time is 3,600 s; the time required for the CAV to enter the DBL,  $T_{\text{borrow}}$ , is 15 s; the time required for the CAV to exit the DBL,  $T_{\text{return}}$ , is 12 s; the minimum safety headway time during lane changing,  $T_{\text{head}}$ , is 2 s; the minimum time for using the DBL,  $T_{\text{min}}$ , is 30 s [22]; and the search radius,  $R$ , is 20 m. Considering the background of multiplexing DBL is the road traffic has reached saturation, the single lane input volume is set as  $q = 1,800$  pcu/h. The average delay, average



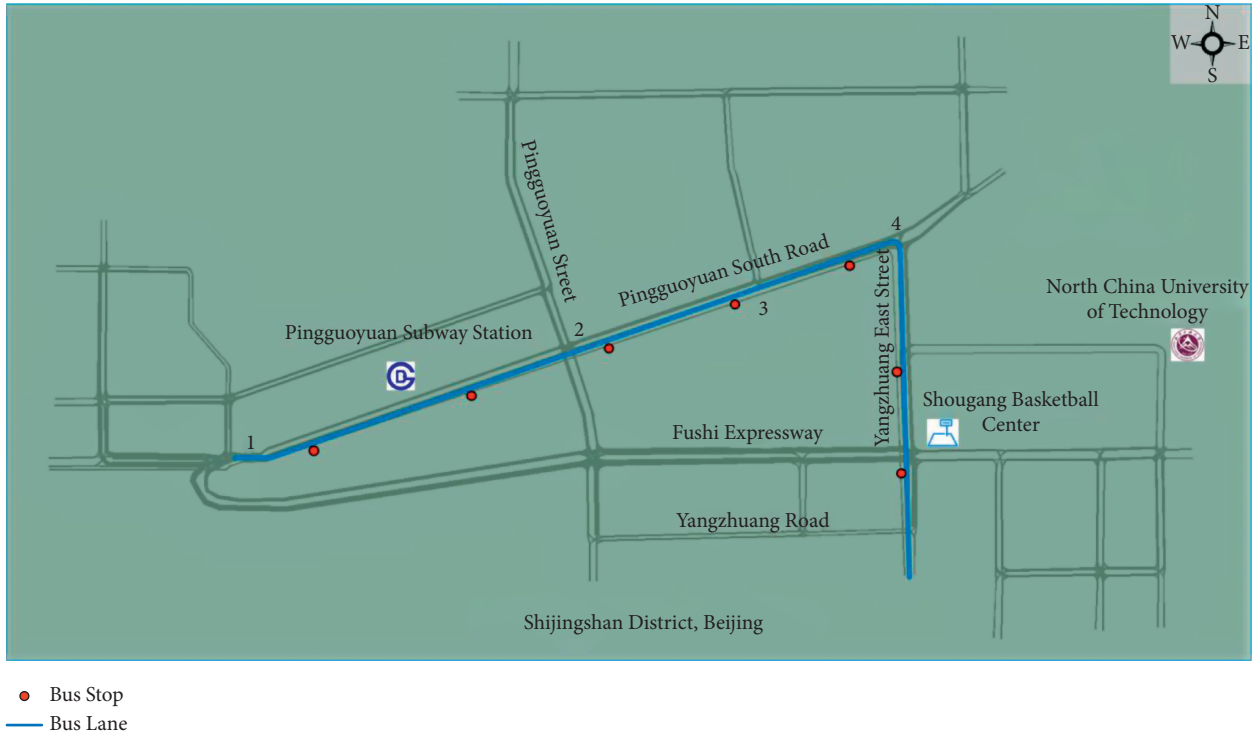


FIGURE 5: The traffic simulation road network.

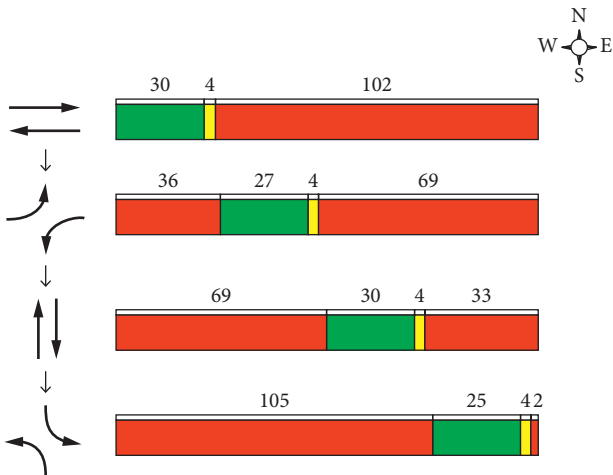


FIGURE 6: The phases and duration time of intersection 1 and intersection 2.

number of stops, and travel speed are selected as the indicators for the effect evaluation of multiplexing DBL.

Three simulation experiments were conducted: normal use of DBL (normal), multiplexing DBL by CAV controlled by signal light (method 1), and multiplexing DBL by CAV controlled by real-time situation (method 2). Figures 9–11 show the average delay, the average number of stops, and the travel speed of different vehicles in the three situations.

The simulation results showed that the two control methods were implemented under the premise of bus priority. Both method 1 and method 2 can reduce the delay of CAVs and other vehicles most of the time.

As shown in Figure 9(b), method 2 had a greater effect on the delay reduction of CAVs than method 1. The reason was that method 2 is more flexible in real-time monitoring and judgment of the vehicle position than the roadside unit signal light in method 1. Figure 9(a) shows that both methods increase the average delay of other vehicles at specific time. The merging lanes of CAVs had impacted on other general vehicles.

Figure 10 shows that under the premise of the average number of bus stops did not significantly increase, both methods can reduce the number of stop times of CAVs and other vehicles most of the time, while method 2 performed better than method 1.

Through the analysis and verification of visualized data, the results in Figure 11 showed that both method 1 and method 2 have improved the travel speed of CAVs and other vehicles, and the priority of buses was not intervened.

During the simulation experiment period, the travel speed of CAVs and other vehicles without control methods was 44.7 km/h and 36.4 km/h, respectively. In method 1, the travel speed of CAVs and other vehicles was 47.3 km/h and 37.8 km/h, respectively, whereas the numbers were 48.8 km/h and 39.9 km/h in method 2. Compared with the normal situation, method 1 increased the travel speed of normal vehicles and CAVs by 5.8% and 3.8%, respectively, and method 2 increased that of normal vehicles and CAVs by 9.2% and 9.6%, respectively. The improvement effect of method 2 was clearly greater than that of method 1. The reason was that the real-time detection used by method 2 was more flexible than the roadside unit signal light control,

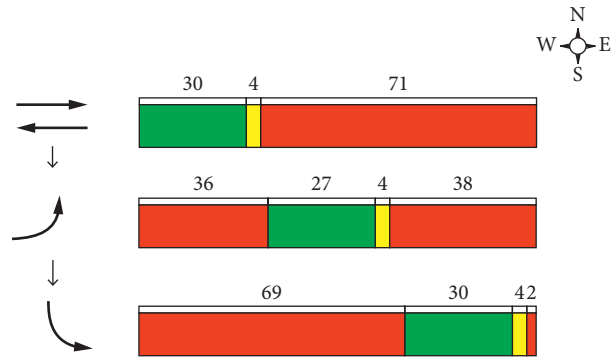


FIGURE 7: The phases and duration time of intersection 3.

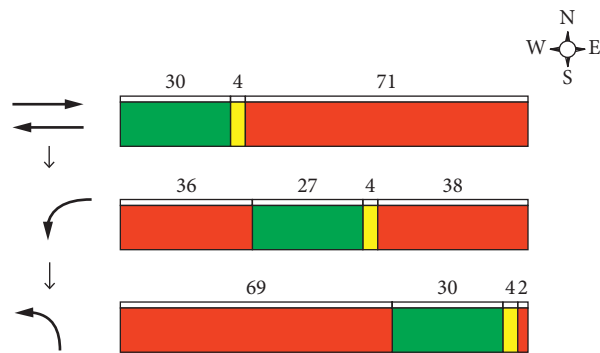


FIGURE 8: The phases and duration time of intersection 4.

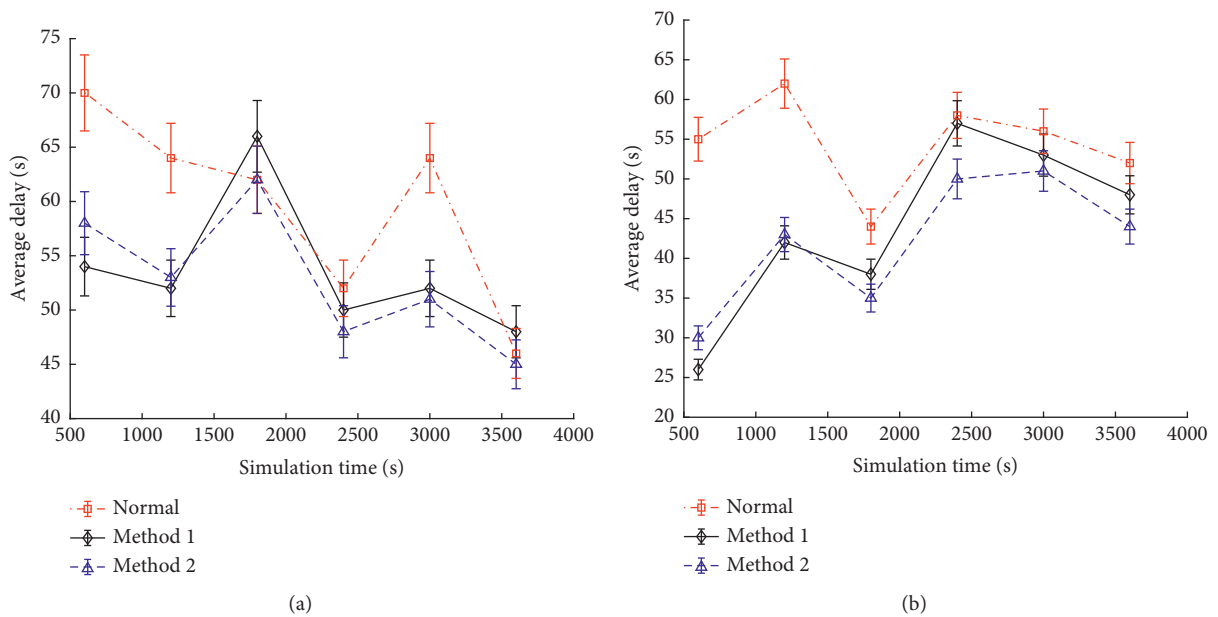
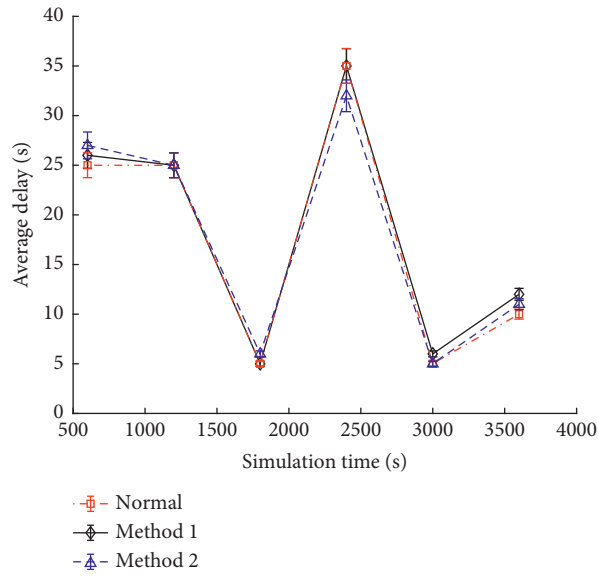
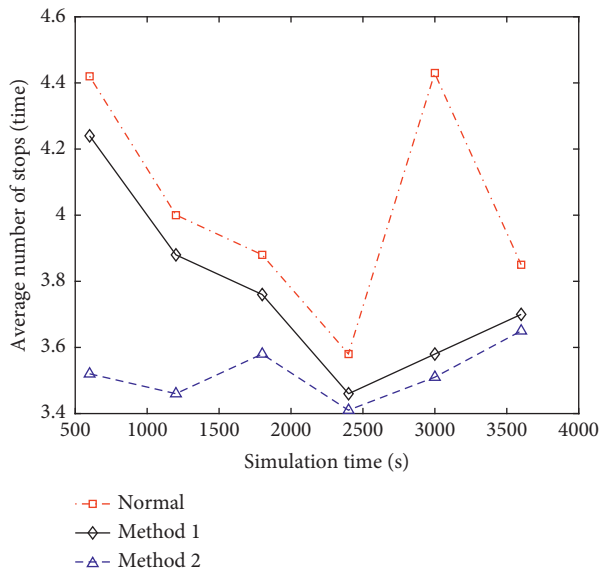


FIGURE 9: Continued.

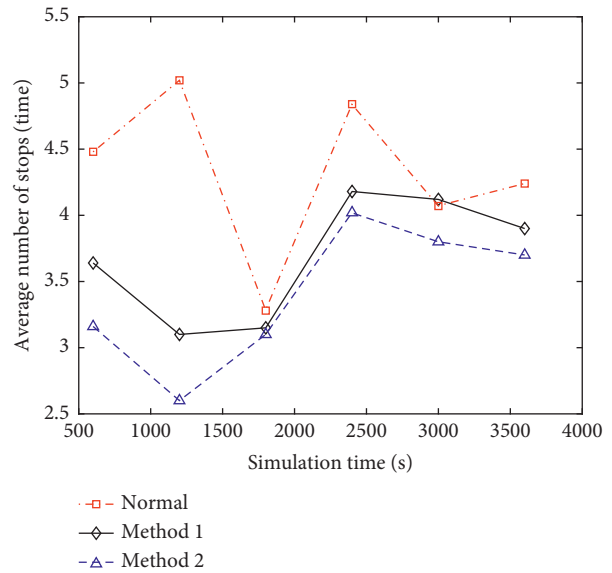


(c)

FIGURE 9: Average delay of different vehicles in the three situations. (a) Average delay of general vehicles in the three situations. (b) Average delay of CAVs in the three situations. (c) Average delay of buses in the three situations.

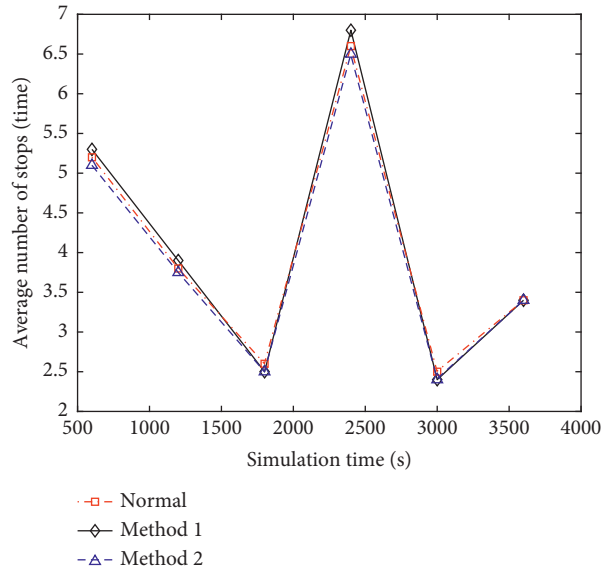


(a)



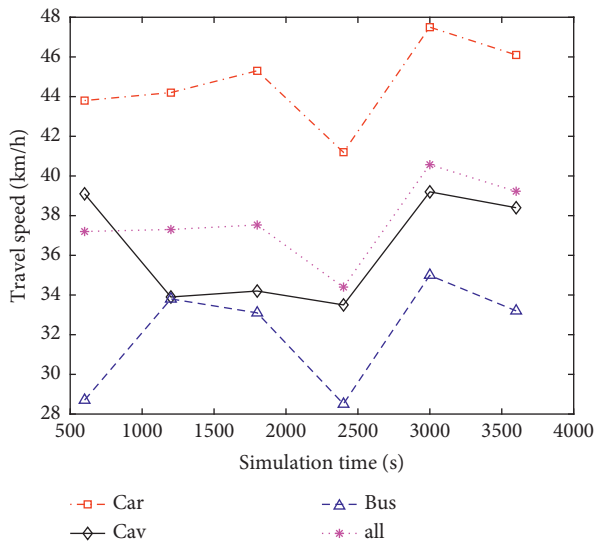
(b)

FIGURE 10: Continued.

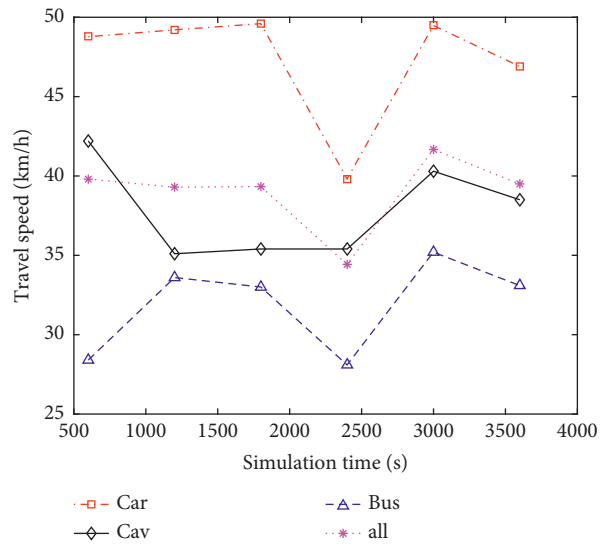


(c)

FIGURE 10: Average number of stops of different vehicles in the three situations. (a) Average number of stops of general vehicles in the three situations. (b) Average number of stops of CAVs in the three situations. (c) Average number of stops of buses in the three situations.



(a)



(b)

FIGURE 11: Continued.

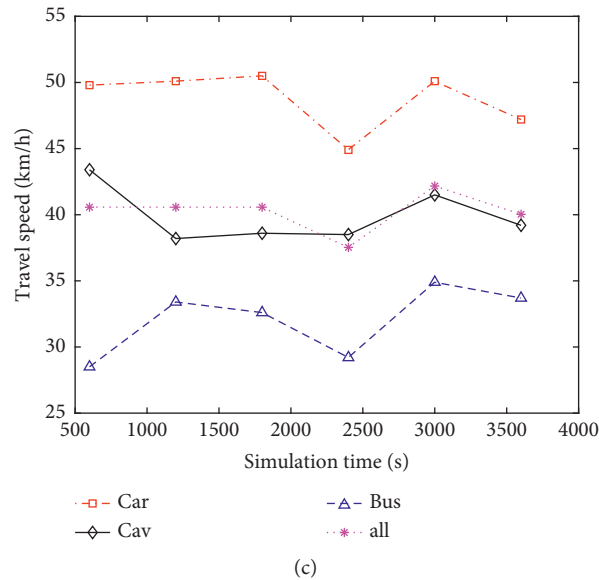


FIGURE 11: Travel speed of different vehicles in the three situations. (a) Travel speed of different vehicles in normal control situation. (b) Travel speed of different vehicles in method 1. (c) Travel speed of different vehicles in method 2.

and method 2 maximized the use of road resources under the premise of ensuring the priority of buses.

## 5. Conclusion

This paper investigated the multiplexing of DBL for CAVs through the microscopic traffic simulation model; two different control methods were implemented under the same road condition, and traffic volume was analyzed. The results indicated that

- (1) Both methods could improve the driving performance of CAVs and other vehicles, and the efficiency of DBL and the capacity of roads are increased under the premise of ensuring bus priority.
- (2) The real-time control method based on the CAV technology is more efficient than the improved signal light control method, which fully shows that with the development of the CAV technology, the method with CAVs as the main control subject will be more flexible and effective.
- (3) The multiplexing DBL control method for CAVs proposed in this paper can be used as a transition plan from the existing signal light control method to the future application of CAVs. The future study will mainly focus on two parts: exploring the traffic flow characteristics of mixed CAVs and human-driving vehicles; investigating the effects of DBL multiplexing on the bus priority signal control.

## Data Availability

The data used to support the findings of this study are available from the corresponding authors upon request only for research purpose.

## Conflicts of Interest

The authors declare that they have no conflicts of interest.

## Acknowledgments

This research was funded by the Beijing Natural Science Foundation (nos. 4214070 and 4194078), Beijing Municipal Great Wall Scholar Program (CIT&TCD20190304), Cross-Disciplinary Science Foundation from Beijing Institute of Petrochemical Technology (project no. BIPTCSF-006), 2021–2023 Young Talents Promotion Project of Beijing Association for Science and Technology, and Open Project for Beijing Urban Governance Research Base of North China University of Technology (no. 21CSZL34).

## References

- [1] Y. Luo and D. Qian, "Impact scope of bus passenger flow caused by bus lane construction," *Journal of Harbin Institute of Technology*, vol. 51, no. 03, pp. 120–126, 2019.
- [2] Y. Zhao, *Research on Bus Lane Utilizing Technology and Vehicle Fractal Cooperation Method*, Zhejiang University of technology, Hangzhou, China, 2011.
- [3] J. Viegas, "Turn of the century, survival of the compact city, revival of public transport," in *Transforming the port and transportation business*, H. Meersman and E. Van de Voorde, Eds., pp. 51–63, Uitgeverij Acco, Antwerp, Belgium, 1997.
- [4] J. Viegas and B. Lu, "The Intermittent Bus Lane signals setting within an area," *Transportation Research Part C: Emerging Technologies*, vol. 12, no. 6, pp. 453–469, 2004.
- [5] M. Eichler and C. F. Daganzo, "Bus lanes with intermittent priority: strategy formulae and an evaluation," *Transportation Research Part B: Methodological*, vol. 40, no. 9, pp. 731–744, 2006.
- [6] J. Song, X. Yang, Z. Cui, and C. Zhou, "Research on time division multiplexing system for bus lanes based on vehicle-road coordination and vehicle-to-vehicle communication,"

- Information Recording Materials*, vol. 020, no. 007, pp. 195–198, 2019.
- [7] Y. Lun, “Development status and trend of autonomous driving industry,” *Telecommunications Network Technology*, vol. 6, no. No.276, pp. 40–43, 2017.
- [8] H. Lin, Q. Fu, and H. Zhang, “Moving bottleneck theory-based new countermeasure for influence of heavy vehicles,” *Journal of Tongji University: Natural Science*, vol. 35, no. 09, pp. 1209–1213, 2007.
- [9] D. C. Gazis and R. Herman, “The moving and “phantom” bottlenecks,” *Transportation Science*, vol. 26, 1992.
- [10] C. Lattanzio, A. Maurizi, and B. Piccoli, “Moving bottlenecks in car traffic flow: a PDE-ODE coupled model,” *SIAM Journal on Mathematical Analysis*, vol. 43, no. 1, pp. 50–67, 2011.
- [11] G. Piacentini, P. Goatin, and A. Ferrara, “Traffic control via moving bottleneck of coordinated vehicles,” *IFAC-PapersOnLine*, vol. 51, no. 9, pp. 13–18, 2018.
- [12] H. B. Zhu, “Numerical study of urban traffic flow with dedicated bus lane and intermittent bus lane,” *Physica A: Statistical Mechanics and Its Applications*, vol. 389, no. 16, pp. 3134–3139, 2010.
- [13] V. Zyryanov and A. Mironchuk, “Simulation study of intermittent bus lane and bus signal priority strategy,” *Procedia - Social and Behavioral Sciences*, vol. 48, no. 1, pp. 1464–1471, 2012.
- [14] W. Wu, L. Head, W. Ma et al., *BLIP: Bus Lanes with Intermittent Priority*, Transportation Research Board Meeting, Washington, D C, 2013.
- [15] H. Yang and W. Wang, “An innovative dynamic bus lane system and its simulation-based performance investigation,” in *Proceedings of the IEEE Intelligent Vehicles Symposium*, pp. 105–110, Xian, June 2009.
- [16] I. F. Joskowicz, *Dynamic Bus Lane*, The University of Texas at Arlington, Arlington, Texas, 2012.
- [17] H. Dong and Y. Zhao, *Optimization of Time Division Multiplexing for Dedicated Bus Lanes Based on Paramics*, Journal of Zhejiang University of Technology, no. 01, pp. 65–69, China, 2012.
- [18] N. Chiabaut and A. Barcet, “Demonstration and evaluation of an intermittent bus lane strategy,” *Public Transport*, vol. 11, no. 1, pp. 443–456, 2019.
- [19] X. Song, L. Ma, L. Li, Y. Gao, and M. Liu, “Simulation analysis and benefit evaluation of bus and right turn exclusive lanes,” *China Journal of Highway and Transport*, vol. 32, no. 05, pp. 146–156, 2019.
- [20] H. Xu, Q. Zheng, and K. Zhang, “Arterial road BRT signal priority method based on vertical equality,” *China Journal of Highway and Transport*, vol. 32, no. 001, pp. 144–153, 2019.
- [21] National Research Council (U.S), *HCM2010: Highway Capacity Manual*, Transportation Research Board, Washington, D.C., 5th ed edition, 2010.
- [22] J. Yang, *Research on the Impact of Frequent Lane Changes on Road Efficiency and Safety*, Chang’an University, Xian, China, 2016.

## Research Article

# The Impact of Automated Vehicles on Traffic Flow and Road Capacity on Urban Road Networks

Ji Eun Park <sup>1</sup>, Wanhee Byun <sup>2</sup>, Youngchan Kim <sup>1</sup>, Hyeonjun Ahn <sup>1</sup>,  
and Doh Kyoum Shin <sup>3</sup>

<sup>1</sup>Department of Transportation Engineering, University of Seoul, Seoul 02504, Republic of Korea

<sup>2</sup>Department of Urban Regeneration, Land & Housing Institute, Daejeon 34047, Republic of Korea

<sup>3</sup>Department of Balanced Development & Global Business, Land & Housing Institute, Daejeon 34047, Republic of Korea

Correspondence should be addressed to Doh Kyoum Shin; [dkshin@lh.or.kr](mailto:dkshin@lh.or.kr)

Received 27 August 2021; Revised 5 October 2021; Accepted 25 October 2021; Published 3 November 2021

Academic Editor: Peter Chen

Copyright © 2021 Ji Eun Park et al. This is an open access article distributed under the Creative Commons Attribution License, which permits unrestricted use, distribution, and reproduction in any medium, provided the original work is properly cited.

Automated vehicles (AVs) are believed to have great potential to improve the traffic capacity and efficiency of the current transport systems. Despite positive findings of the impact of AVs on traffic flow and potential road capacity increase for highways, few studies have been performed regarding the impact of AVs on urban roads. Moreover, studies considering traffic volume increase with a mixture of AVs and human-driven vehicles (HDVs) have rarely been conducted. Therefore, this study investigated the impact of gradual increments of AV penetration and traffic volume on urban roads. The study adopted a microsimulation approach using VISSIM with a Wiedmann 74 model for car-following behavior. Parameters for AVs were set at the SAE level 4 of automation. A real road network was chosen for the simulation having 13 intersections in a total distance of 4.5 km. The road network had various numbers of lanes from a single lane to five lanes in one direction. The network consists of a main arterial road and a parallel road serving nearby commercial and residential blocks. In total, 36 scenarios were investigated by a combination of AV penetrations and an increase in traffic volumes. The study found that, as AV penetration increased, traffic flow also improved, with a reduction of the average delay time of up to 31%. Also, as expected, links with three or four lanes had a more significant impact on the delay. In terms of road capacity increase, when the penetration of AVs was saturated at 100%, the road network could accommodate 40% more traffic.

## 1. Introduction

Automated vehicles (AVs) are almost commercially ready for the public in many countries. Boston consulting group [1] predicts that manufacturers will introduce AVs into the car market by 2025 and that by 2035 they will have a 10% share of the market. Litman [2] estimates that 80~100% of cars on the roads by 2045 will be AVs, while Bansal and Kockelman [3] predict that the market share of AVs will be between 24% and 87%. Regardless of the detailed figures in the predictions, it is certain that AVs will fill up the roads within 20 years.

In terms of mobility, AVs will bring a fundamental revolution to our life. People will not need to drive and therefore will be free from the stress of driving. They can enjoy their time pursuing other activities in their car.

Transport planners and policymakers believe that AVs have great potential for resolving many traffic-related problems, e.g., traffic congestion. The traditional solution to mitigate traffic congestion is capacity expansion. However, building more roads is not a feasible solution, as there is little space available for roads in urban areas [4].

AVs can drive accurately on roads and with better sensing ability than humans. Specifically, they require a much smaller gap, or shorter headway, than human-driven vehicles (HDVs), since they have more information about the surrounding driving environment and a slower reaction time delay [5–8]. Vehicle-to-vehicle (V2V) communication will allow vehicles to form platoons [6, 9]. These technological advances will be able to increase traffic flow efficiency and road capacity.



However, there are still gaps in the estimation of improvement by AVs depending on road categories and the relative proportion of AVs and HDVs. According to previous studies, AVs can improve traffic flow [10–12], consequently, allowing increased road capacity [13, 14] of up to 50% in uninterrupted flow [5, 6, 8]. However, another study reports that the improvement will not be significant (or could even worsen) until a penetration rate of 40% is achieved [15]. Most of the previous studies report the impact of AVs on highways, but the impact on urban roads is rarely reported. The final objective of AV technology is to allow AVs to run on all roads, regardless of road environment or category. While highways are relatively easy for AVs, vehicle movements on urban roads are restricted by the environment, such as traffic signals at intersections, so the impact of AVs will be different on urban roads. Therefore, studies are necessary to investigate the impact of AVs on traffic flow on urban road networks.

This study aims to investigate and predict the impact of AVs on traffic flow in three aspects. First, the study focuses on urban roads, with their characteristic interrupting traffic flow. Second, it will investigate the impact of penetration rate changes of the AVs (a mixed condition of AVs and HDVs). Third, it will investigate the impact of AVs on road capacity—how much more traffic the current road network can accommodate by introducing AVs. In addition, the study focuses on AVs at level 4 of vehicle automation by the Society of Automotive Engineers (SAEs) [16]. The SAE defines level 4 as embodying a high degree of automation. In level 4, the cars do not require human intervention in most circumstances.

## 2. Literature Review

The following sections summarize the previous studies that investigated the impact of AVs and their methods.

Several studies reported that AVs improve traffic flow and increase road capacity. These improvements would get larger as the AV penetration rate increased [7, 17–20]. Talebpour et al. [18], in a study for a four-lane highway using simulation modeling, found that traffic flow improved for AV penetration above 30%. Similarly, Van Arem et al. [19] noted that the impact of AVs was noticeable when the penetration rate exceeded 40%. They also reported that road capacity was increased when the penetration rate exceeded 50%. Likewise, Jones and Philips [20] reported that vehicles with Cooperative ACC (CACC) would improve traffic flow when the penetration rate exceeded 40%.

In contrast, Calvert et al. [21], in the study about the impact of Adaptive Cruise Control (ACC), simulated a motorway of 19 km with three lanes. They found that an improvement in traffic flow was only identified at a penetration rate above 70%. Moreover, there was a small drop in road capacity up to a penetration rate of 80%. A study by Tientrakool et al. [22] found that road capacity significantly improved after the vehicle penetration rate with CACC exceeded 85%.

There are a few studies that deal with urban roads. Lu et al. [17] focused on the impact of AVs on urban road capacity using a microsimulation model. They found a 16% increase in road capacity with an artificial grid network at an

AV penetration rate of 100% while a 23.8% increase for the real road network in Budapest, Hungary. Yongseok Ko et al. [7] investigated the impact of AVs on travel time savings at the macrolevel. They reported that AVs reduced travel time from a penetration rate of 20% in the Seoul Metropolitan area. On the other side, the reduction in travel time started from a penetration rate of 60% in an interregional network. They concluded that AVs were more effective on congested roads. However, the study by Friedrich [13] reported a contrast from the findings of Ko et al. They concluded that, at an AV penetration rate of 100%, road capacity increased by 40% in urban areas compared to 80% on highways.

There are also a few studies regarding the impact of AVs at intersections. Zohdy and Rakha [23] and Bichiou and Rakha [24] investigated the impact of Cooperative Automated Vehicles (CAVs) on a signalized intersection and a roundabout. They focused on the cooperative and connected function of AVs and modeled a single intersection. They found that there was a 70~80% reduction in delay.

Meyer et al. [25] and Park et al. [26] noted the possibility of increased car use demand and consequent lack of road capacity. They argued that travel demand by kids, the elderly, and the handicapped would rapidly increase, as well as moving from public transport use to car use since there would be no burden to drive themselves.

In terms of methods for AV-related studies, transport simulation modeling is a significant approach to evaluate the impact of AVs [27]. The majority of the previous studies adopted a simulation modeling approach based on traffic [7, 13, 17–22, 24, 25]. Some of them were studied at the macroscopic level [7, 13, 25], while many of them were investigated at the microscopic level [17–22, 24]. However, with low penetration of AVs, there are no available definitive characteristics of traffic made up mainly of AVs. As part of the mainstream, AVs are still being tested, so a microscopic modeling approach is useful as it reflects detailed and different behaviors between AVs and HDVs in a model [8, 27–33].

## 3. Methods

The study adopted a microsimulation approach, since our primary concern is to assess the impact of AVs based on their behavior, and no AVs currently run on roads, except for a few test cars. The study also took a real-world road network in South Korea. An artificial road network can be helpful to identify the impact of AVs; however, this will have limitations regarding reflecting real road situations.

**3.1. Study Area and Data Collection.** A road network was selected to reflect the numbers of lanes and traffic flows of newly developed cities of Korea (Figure 1). The central area of the Bundang district in Seongnam city was selected. The area has mixed land uses of mass residential blocks with commercial and business blocks nearby. The road network is 4.5 km in total length with 13 intersections and from one lane to five lanes in one direction. In Figure 1, No. 6 and No. 7 are T-intersections with median barriers. So, the left-turn movement from all intersection approaches is prohibited.



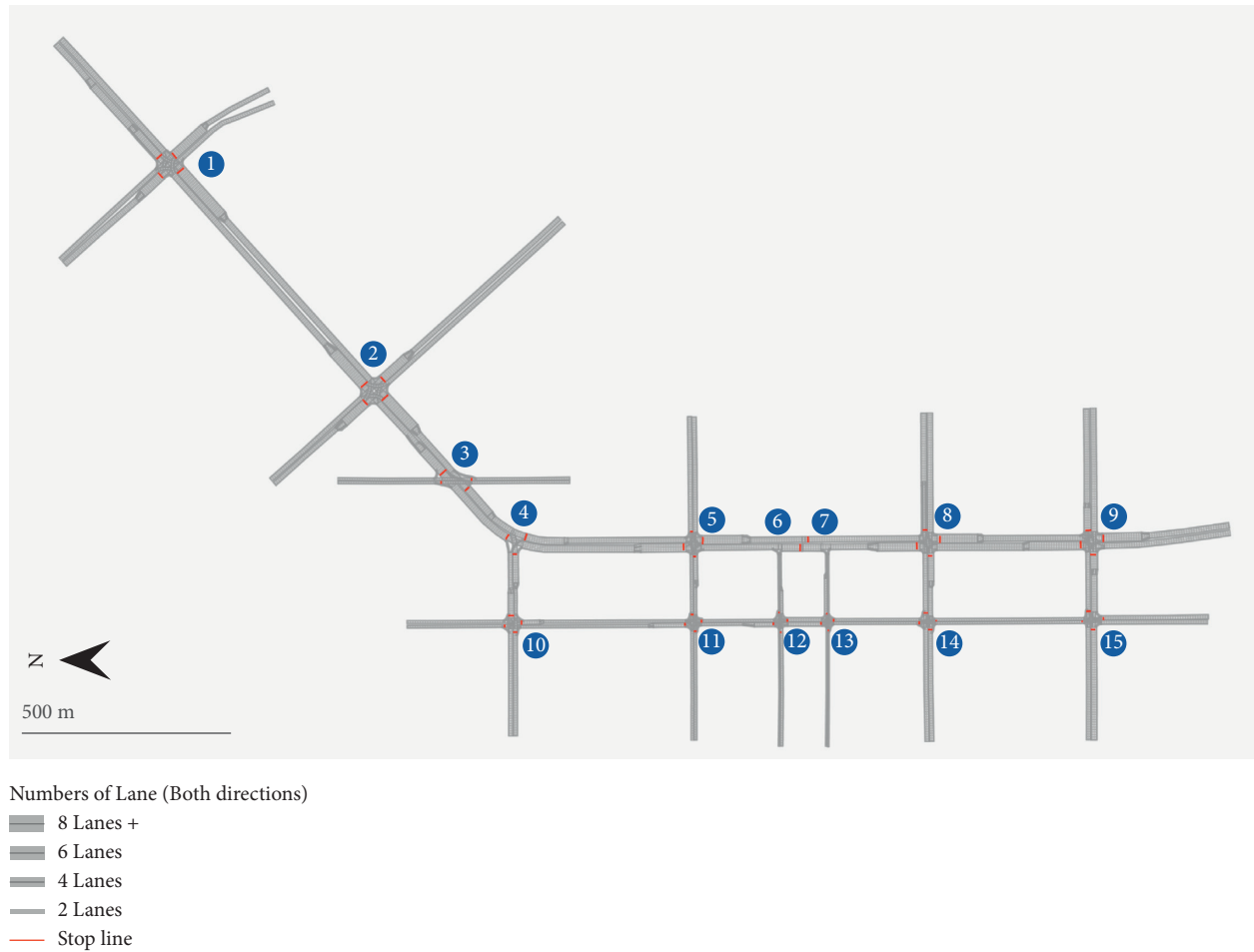


FIGURE 1: Layout of the road network.

The selected site has a main arterial road (from No. 1 to No. 9) connecting northern and southern areas of Seongnam city, and a road section in parallel with the arterial road (from No. 10 to No. 15) serves commercial and residential blocks. Moreover, the arterial road section is the main commuting route for Seoul. All the roads have well-designed pedestrian paths but there are no bike lanes on the roads. Therefore, bike traffic was not considered as only 1.8% of transport demand is served by bicycles [34].

In terms of the composition of lanes of road links, the arterial road section from No. 1 to No. 9 has four or five lanes in each direction (eight or more lanes in both directions). Only one link starting from No. 2 to No. 3 has five lanes. Links from No. 8 to No. 14 and from No. 9 to No. 15 have three lanes in each direction. A link from No. 10 to No. 4 also has three lanes. Links from No. 6 to No. 12 and from No. 7 to No. 13 have a single lane in each direction. All the remains have two lanes in each direction (mainly a road from No. 10 to No. 15).

Data collection was conducted to reflect the traffic conditions found in a real road network. It was carried out for three weekdays in July 2020. The team recorded traffic flows using video cameras for two hours from 7 am to 9 am at each intersection of the network. The volume of traffic

passing the intersections in each direction, queue lengths, and traffic signal changes were recorded. The traffic counts were used as input traffic data for modeling and the calibration and validation of modeling HDVs, while the traffic signal data were used to check the traffic signal data provided by the city council.

The arterial road section had 1,904 vehicles per hour on average in the northbound direction and 1,414 vehicles per hour in the southbound direction, while the parallel section had 202 vehicles per hour in the northbound direction and 216 vehicles per hour in the southbound direction. According to the arterial level of service for urban street class III by Highway Capacity Manual [35], links of the arterial road had a level of service that ranged from B to D while links of the parallel road had a level of service of D or F. The traffic signal cycles ranged between 120 s and 180 s.

**3.2. Simulation Environment.** As discussed in the Literature Review section, microsimulation traffic modeling is the main approach for AVs-related studies, especially focusing on traffic performance [32, 33]. VISSIM provides two car-following models: Wiedemann 74 and Wiedemann 99. The 74 model is suitable for urban roads, while the 99 model is

better for motorway traffic [36]. As our interest is on the impact of AVs on urban roads, the 74 model was deployed.

VISSIM allows users to set parameters for behaviors of car-following, lane changing, and drivers' characteristics. Various parameters were modified to model the movements of AVs. Default values of the parameters for AVs in VISSIM are at the SAE level 3 of automation [28]. However, as mentioned in the introduction, this study set AVs at level 4 of SAE and the values of parameters for them were derived from previous studies [28, 30, 37, 38]. The SAE defines level 3 and level 4 as high driving automation. In level 3, human drivers usually do not need to drive, but they have to be able to drive when driving is requested. In level 4, human drivers never need to take over driving.

Table 1 shows the various parameters used. The parameters for car-following and lane change for AVs were set to reflect more aggressive and sensitive behaviors of AVs than humans [38]. Cooperative lane change was also allowed for AVs. In terms of driver characteristics, it was assumed that AVs could communicate with other AVs and more easily obtain information about the traffic situation ahead and behind. The desired speed of AVs was fixed at 50 km/h, but it ranged from 48 to 58 for HDVs. The study assumed the HDV had 10% of driver errors, causing unnecessary conflicts of HDVs on the roads. In the model, platooning features were allowed only for AVs. The parameter values for HDVs used the default values of VISSIM.

**3.3. Scenarios and Run.** The study assumed that the penetration of AVs increases and traffic volumes also increase, due to increased demand for car use. The study considered six different rates including 0%, 20%, 40%, 60%, 80%, and 100% for each.

36 scenarios were developed and run for analysis by a combination of AV penetration rate and traffic volume increase, 6 cases for AV penetration rate and 6 cases for traffic volume increase (Figure 2). The base scenario, with the penetration rate of 0% and traffic volume increase of 0%, represents a current traffic environment with no AVs and no traffic volume increase. As expected, the penetration of 100% represents a fully AV environment and a traffic volume increase of 100% means that traffic volumes double.

Simulation runtime was set at 2 hours, including a warm-up period of 15 minutes before and after the simulation. In addition, all scenarios were run ten times with different seed numbers to obtain reliable outputs [39].

Four network performance indicators (average travel time, average vehicle speed, average delay, and stop frequency at intersections) were used to assess the impact of AVs and the increase in traffic volumes on urban roads.

A set of 4 virtual detectors were installed at the start of each link (Figure 3). The detectors measured vehicle speed and travel time in all directions (forward, left turn, and right turn). Delays were calculated from the measured travel time and free-flow time for links.

**3.4. Calibration.** Calibration was carried out using traffic volumes, collected to accurately represent the field

conditions. The process was only for the base case since the exact behaviors of AVs are still unavailable in many areas.

The calibration was performed with all the parameters for HDVs. The more sensitive parameters were identified and given priority for modification. Minimum headway, safety distance reduction factor, desired speed, and driver errors were the most sensitive.

After every modification, the model was run 10 times. The calculated traffic volumes and field observed traffic volumes were then compared for each intersection of the network. After many repetitions, the final difference was within 15% on average. However, not all the differences in the traffic counts for each direction at the intersections were within 15%. The difference along main corridors was generally within 15%. On the other hand, the minor corridors had much larger differences.

## 4. Results and Discussions

**4.1. Change in Traffic Flow by the Penetration Rates of AVs.** In this section, results from the scenarios only with increased AV penetration rate are presented (no traffic volume increase).

Overall, AVs improved traffic flow over the whole network (Table 2). The reduction of delay time was especially significant. As the penetration rate increased from 0% to 100%, the average travel time and average delay of the network decreased by 17% (from 229.99 s to 189.75 s) and 31% (from 126.65 s to 87.74 s), respectively. The average vehicle speed increased by 21% (from 22.08 km/h to 26.71 km/h).

The three indicators above were investigated at an individual link level. Detailed results for delay are presented (Figure 4) since they are clearer. As expected, delay improvement was not uniform, some links had a greater reduction, while others experienced an increase.

In general, the links with more lanes had greater improvement (reduced delay). However, for the links with two lanes, the delay was less reduced than for the links with a single lane. Another interesting point was that the left-turn traffic had better improvement in a delay overall, especially for single lane links.

The links with three or more lanes have a dedicated lane for left turns, while the links with a single and two lanes do not. For single lanes, vehicles drive one by one at intersections with a simple green light for all directions, so that AVs can improve traffic flow in general. On the other hand, for links with two lanes, there would be a conflict between vehicles turning left and those moving forward, depending upon traffic signal phase settings.

In terms of stop frequency at intersections (Table 3), vehicles made 2.67 stops on average for the penetration of 0% and 2.1 stops for the 100% penetration. The stop frequency decreased, as the penetration rate increased, for both AVs and HDVs, with HDVs stopping slightly less than AVs. HDVs stopped 2.67 times for the penetration rate of 0% and 1.85 times for the penetration rate of 80%. AVs stopped 2.4 times for the penetration rate of 20% and 2.07 times for the penetration rate of 80%.

TABLE 1: Parameters for modelling AVs and HDVs.

Parameters		AVs	HDV	
Car-following (Wiedemann 74)	Standstill distance (m)	0.5	1.5	
	Headway time (s)	0.5	0.9 ± 0.2	
Lane change	Min. headway (m)	0.2	0.5	
	Safety distance reduction factor (%)	30	60	
	Cooperative lane change      Min. speed difference(km/h)	10	N/A	
	Max. collision time (s)	10	N/A	
Driver characteristics	Look ahead distance (m)	Min.	0	5
		Max.	500	100
	Look back distance (m)	Min.	0	5
		Max.	500	50
	Desired speed (km/h)	Lower bound	50	48
Upper bound		50	58	
	Driver errors (%)	0	10	
Automated driving/platooning possible	Max. number of vehicles	7	N/A	
	Max. desired speed (km/h)	50	N/A	
	Max. distance for catching up to a platoon (m)	30	N/A	
	Gap time (s)	0.2	N/A	
	Minimum clearance (m)	2	N/A	

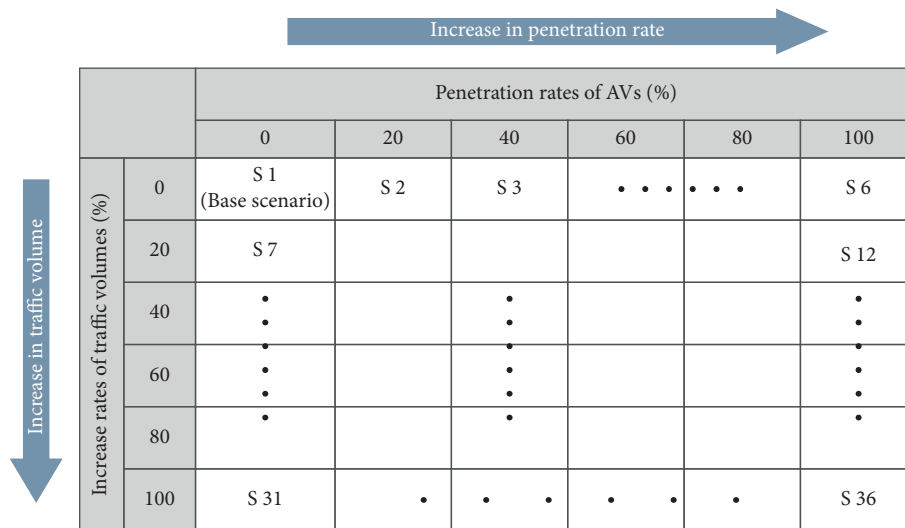


FIGURE 2: Scenario matrix.

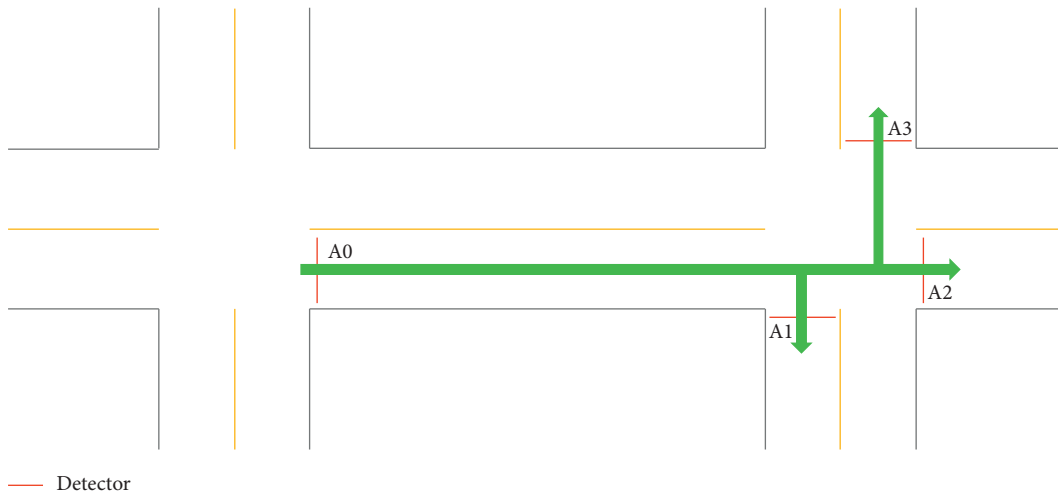


FIGURE 3: Location of detectors.

TABLE 2: Summary of road network performance by AV penetration rate.

Penetration rate (%)	Avg. travel time (s)	Avg. delay time (s)	Avg. vehicle speed (km/h)
0	229.99	126.65	22.08
20	213.18	109.71	23.88
40	204.21	100.88	24.92
60	198.95	95.91	25.56
80	194.46	91.82	26.12
100	189.75	87.74	26.71

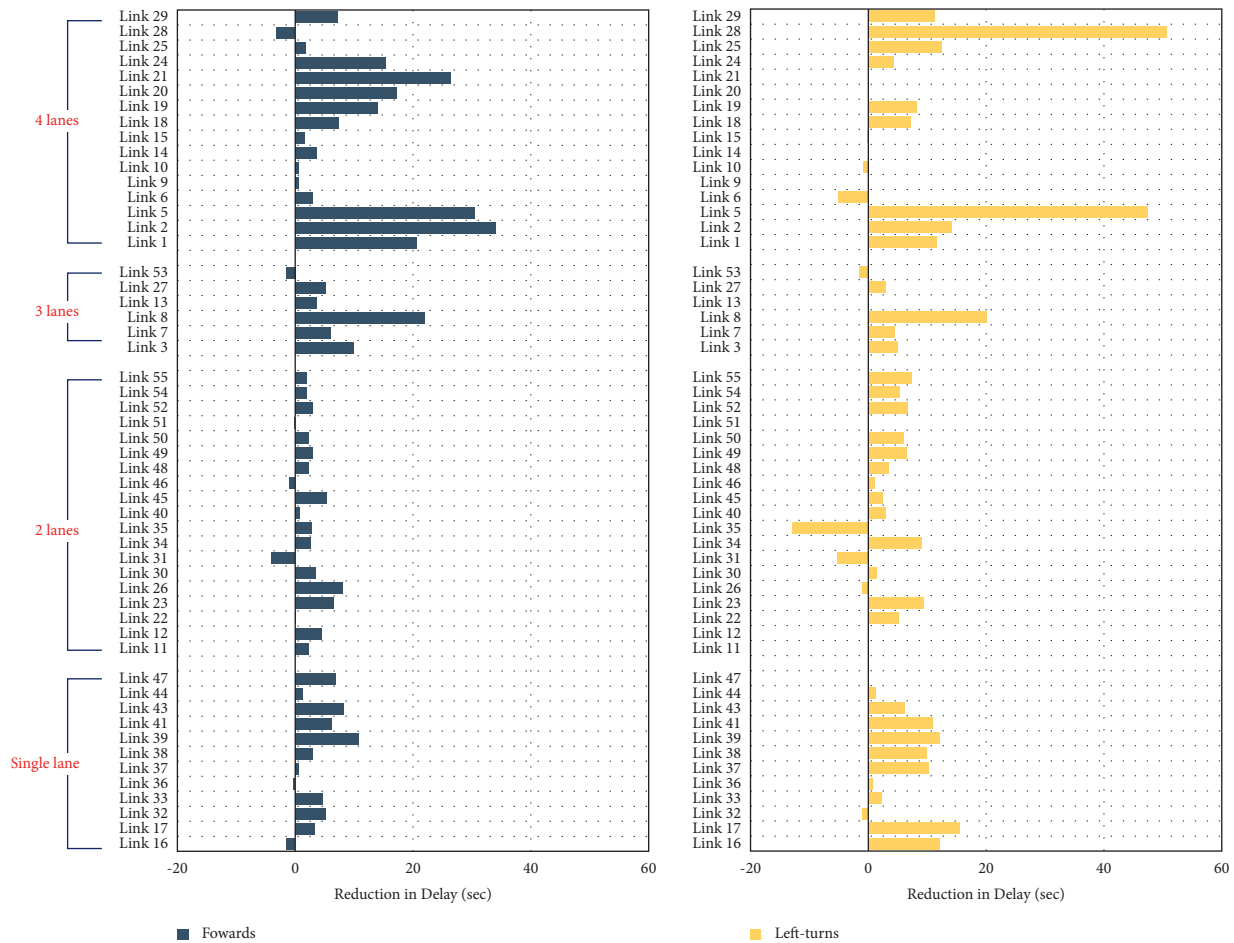


FIGURE 4: Reduction in delays of the links by lane numbers at 100% penetration rate.

Interestingly, the stop frequency for AVs increased slightly to 2.1 stops for the penetration rate of 100%, though there is no significant difference between 2.07 and 2.1. Further analysis found that the stop frequency for AVs increased at a penetration rate of 84%. The difference between HDVs and AVs in the stop frequency seems to be influenced by the value of the parameter of desired speed. The desired speed of AVs was set at 50 km/h, but the speed of HDVs varied from 48 to 58 km/h, so HDVs could drive more quickly and aggressively with a small violation of traffic signals.

4.2. Impact of AV Penetration Rate and Traffic Volume Increase on Traffic Flow. This section details the effect of AV

penetration rate and traffic volume increase on traffic flow. The impact on average travel time, average vehicle speed, and the average delay is presented in Figure 5.

Average travel time, average vehicle speed, and average delay increased dramatically as traffic volume increased. However, this was suppressed by an increase in the AV penetration rate. For example, as the traffic volume increased and the penetration rate remained at 0% (orange line), the average travel time increased by 158% (from 229.99s to 592.24s). On the other hand, when the traffic volume increased and the penetration rate remained at 100% (dark blue line), the average travel time increased by 91% (from 189.75s to 362.95s). In terms of the average delay, the changes were more significant. When the penetration rate was 0% and traffic volume increased, the average delay

TABLE 3: Stop frequency at intersection by AV penetration.

Penetration rate (%)	HDVs	AVs	Average
0	2.67	—	2.67
20	2.19	2.4	2.23
40	2.03	2.17	2.09
60	1.96	2.1	2.04
80	1.85	2.07	2.03
100	—	2.1	2.1

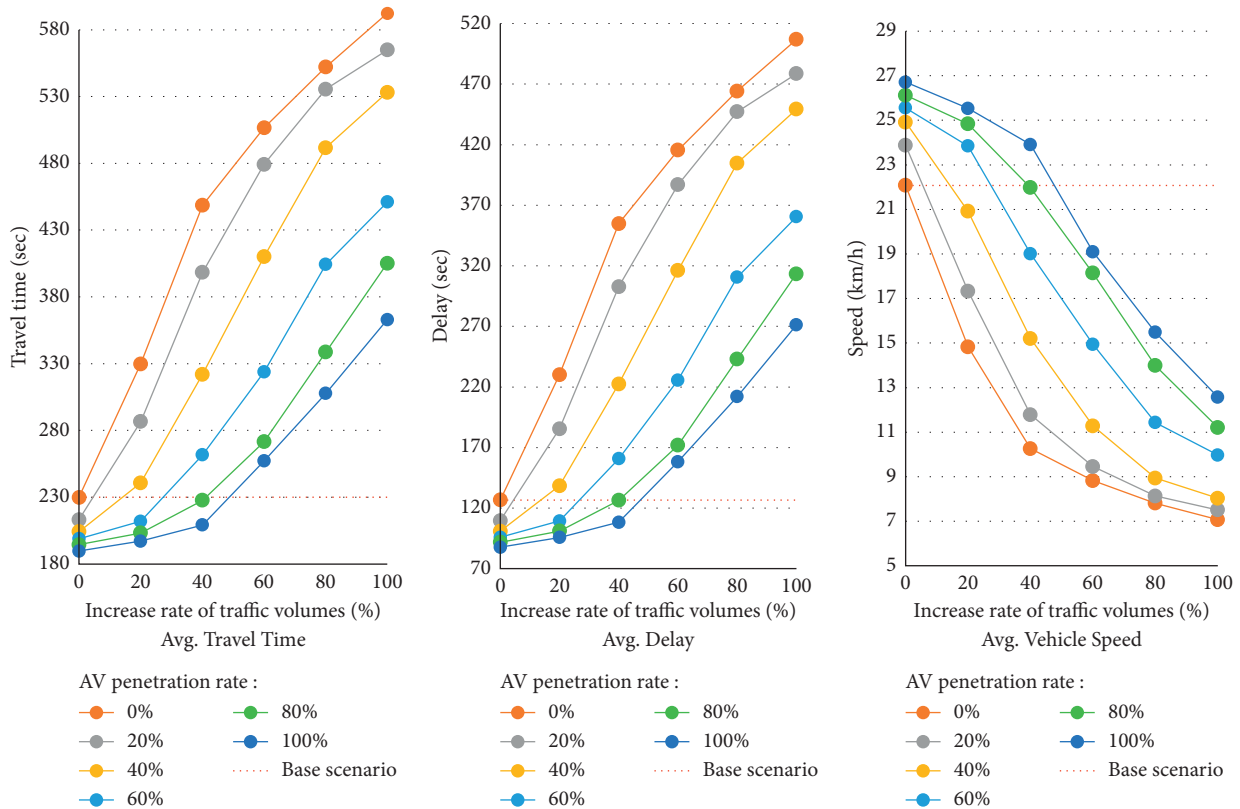


FIGURE 5: Traffic flow by AV penetration rate and traffic volume increment.

increased by 336% (from 109.71 s to 478.65 s), while at the penetration rate of 100%, it changed by 209% (from 87.74 s to 271.15 s). The change of the average speed also showed a similar pattern, where the increase of AV penetration rate dramatically mitigates worsening traffic conditions by traffic volume increase.

In addition, the distances between the lines on the y-axis were getting greater as the traffic volumes increased (x-axis) and then getting narrower again. For example, as traffic volume increased from 0% to 100% by 20%, differences between the average travel time for the penetration rate of 0% and of 100% were 40.24 s, 132.75 s, 239.43 s, 249.41 s, 244.48 s, and 229.28 s, respectively. At the penetration rate of 60%, the mitigation effect by AVs on travel time increase by traffic volume was most intensive.

Automated vehicles reduce the pressure from increased traffic volumes. This means that, without building more roads, road network capacity will increase as the number of AVs increases. For example, in the graph of average travel

time in Figure 5, the red dotted line is the current average travel time of the network (229.99 s). The red dot line can be set as a limit of upper acceptable travel time for worsening traffic flow by increased traffic volumes. In the graph of average travel time in Figure 5, when the penetration rate was 100%, the average travel time was still below the red dot line. This means the road network can accommodate 50% more traffic volume.

4.3. Discussion: AVs, Traffic Flow, and Road Capacity. So far, the results indicate that introducing AVs will have the potential to improve traffic flow, even on urban roads. For the case study areas, the travel time decreased by 17% when the penetration rate was 100%. They also showed that traffic flow could be improved, even with a low penetration rate. When the penetration rate was 20% without traffic increase, the average travel time decreased by 7% and the average delay decreased by 13%, while the average speed increased by



8%. This improvement will be possible due to shorter headway, better sensor system, and less errors of AVs compared to HDVs. Probably, it will be because of the parameter setting for more aggressive driving behaviors, based on assuming better and more accurate driving ability of AVs.

However, there is still a debatable point. Some studies report that traffic flow will become worse with a low or medium AV penetration rate, between around 20% and 70% [5, 7, 8, 15, 28]. The studies considering vehicles on highways with ACC emphasized that AVs would make it possible to reduce headway between vehicles and that this will lead to an improvement in traffic flow and even road capacity. Conversely, few studies were performed for urban roads. Lu et al. [17] investigated the impact of AVs on urban roads. They found that, with a penetration increase from 0% to 100%, there was an improvement of 16% in traffic flow in an artificial grid network, while an improvement of 23.8% was found for the real-world network. Their study did not show a negative impact on the traffic volume at a low AV penetration rate and indicated that the impact of AVs would differ depending on road categories.

The study found that road capacity will increase by AVs even on urban roads. A few other studies showed a similar capacity increase by 20~25% in the urban roads (interrupted flow) due to an increase in the AV penetration rate [13, 17, 24]. However, 20~40% increase in road capacity on urban roads seems rather low compared to the increase of 80% on highways (uninterrupted flow) [40]. This will be due to traffic signals at the intersections and the intersections themselves. Vehicles on urban roads must wait for their right of way at an intersection. Halting at an intersection and waiting for a green signal causes delay, regardless of AVs or HDVs. Under a mixed condition of AVs and HDVs, traffic signals will be necessary at most intersections. Although all vehicles on roads will be AVs in the future, they would wait for their turn to pass through an intersection. This would reduce the benefit of AVs on urban roads.

## 5. Conclusions

The study investigated the impact of AVs on traffic flow and road capacity. The study adopted a case study with a real-world network and a microsimulation approach using VISSIM to simulate the accurate behaviors of vehicles, interactions among vehicles, and movements by traffic signals in an urban road network. The team collected traffic data on-site and traffic signal data from a local council. The parameters were set for AV behaviors at SAE level 4, based on previous studies [28, 30, 37, 38]. However, a few possible AV features, for example, V2V communication, were not implemented in the simulation. A total of 36 scenarios were simulated. Among them, 6 scenarios were to consider the increase of only AV penetration rate from 0% to 100%, with 20% increment. The other 30 scenarios took account of both the AV penetration rates and traffic volume increase (also from 0% to 100%, with a 20% increment).

As expected, AVs have the potential to improve traffic flow and reduce the burden of traffic volume increase. The

results showed that AVs improved traffic flows by decreasing travel time and delay and increasing vehicle speed. As the penetration rate increased, the improvement also increased. For the penetration of 100%, there was an average travel time saving of 17%, delay reduction of 31%, and vehicle speed improvement of 21%. Analysis at the link level indicated that the links with three or more lanes had more traffic flow improvement than the links with one or two lanes.

The study also found that AVs reduce worsening traffic flow. However, if using AVs leads to increased demand for car use, AVs will become a potential risk regarding traffic management. However, when all the vehicles are AVs, the current road network could afford 40% more traffic, without building extra roads and worsening traffic conditions.

Although there is huge interest and investment in AV-related technologies, it is still unclear how AVs would improve the future transport system. Most of the previous studies investigated the impact of AVs in the case of highways. However, despite most car use taking place in urban areas, studies for urban roads have rarely been done.

This study indicated that even a low penetration rate of AVs can improve traffic flow on urban roads. Moreover, as AVs can improve road network capacity by 40%, transport planners or policymakers should consider AVs for planning transport systems for the future, probably over 15 or 25 years. With car-sharing trends and shared automated vehicles (SAVs), planners need to rethink issues around car use and road capacity. Probably, there will be an overcapacity of current road networks for car use demand in the future. In that case, city planners need to redesign roads for cities or to find another use for the spare capacity achieved by using AVs.

Although the study tried to investigate the impact of AVs on urban roads, there were many limitations. The parameters in the model need to be more accurately calibrated. For example, the 15% error in passing traffic counts, between model-generated counts and field data, was relatively large and could be improved on. The calibration was also carried out focusing on main corridors, so minor corridors were not as well-calibrated. The study assumed the homogeneous behavior of AVs. In the study, AVs were set to drive more aggressively than HDVs because they were believed to have better sensors and more accurate steering ability. However, another possible behavior is being more cautious to reduce the possibility of accidents. Another limitation was the changes in vehicle behaviors by interactions between AVs and HDVs, in that AVs will influence HDVs under a mixed condition of AVs and HDVs. Ramati et al. [41] reported that human drivers' behaviors will change when they are following AVs. They found that human drivers felt more comfortable with following AVs than HDVs. However, our study assumed that HDVs were not affected by the existence of AVs and the increased penetration, so the next step will be to reflect human drivers' behavior changes by introducing AVs in microscopic simulation models [41]. There was a debatable point regarding the improvement of traffic flow at low penetration rates, around 20~40%. Many researchers forecast a confusing period as AVs and HDVs will be mixed on roads for a long time. The study did not show such a

result, although this could be a matter of parameters or calibration.

## Data Availability

The VISSIM data used to support the findings of this study are available from the corresponding author upon request.

## Conflicts of Interest

The authors declare that there are no conflicts of interest regarding the publication of this paper.

## Acknowledgments

This research was sponsored by the project “Impact of Automated Vehicles on Parking Spaces and Roads” of the Land and Housing Institute (LHI) of Korea Land and Housing Corporation.

## References




- [1] Boston Consulting Group, *Revolution in the Driver's Seat: The Road to Autonomous Vehicles*, Boston Consulting Group, Boston, MA, USA, 2014.
- [2] T. Litman, *Autonomous Vehicle Implementation Prediction: Implications for Transport Planning*, Victoria Transport Policy Institute, Victoria, Canada, 2015.
- [3] P. Bansal and K. M. Kockelman, “Forecasting Americans’ long-term adoption of connected and autonomous vehicle technologies,” *Transportation Research Part A: Policy and Practice*, vol. 95, pp. 49–63, 2017.
- [4] T. Ajitha, L. Vanajakshi, and S. C. Subramanian, “Real-time traffic density estimation without reliable side road data,” *Journal of Computing in Civil Engineering*, vol. 29, no. 2, pp. 04014033-1-04014033-8, 2015.
- [5] G. M. Arnaout and S. Bowling, “A progressive deployment strategy for cooperative adaptive cruise control to improve traffic dynamics,” *International Journal of Automation and Computing*, vol. 11, no. 1, pp. 10–18, 2014.
- [6] P. Fernandez and U. Nunes, “Platooning with IVC-enabled autonomous vehicles-strategies to mitigate communication delays,” *Improves safety and traffic flow, IEEE transactions on ITS*, vol. 13, no. 1, pp. 91–106, 2012.
- [7] Y. S. Yongseok Ko, D. H. Jeong Hyun Rho, and J. H. Yook Donghyung, “Assessing benefits of autonomous vehicle system implementation through the network capacity analysis,” *The Korea Spatial Planning Review*, vol. 93, pp. 17–24, 2017.
- [8] I.-S. Park, J. D. Lee, J.-D. Lee, J.-Y. Lee, and K.-Y. Hwang, “Impacts of automated vehicles on freeway traffic-flow,” *The Journal of The Korea Institute of Intelligent Transport Systems*, vol. 14, no. 6, pp. 21–36, 2015.
- [9] M. Hu, X. Zhao, and F. Hui, “Modeling and analysis on minimum safe distance for platooning vehicles based on field test of communication delay,” *Journal of Advanced Transportation*, vol. 2021, Article ID 5543114, 15 pages, 2021.
- [10] J. VanderWerf, S. Shladover, and M. A. Miller, *Conceptual Development and Performance Assessment for the Deployment Staging of Advanced Vehicle Control and Safety Systems*, California Partners for Advanced Transit and Highways (PATH), Berkeley, CA, USA, 2004.
- [11] A. Kesting, M. Treiber, M. Schönhof, F. Kranke, and D. Helbing, “Jam-avoiding adaptive cruise control (ACC) and its impact on traffic dynamics,” in *Traffic and Granular Flow'05*, pp. 633–643, Springer, Berlin, Germany, 2007.
- [12] S. E. Shladover, D. Su, and X.-Y. Lu, “Impacts of cooperative adaptive cruise control on freeway traffic flow,” *Transportation Research Record: Journal of the Transportation Research Board*, vol. 2324, no. 1, pp. 63–70, 2012.
- [13] B. Friedrich, “The effect of autonomous vehicles on traffic,” in *Autonomous Driving*, M. Maurer, J. Gerdes, B. Lenz, and H. Winner, Eds., Springer, Berlin, Germany, pp. 317–334, 2016.
- [14] PSC and CAR, *Planning for Connected and Automated Vehicles*, Public Sector Consultants (PSC) Center for Automotive Research (CAR), Lansing, MI, USA, 2017.
- [15] J. Vander Werf, S. E. Shladover, M. A. Miller, and N. Kourjanskaia, “Effects of adaptive cruise control systems on highway traffic flow capacity,” *Transportation Research Record: Journal of the Transportation Research Board*, vol. 1800, no. 1, pp. 78–84, 2002.
- [16] SAE, *Taxonomy and Definitions for Terms Related to On-Road Motor Vehicle Automated Driving Systems*, SAE, Warrendale, PA, USA, 2021.
- [17] Q. Lu, T. Tettamanti, D. Hörcher, and I. Varga, “The Impact of autonomous vehicles on urban traffic network capacity: an experimental analysis by microscopic traffic simulation,” *Transportation Letters*, vol. 12, no. 8, pp. 540–549, 2020.
- [18] A. Talebpour, H. S. Mahmassani, and A. Elfar, “Investigating the effects of reserved lanes for autonomous vehicles on congestion and travel time reliability,” *Transportation Research Record: Journal of the Transportation Research Board*, vol. 2622, no. 1, pp. 1–12, 2017.
- [19] B. Van Arem, C. J. G. Van Driel, and R. Visser, “The impact of cooperative adaptive cruise control on traffic-flow characteristics,” *IEEE Transactions on Intelligent Transportation Systems*, vol. 7, no. 4, pp. 429–436, 2006.
- [20] S. R. Jones and B. H. Philips, “Cooperative adaptive cruise control: critical human factors issues and research questions,” in *Proceedings of the 7th International Driving Symposium on Human Factors in Driver Assessment, Training, and Vehicle Design*, Bolton Landing, NY, USA, June 2013.
- [21] S. C. Calvert, W. J. Schakel, and J. W. C. van Lint, “Will automated vehicles negatively impact traffic flow?” *Journal of Advanced Transportation*, vol. 2017, Article ID 3082781, 17 pages, 2017.
- [22] P. Tientrakool, H. Ya-Chi, and N. F. Maxemchuk, “Highway capacity benefits from using vehicle-to-vehicle communication and sensors for collision avoidance,” in *Proceedings of the Vehicular Technology Conference (VTC Fall)*, pp. 1–5, San Francisco, CA, USA, September 2011.
- [23] I. H. Zohdy and H. A. Rakha, “Enhancing roundabout operations via vehicle connectivity,” *Transportation Research Record: Journal of the Transportation Research Board*, vol. 2381, no. 1, pp. 91–100, 2013.
- [24] Y. Bichiou and H. A. Rakha, “Developing an optimal intersection control system for cooperative automated vehicles,” *IEEE Transactions on ITS*, vol. 20, no. 5, pp. 1–9, 2018.
- [25] J. Meyer, H. Becker, P. M. Bösch, and K. W. Axhausen, “Autonomous vehicles: the next jump in accessibilities?” *Research in Transportation Economics*, vol. 62, pp. 80–91, 2017.
- [26] J. Y. Park, S. K. Wu, and D. Y. Lee, *Impact Analysis of Autonomous Vehicles and Policy Implications*, The Korea Transport Institute, Sejong City, Republic of Korea, 2018.
- [27] H. U. Ahmed, Y. Huang, and P. Lu, “A Review of car-following models and modeling tools for human and

- autonomous-ready driving behaviors in micro-simulation,” *Smart Cities*, vol. 4, no. 1, pp. 314–335, 2021.
- [28] ATKINS, *Research on the Impacts of Connected and Autonomous Vehicles (CAVs) on Traffic Flow: Stage—Traffic Modelling and Analysis Technical Report*, ATKINS, London, UK, 2016.
- [29] D. Li and P. Wagner, “Impacts of gradual automated vehicle penetration on motorway operation: a comprehensive evaluation,” *European Transport Research Review*, vol. 11, no. 1, p. 36, 2019.
- [30] M. H. Kang, J. E. Song, K. Y. Hwang, and I. J. Im, “Analysing traffic impacts of automated vehicles on expressway weaving sections,” *Journal of Transport Research*, vol. 26, no. 4, pp. 33–47, 2019.
- [31] W. Ko, S. M. Park, S. Park, J. So, and I. Yun, “Analysis of effects of autonomous vehicle market share changes on expressway traffic flow using IDM,” *The Journal of The Korea Institute of Intelligent Transport Systems*, vol. 20, no. 4, pp. 13–27, 2021.
- [32] E. Aria, J. Olstam, and C. Schwietering, “Investigation of automated vehicle effects on driver’s behavior and traffic performance,” *Transportation Research Procedia*, vol. 15, pp. 761–770, 2016.
- [33] S. He, X. Guo, F. Ding, Y. Qi, and T. Chen, “Freeway traffic speed estimation of mixed traffic using data from connected and autonomous vehicles with a low penetration rate,” *Journal of Advanced Transportation*, vol. 2020, Article ID 1361583, 13 pages, 2020.
- [34] Gyenggi Transportation Information Center, “Transportation DB: modal share by purpose,” 2021, [https://gits.gg.go.kr/gtdb/web/trafficDb/newzone/HB004/2/ASSPER/2\\_ASSPER\\_OBJ\\_MOD.do](https://gits.gg.go.kr/gtdb/web/trafficDb/newzone/HB004/2/ASSPER/2_ASSPER_OBJ_MOD.do).
- [35] Transportation Research Board, *Highway Capacity Manual 2000*, National Academy of Sciences, Transportation Research Board, Washington, D.C, WA, USA, 2000.
- [36] PTV vision, VISSIM 2020 user manual, 2020.
- [37] D.-H. Yook, B. K. Lee, B.-J. Lee, and J.-T. Park, “Exploring the impacts of autonomous vehicle implementation through microscopic and macroscopic approaches,” *The Journal of The Korea Institute of Intelligent Transport Systems*, vol. 17, no. 5, pp. 14–28, 2018.
- [38] M. M. Morando, Q. Tian, L. T. Troung, and H. L. Vu, “Studying the safety impact of autonomous vehicles using simulation-based surrogate safety measures,” *Journal of Advanced Transportation*, vol. 2018, Article ID 6135183, 11 pages, 2018.
- [39] L. T. Truong, M. Sarvi, G. Currie, and T. M. Garoni, “Required traffic micro-simulation runs for reliable multivariate performance estimates,” *Journal of Advanced Transportation*, vol. 50, no. 3, pp. 296–314, 2016.
- [40] A. R. Pinjari, B. Augustine, and N. Menon, *Highway Capacity Impacts of Autonomous Vehicles: An Assessment*, University of South Florida, Tampa, FL, USA, 2013.
- [41] Y. Rahmati, M. Khajeh Hosseini, A. Talebpour, B. Swain, and C. Nelson, “Influence of autonomous vehicles on car-following behavior of human drivers,” *Transportation Research Record: Journal of the Transportation Research Board*, vol. 2673, no. 12, pp. 367–379, Article ID 036119811986262, 2019.



## Research Article

# An Algorithm for Detecting Collision Risk between Trucks and Pedestrians in the Connected Environment

Seung-oh Son <sup>1</sup>, Juneyoung Park <sup>1,2</sup>, Cheol Oh <sup>1,2</sup> and Chunho Yeom <sup>3</sup>

<sup>1</sup>Department of Smart City Engineering, Hanyang University, 15588 Ansan, Republic of Korea

<sup>2</sup>Department of Transportation and Logistics Engineering, Hanyang University, 15588 Ansan, Republic of Korea

<sup>3</sup>International School of Urban Sciences, University of Seoul, 02592 Seoul, Republic of Korea

Correspondence should be addressed to Juneyoung Park; [juneyoung@hanyang.ac.kr](mailto:juneyoung@hanyang.ac.kr)

Received 25 August 2021; Accepted 16 October 2021; Published 28 October 2021

Academic Editor: Xiaoyue Liu

Copyright © 2021 Seung-oh Son et al. This is an open access article distributed under the Creative Commons Attribution License, which permits unrestricted use, distribution, and reproduction in any medium, provided the original work is properly cited.

This study develops an algorithm to detect the risk of collision between trucks (i.e., yard tractors) and pedestrians (i.e., workers) in the connected environment of the port. The algorithm consists of linear regression-based movable coordinate predictions and vertical distance and angle judgments considering the moving characteristics of objects. Time-to-collision for port workers (TTCP) is developed to reflect the characteristics of the port using the predictive coordinates. This study assumes the connected environment in which yard tractors and workers can share coordinates of each object in real time using the Internet of Things (IoT) network. By utilizing microtraffic simulations, a port network is implemented, and the algorithm is verified using data from simulated workers and yard trucks in the connected environment. The risk detection algorithm is validated using confusion matrix. Validation results show that the true-positive rate (TPR) is 61.5~98.0%, the false-positive rate (FPR) is 79.6~85.9%, and the accuracy is 72.2~88.8%. This result implies that the metric scores improve as the data collection cycle increases. This is expected to be useful for sustainable transportation industry sites, particularly IoT-based safety management plans, designed to ensure the safety of pedestrians from crash risk by heavy vehicles (such as yard tractors).

## 1. Introduction

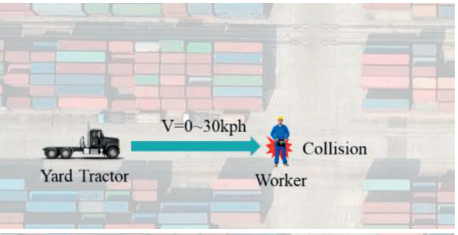
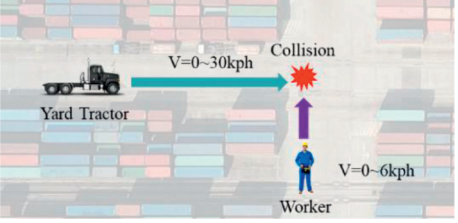
Technologies, educational programs, and policies designed to prevent industrial accidents have been widely implemented, and accidents are on the decline in various industrial sectors. However, accidents are still common at ports. According to the Korea Maritime Institute, the accident rate for port workers stood at 9.46 per thousand as of 2017, double the average of 4.84 for all Korean industries. This is 1.5 times greater than the rate in the transportation sector, in which traffic accidents occur more frequently. Port activities involve manual tasks associated with binding and, depending on the type of cargo, loading and unloading, and storage methods. Collisions, falling objects, and falling accidents occur frequently in ports [1]. The severity of an accident is higher compared to those in the industrial sector in general because heavy equipment is involved. The most frequent and accidental accident is collision. At a port, most

heavy equipment emits a warning sound to prevent collisions in advance. This makes it difficult for the operator to recognize access equipment (such as yard tractors), and accidents in these circumstances can be fatal. In the yard area of a port, there are two main cases of collision that can occur between workers and trucks (Table 1).

Collisions between workers and equipment in port yards are similar to pedestrian-vehicle crashes on roads, which constitute a leading concern in traffic safety. Multiple algorithm-based technologies have been developed to avoid collisions, including the forward crash warning system [2–5]. The concept of time-to-collision (TTC), which is used frequently in these algorithms, is defined in relation to the preceding and following vehicles [6]. The following equation [7, 8] provides a mathematical description of the concept:

$$TTC = \frac{h - L}{V_F - V_P}, \quad (1)$$

TABLE 1: Examples of collision-risk situations between pedestrian and truck.

No.	Situation	Visualization
1	The worker is working or waiting in the yard. The yard tractor is driving on the road at normal speed and approaching the worker's location. The worker is not aware of the approaching tractor.	
2	The worker is on the move. The yard tractor is driving on the road at normal speed and approaching the worker's location. The worker is not aware of the approaching tractor.	

where  $h$  is the space headway and  $L$  is the length of the preceding vehicle.  $V_F$  and  $V_P$  refer to the speeds of the following and preceding vehicles, respectively. The TTC assumes that the preceding vehicle maintains a constant speed. As a result, traditional TTCs are limited in their ability of expressing dynamic situations in which speed changes rapidly on real roads. To address this shortcoming, researchers have developed complementary algorithms such as inverse TTC, time-exposed TTC, and time-integrated TTC, for use in collision-risk detection technologies [9–13].

TTC is used not only in detection algorithms as an indicator of real-time collisions, but also in assessing safety levels based on trajectory [14]. TTC is a representative indicator for the assessment of safety, and indicators such as postencroachment time (PET) and the deceleration rate to avoid a crash are used for analysis [15, 16]. In 2003, Yang et al. developed a hydraulically based system for use in a rear-end collision warning and avoidance [17]. In the car-following situation, the warning system was designed with a condition-space-based approach. In 2018, Wu et al. developed an algorithm to determine the risk of a rear-end collision using real-time data. Unlike previous research, the Wu et al. study developed collision-prevention algorithms by processing real-time data that can be used in connected vehicle environments [18]. In 2019, Wu et al. used PET as an indicator for a safety analysis of the conflicting section between the bicycle road and the vehicle driveway. The authors analyzed the mechanical behavior between bicycles and vehicles to develop an algorithm that estimated crash risks and triggered a warning alarm [19]. In 2006, Oh et al. proposed a method of determining the risk of rear-end crashes using loop-detector data and applying the concept of a safe stopping distance. The relationship between the preceding and following vehicles in a collision can be expressed mathematically [20]. In 2016, Lee and Yeo developed a collision-warning algorithm based on a multilayer perceptron neural network. An algorithm was proposed to provide collision-warning information by predicting the right of influence and deceleration of passage time and

utilizing segment information collected by a roadside communication unit [7]. In 2020, Yue et al. conducted a study from the vehicle's perspective using a pedestrian-to-vehicle (P2V) driving simulator to predict and avoid pedestrians in pedestrian-vehicle collisions. Research has been conducted to improve P2V technology from the driver's perspective, which differs from the pedestrian's perspective, to increase pedestrian safety [21]. In 2019, Wu et al. proposed a system of risk assessment for pedestrian-vehicle collisions. Using data collected from Lidar and other sensors, they predicted pedestrian crossing intentions using a trajectory prediction model and analyzed risks based on a dynamic Bayesian network [22].

Other studies developed vehicle-to-vehicle communications systems that assume a smooth communications environment and perform a rear-end collision-risk analysis based on intervehicle information and collected communications [23–25]. Sensor-based studies that prioritize near-field networks to determine accident risks are already being used throughout the industry. However, research on long-distance communication using global positioning satellite (GPS) data is still being carried out with an eye to commercialization as it requires technical improvements, such as less battery maintenance and superior GPS reception. In 2017, Chen et al. calculated alternative safety indicators, such as TTC and PET between vehicles and pedestrians, to assess safety at intersections under specific conditions and times [26]. The study featured an analysis of traditional TTC problems and P2V relationships by applying formulas. In 2019, Li et al. attempted to predict the maneuverability of adjacent vehicles through inferences based on probability methodologies such as Bayesian networks. The resulting dynamic features have been presented and are considered significant advancements in terms of real-time risk management [27].

Most TTC-based algorithm technologies have been approached from a vehicle perspective [7, 17, 21, 23, 26, 28, 29] and little relevant research has been conducted to help pedestrians avoid collisions with vehicles [26, 30]. In

this study, a vehicle-collision avoidance algorithm is proposed from the perspective of the pedestrian (worker). In a port, devices can be distributed to workers to facilitate the collection and management of data. The device is developed using IoT-based GPS technology and can determine the real-time location of workers and equipment. These IoT-based collision-risk detection technologies are expected to be applied first in traffic environments that guarantee the safety of pedestrians. The algorithm technology described in this study is expected to play an important role in planning pedestrian traffic safety measures in future sustainable pedestrian-oriented traffic environments.

The purpose of this study is to develop detection techniques that can predict pedestrian collision risks using connected technology under special conditions, such as low-traffic ports or nonsignal intersections. The movable objects of the port terminal travel in a designated direction through a designated road, but pedestrians cannot specify the direction of progress due to their characteristics. Considering this, in this study, the speed, direction, and location of the equipment are defined by the change in relative distance as predictions. A collision-risk detection algorithm is developed reflecting the defined concept, which is validated using microtraffic simulations. With reference to the performance of the device that can be applied to the field, a simulation scenario with different data collection cycles is designed. Validation of the algorithm was performed by considering differences in risk detection accuracy on a collection cycle basis.

## 2. Methodologies

**2.1. Prediction of Relative Space.** In this study, risk indicators were calculated based on traditional TTC concepts. Traditional TTCs are used not only for crash risk detection, but also for conflict-based safety analysis at intersections and certain other sections. This study used a risk detection methodology using latitude and longitude coordinates. The relative distance is then calculated to determine the risk as in the following equation. Euclidean distances were used to calculate the distance between coordinates:

$$l_r = \sqrt{(x_p - x_e)^2 + (y_p - y_e)^2}, \quad (2)$$

where  $l_r$  is the distance between port worker and equipment and  $(x_p, y_p)$  and  $(x_e, y_e)$  are the coordinates of the port worker and equipment (based on geographical distances), respectively. This study produced a changing relative distance-based TTC between worker and equipment. Alternative safety indicators were then proposed to respond to and avoid expected collisions. Considering the spatial characteristics of the port, a general straight section predicted future coordinates using a linear regression model. In many previous studies of collision-warning algorithms, the perception reaction time (PRT) is assumed to be between 0 and 2.5 s [31–33]. In this study, response time is set in consideration of the PRT by taking into account the vehicles, the work of the port workers, and mobility characteristics. The movement of the equipment is predicted for more than 10 s from detection and recognition of, and response to,

collision risk, and verification of the research methodology is carried out.

A criterion of 10 s for detecting accident risks is set given the characteristics of the port container yards. A one-yard block is compartmentalized so that it can accommodate 15 containers (20 ft) horizontally and six vertically. A block is 90 m wide and 15 m long. The speed limit of moving equipment (such as yard tractors) in the port is 30 km/h (8.3 m/s). The maximum distance the equipment can travel in 10 s is therefore 83 m. Because the width of a one-yard block is 90 m, the time of 10 s in the algorithm is the maximum prediction time to ensure that all movement up to the next direction selection can be predicted. Because the port is a difficult working environment to recognize approaching equipment, collision accidents caused by low speeds continue to occur. For example, if a yard tractor moves at a speed of 5 km/h, it can travel 13.9 m in 10 s. Due to the reduction of the hazard radius and sudden acceleration and deceleration behavior, it is necessary to select the forecast range for the next 10 s. In this study, a complementary TTC is proposed based on predicting a minimum collision distance with workers within 10 s. The minimum relative distance based on recursive algorithms can be found in the following equation:

$$l_{r,t} = \sqrt{(x_{p,t} - x_{e,t})^2 + (y_{p,t} - y_{e,t})^2}, \quad (0 < t < 10 \text{ s}), \quad (3)$$

where  $l_{r,t}$  is the relative distance between worker and equipment at any time  $t$  and  $(x_{p,t}, y_{p,t})$  and  $(x_{e,t}, y_{e,t})$  are the coordinates of port worker and equipment, respectively, at any time  $t$ . The collision risk is calculated based on the minimum value among the relative distances calculated by location information within 10 s of the future.

In order to use the collected position coordinates for analysis, a transformation work is required. Because the latitude and longitude coordinates used in this study are spherical coordinates, they should be converted to Cartesian coordinates to obtain relative distances. The haversine formula is used to convert orthogonal coordinates to the Cartesian system, and the relative distance is calculated after conversion. In this study, a regression model with recursive concept is developed to predict location coordinates. In other words, it is a method of using historical location information to produce future forecast information. In Figure 1, the recursive concept is illustrated.

When the current time is  $t_0$  and the historical coordinates recorded before  $t$  seconds are supplied, a linear regression model can be constructed with the slope dependent on the amount of change and the regression coefficient and dependent variables as the predicted coordinates. The  $y$ -axis coordinates (latitude) and  $x$ -axis coordinates (longitude) were predicted by building separate equations as follows:

$$\begin{aligned} y_{\text{predicted},e,t} &= \frac{(y_{e,t} - y_{e,t+1})}{(x_{e,t} - x_{e,t+1})} \cdot x_{\text{predicted},e,t} + e \\ &= f'(t) \cdot x_{\text{predicted},e,t} + e, \end{aligned} \quad (4)$$

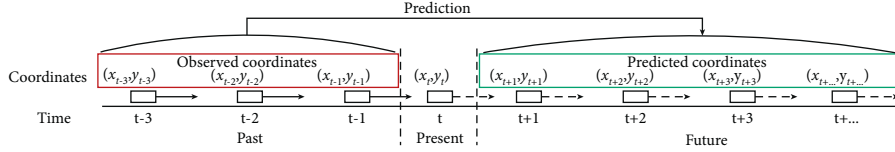


FIGURE 1: A recursive algorithm for predicting coordinates by time.

where  $y_{\text{predicted},e,t}$  and  $x_{\text{predicted},e,t}$  are the predicted  $y$ -axis (latitude) and  $x$ -axis (longitude) coordinates of equipment, respectively.  $e$  is a residual, and  $f'(t)$  is the regression coefficient of the prediction model, such that

$$d_t = \frac{|ax_{\text{predicted}} + by_{\text{predicted}} + c|}{\sqrt{a^2 + b^2}} \quad (5)$$

$$= \frac{|f'(t) \cdot x_{\text{predicted},t} - y_{\text{predicted},t} + e|}{\sqrt{f'(t)^2 + (-1)^2}}$$

$$x = \frac{-b \pm \sqrt{b^2 - 4ac}}{2a} \theta_t = a \sin\left(\frac{d_t}{l_r}\right) \times \frac{180^\circ}{\pi}, \quad (6)$$

where  $d_t$  is the vertical distance between the predicted directional line of the moving equipment and the worker.  $\theta_t$  is the degree between the equipment and the worker (Figure 2).

**2.2. Time-to-Collision for Port Workers (TTCP).** The relative distance ( $l_r$ ) from the current time to the predicted coordinates after 10 s has been aggregated to define the time at which  $l_r$  is minimal, as seen in equation (7). In addition, changes in  $l_r$  and relative velocity ( $v_r$ ) between the forecast coordinates for a worker and equipment can provide a real-time rate of change ( $v_{l,\Delta t}$ ) of the current relative speed. The time-to-collision for port workers (TTCP) can be calculated using the relationship between relative distance and real-time rate of change:

$$\text{TTCP} = t_{\min} - t_0 = \frac{l_{r,t}}{(l_{r,t_2} - l_{r,t_1}) / (t_2 - t_1)} = \frac{l_{r,t}}{v_{r,\Delta t}}, \quad (7)$$

where  $t_{\min}$  is the time at which the relative distance between objects for the future 10 s is minimum.  $t_0$  is current time.  $l_{r,t}$  is relative distance, and  $v_{r,\Delta t}$  is the relative distance reduction rate at time  $t$ . TTCP is the time calculated for the rate at which the relative distance and relative velocity can be obtained through the prediction coordinates and the relative velocity is reduced by the amount of change in this indicator. It is the time taken to minimize  $l_{r,t}$  from the worker, assuming that the worker's presence is recognized within a certain relative distance and that the worker moves in the predicted direction at the current speed for 10 s. The set 10 s is the maximum value that can detect all accessible objects. In this study, the TTCP threshold to determine the presence or absence of a dangerous situation is set to 4 s. According to Yue et al., given a brake reaction rate of 1.25 to 1.5 s (from the previous study), a TTC of 2 s is considered a serious precrash accident [21]. In addition, given a brake response speed and the worker's response speed of 2.5 s, a TTC of 4 s is

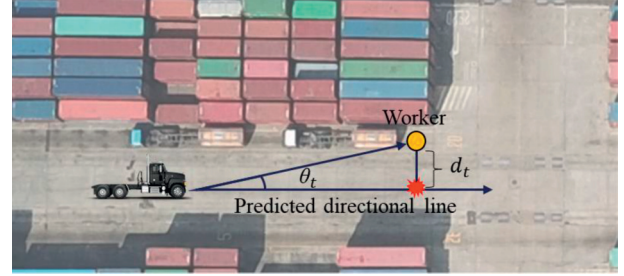


FIGURE 2: Illustration of the distance between the tractor's predicted directional line and a worker.

considered dangerous. Therefore, in this study, when the proposed TTCP is 4 s, the situation is considered dangerous (precrash situation). Because the maximum travel distance for 4 s at a design speed of 30 km/h is approximately 33.3 m, this is almost consistent with the relative distance-based risk assessment standard of 30 m.

**2.3. Development of a Crash Risk Detection Algorithm for Port Workers.** To detect accident risks in real time by combining the proposed alternative safety indicators such as TTCP requires defining and classifying various behaviors of workers and equipment. In this study, given the basic characteristics of accidents occurring within the port, directly relevant variables were derived and considered in the algorithm. Factors judged important and reflected in the development of algorithms are work status, location (place), distance from objects (relative distance,  $l_r$ ), vertical distance ( $d_t$ ), degree ( $\theta_t$ ), and approach direction ( $v_r$ ).

According to Layton and Dixon (2012), the stopping sight distance is 31.2 m at a design speed of 30 km/h, and the typical emergency stopping distance is 14.2 m on dry road surfaces (with a response time of 2.5 s) [31]. By referring to this standard, yard trucks within 30 m of the worker and approaching the worker's direction were detected as dangerous objects. In this study, an algorithm was developed by largely dividing it into two stages based on these criteria. The first is the "risk situation judgement algorithm" that detects objects approaching within a relative distance of 15 m. The second is "collision-risk detection algorithm," which determines the designated TTCP criterion according to vertical distance ( $d_t$ ) and angle ( $\theta_t$ ). Collision-risk detection algorithm is performed only for objects determined to be dangerous by risk situation judgement algorithm. The developed algorithm is shown in Figure 3.

Figure 4 provides a diagram of the algorithm to determine the risk of collision at a port. It is the process of calculating the indicators according to changes in the



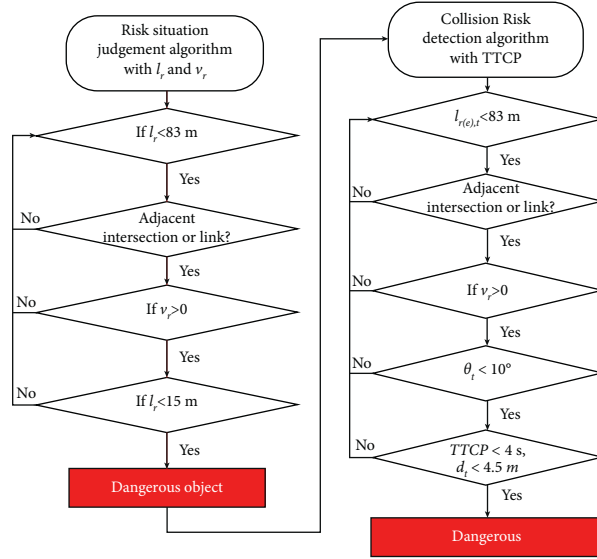


FIGURE 3: Risk detection algorithm with TTC.

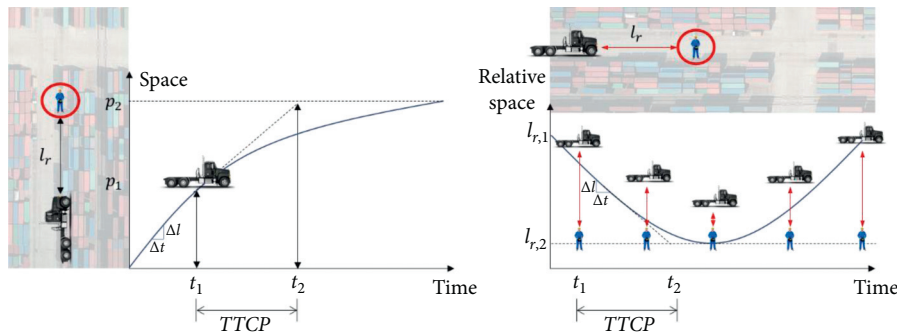


FIGURE 4: Risk detection algorithm with TTC.

relative space between trucks and workers. This figure expresses a simple situation for understanding. In practice, the change in speed of the object can be reflected to detect changes in the TTC according to the speed.

**2.4. Data Description.** This study assumes a situation in which the real-time locations of workers and equipment are collected using IoT devices. This allowed us to derive the risk of a collision accident between workers and equipment in a port yard in the form of a TTC-based risk index and detection using the collected data. Technical research is currently being carried out at the port in anticipation of the introduction of IoT devices. To implement and evaluate accident-risk detection technologies in an IoT communication environment, a virtual environment is established using microtraffic simulations. Previous studies used data collected from actual roads [12, 34], where it is difficult to ensure a fully controlled environment for experimentation and implement the desired scenario. Thus, in this study, simulation analyses were performed that enabled the full implementation of the planned risk scenario. In this study, the risk of a collision within a port is divided into scenarios.

The actual environment and working characteristics were classified and analyzed to capture all possible situations between workers and equipment in the simulation network, and the risk of collision at the port is separated into four distinct scenarios. Trace data on workers and equipment were collected for each scenario using VISSIM, a microtraffic simulation program. The simulation time is set to a total length of 1,200 s for the collection of data, and analysis is performed by dividing the collection cycle into three categories, considering the communication performance of an actual IoT device.

The period for the analysis is set to 1 Hz, 2 Hz, or 10 Hz. To simulate the movement of equipment and yard tractors in the port, movement at the actual port is analyzed and the average speed is below 30 km/h. Network settlement and verification efforts were not carried out because the objective is to detect the risk of collision between workers and equipment in certain situations without considering intervehicle interactions and delays in traffic. The spatial background applied in this study is Busan Sinseondae Pier (Figure 5). The same spatial network is established using Google and Kakao maps, and photos are taken at real-world sites.



FIGURE 5: Study area (Sinseondae Pier, Busan Port Terminal).

TABLE 2: Confusion matrix.

Classification	Actual class		
	Dangerous	Normal	
Prediction	Dangerous	True positive (TP)	False positive (FP)
	Normal	False negative (FN)	True negative (TN)

### 3. Results and Discussion

Algorithm verification is carried out to detect the risk of a collision between a worker and equipment within the port using trajectory data collected in the analysis network and VISSIM. The analysis is performed by dividing the data into three scenarios according to the frequency of the information collection. Simulation experiments were conducted according to the information collection cycle. To evaluate the risk detection performance of the algorithm, the risk situation is defined as follows:

- (1) If the relative distance is within 30 m and the relative distance is decreasing, the relative velocity ( $v_r$ ) is positive and the mobile device is approaching
- (2) Relative distance within 15 m

In this study, the confusion matrix is used to evaluate the detection performance of the algorithm. As a criterion for determining the accuracy of the predicted value, the above two situations were set as the actual class (Table 2). The confusion matrix is used to compare the number of true and false predicted values and actual values. The simulation results of algorithm are classified into four categories to evaluate detection accuracy as follows:

True positive (TP): the algorithm predicted that a situation is dangerous, and it is true

False positive (FP): the algorithm predicted that a situation is dangerous, and it is false

False negative (FN): the algorithm predicted that a situation is normal, and it is false

True negative (TN): the algorithm predicted that a situation is normal, and it is true

True positive rate (TPR) = recall (sensitivity)

$$= \frac{TP}{TP + FN} \quad (8)$$

False positive rate (FPR) = 1 – specificity

$$= \frac{FP}{FP + TN} \quad (9)$$

$$\text{accuracy} = \frac{TP + TN}{TP + FN + FP + TN} \quad (10)$$

True-positive rate (TPR), also called sensitivity, refers to how accurately the algorithm classifies dangerous situations (TP + FN), as seen in equation (8). False-positive rate (FPR) indicates how accurately the algorithm classifies normal situations (TN + FP), as seen in equation (9). Accuracy is an indicator that considers both TP and TN, which can most intuitively represent the performance of the algorithm [35], as seen in equation (10).

The numbers of samples according to the data collection cycle were 12,811 (1 Hz), 25,147 (2 Hz), and 137,254 (10 Hz), respectively. The confusion matrix and metric scores are presented in Tables 3–6. The metric scores of 1 Hz show 61.5%, 79.6%, and 72.2%. This score is the smallest of three data collection cycle scenarios. Compared to other cycles, 1 Hz has a longer prediction unit. Therefore, this result is seen as an increase in error within the prediction unit. For 2 Hz, the data were every 0.5 s; the metric score shows 91.8%, 85.9%, and 87.5%. Finally, for 10 Hz and the shortest collection cycle, the metric score shows 98.0%, 85.4%, and 88.8%. It is obvious that the score of 10 Hz has the greatest accuracy among the cycles, which suggests that the shorter

TABLE 3: Results (data acquisition cycle = 1 Hz).

Classification		Actual class	
		Dangerous	Normal
Prediction	Dangerous	3,220	1,545
	Normal	2,013	6,032

True-positive rate (TPR) = 0.615; false-positive rate (FPR) = 0.796; accuracy = 0.722.

TABLE 4: Results (data acquisition cycle = 2 Hz).

Classification		Actual class	
		Dangerous	Normal
Prediction	Dangerous	6,249	2,588
	Normal	561	15,748

True-positive rate (TPR) = 0.918; false-positive rate (FPR) = 0.859; accuracy = 0.875.

TABLE 5: Results (data acquisition cycle = 10 Hz).

Classification		Actual class	
		Dangerous	Normal
Prediction	Dangerous	35,967	14,661
	Normal	724	85,901

True-positive rate (TPR) = 0.980; false-positive rate (FPR) = 0.854; accuracy = 0.888.

TABLE 6: Metric scores for algorithm (data acquisition cycle = 1, 2, 10 Hz).

Data acquisition cycle (Hz)	True-positive rate	False-positive rate	Accuracy
1	0.615	0.796	0.722
2	0.918	0.859	0.875
10	0.980	0.854	0.888

the collection cycle, the better the performance of the algorithm.

In summary, sensitivity analysis and comparative studies have been conducted to verify the performance of the algorithm. Sensitivity analysis shows the performance of algorithms associated with data collection cycles, which means that shorter collection cycles are better in terms of detection accuracy of algorithms. Considering current technical level such as battery and equipment size, it is difficult to supply equipment with 10 Hz. Therefore, it is necessary to establish equipment and servers that can provide an appropriate data collection cycle in consideration of the realistic conditions of the industrial site.

#### 4. Conclusions

This study developed and verified an algorithm to detect the risk of collision accidents between port workers and equipment. A risk indicator represented by TTC is selected to provide detection of the risk of collision due to equipment in situations specified by various conditions in the port.

Traditional TTCs are the simplest collision-detection replacement safety indicators and only detect hazardous situations if certain conditions are met. Various studies have suggested improving TTCs to compensate for these problems. The purpose of this study is to develop an algorithm that considers the characteristics of pedestrian behavior by calculating the TTC between workers and equipment, not TTCs, in the situation of the next lane.

As a result, the algorithm shows 61.5–98.0% TPR, 79.6–85.9% FPR, and 72.2–88.8% Accuracy depending on the collection cycle. The algorithm validation results indicate that the metric scores increase as the collection cycle is shortened. This means that the better the performance of individual IoT devices available in the field is, the better the risk detection level of the algorithm can be. Based on these analysis results, this study argues for the need to introduce smart port equipment following technical improvements. Because it is an algorithm developed considering the spatial characteristics of ports, it is significant in terms of safety improvement in industrial sites.

However, some limitations exist in this study. First, since it is a simulation-based algorithm study assuming conditions in the field, further verification using real-world field data is required. Second, improvements are needed on the threshold baseline setting of stopping sight distance and TTC. In this study, the criteria for studies conducted in general traffic flow environments were utilized. Therefore, the stopping sight distance and TTC settings that are optimized for a port environment are needed [30, 36]. Third, the accuracy improvement of the algorithm can be performed by utilizing various prediction and verification methodologies. In this study, predictive method is used for real-time contextual judgement and algorithm optimization. However, since machine learning-based positional coordinate prediction studies have been conducted, various prediction methodologies need to be reviewed to improve the accuracy of algorithms [37]. In addition, studies of collision-prevention methodologies using similar techniques can be applied to improvements [38–40]. Future research will be considered verifying algorithms using device data collected in the field and improving services after introduction. It is expected to help prevent accidents between equipment and pedestrians at ports and other industrial sites.

#### Data Availability

Some or all data, models, or code that support the findings of this study are available from the corresponding author upon reasonable request.

#### Disclosure

This research was a part of the project titled “Development of Port Risk Prediction and Intelligent Port Safety Management Technologies”.

#### Conflicts of Interest

The authors declare no conflicts of interest.

## Acknowledgments

This paper was funded by the Ministry of Oceans and Fisheries, Korea (20190399-08).

## References

- [1] J. Zhang, Â. P. Teixeira, C. Guedes Soares, and X. Yan, "Quantitative assessment of collision risk influence factors in the Tianjin port," *Safety Science*, vol. 110, pp. 363–371, 2018.
- [2] Y. Liu, W. Wang, X. Hua, and S. Wang, "Safety analysis of a modified cooperative adaptive cruise control algorithm accounting for communication delay," *Sustainability*, vol. 12, no. 18, p. 7568, 2020.
- [3] T. Nakazawa, S. Tang, and S. Obana, "CCN-based inter-vehicle communication for efficient collection of road and traffic information," *Electronics*, vol. 9, no. 1, p. 112, 2020.
- [4] L. Wang, H. Zhong, W. Ma, M. Abdel-Aty, and J. Park, "How many crashes can connected vehicle and automated vehicle technologies prevent: a meta-analysis," *Accident Analysis & Prevention*, vol. 136, Article ID 105299, 2020.
- [5] L. Yue, M. Abdel-Aty, Y. Wu, O. Zheng, and J. Yuan, "In-depth approach for identifying crash causation patterns and its implications for pedestrian crash prevention," *Journal of Safety Research*, vol. 73, pp. 119–132, 2020.
- [6] R. van der Horst and J. Hogema, "Time-to-collision and collision avoidance systems," in *Proceedings of the 6th ICTCT Workshop Salzburgna*, Salzburg, Germany, 1994.
- [7] D. Lee and H. Yeo, "Real-time rear-end collision-warning system using a multilayer perceptron neural network," *IEEE Transactions on Intelligent Transportation Systems*, vol. 17, no. 11, pp. 3087–3097, 2016.
- [8] R. Utriainen, "The potential impacts of automated vehicles on pedestrian safety in a four-season country," *Journal of Intelligent Transportation Systems*, vol. 25, no. 2, pp. 188–196, 2020.
- [9] H. C. Chin, S. T. Quek, and R. L. Cheu, "Traffic conflicts in expressway merging," *Journal of Transportation Engineering*, vol. 117, no. 6, pp. 633–643, 1991.
- [10] H.-C. Chin and S.-T. Quek, "Measurement of traffic conflicts," *Safety Science*, vol. 26, no. 3, pp. 169–185, 1997.
- [11] H. Yang, K. Ozbay, and B. Martin, "Application of simulation-based traffic conflict analysis for highway safety evaluation," in *Proceedings of the 12th WCTR*, vol. 4, Lisbon, Portugal, 2010.
- [12] Z. Wei, S. Xiang, D. Xuan, and L. Xu, "An adaptive vehicle rear-end collision warning algorithm based on neural network, communications in computer and information science," in *International Conference on Information and Management Engineering*, pp. 305–314, Springer, Berlin, Germany, 2011.
- [13] R. J. Kiefer, D. J. LeBlanc, and C. A. Flannagan, "Developing an inverse time-to-collision crash alert timing approach based on drivers' last-second braking and steering judgments," *Accident Analysis & Prevention*, vol. 37, no. 2, pp. 295–303, 2005.
- [14] J. Hou, G. F. List, and X. Guo, "New algorithms for computing the time-to-collision in freeway traffic simulation models," *Computational Intelligence and Neuroscience*, vol. 2014, Article ID 761047, 8 pages, 2014.
- [15] B. L. Allen, B. T. Shin, and P. J. Cooper, *Analysis of Traffic Conflicts and Collisions*, McMaster University, Hamilton, Canada, 1978.
- [16] A. Razmpa, *An Assessment of Post-Encroachment Times for Bicycle-Vehicle Interactions Observed in the Field, a Driving Simulator, and in Traffic Simulation Models*, Portland State University, Portland, OR, USA, 2016.
- [17] L. Yang, J. H. Yang, E. Feron, and V. Kulkarni, "Development of a performance-based approach for a rear-end collision warning and avoidance system for automobiles," in *Proceedings of the IEEE IV2003 Intelligent Vehicles Symposium Proceedings (Cat No 03TH8683)*, pp. 316–321, IEEE, Columbus, OH, USA, 2003.
- [18] Y. Wu, M. Abdel-Aty, J. Park, and J. Zhu, "Effects of crash warning systems on rear-end crash avoidance behavior under fog conditions," *Transportation Research Part C: Emerging Technologies*, vol. 95, pp. 481–492, 2018.
- [19] Y. Wu, M. Abdel-Aty, O. Zheng, Q. Cai, and L. Yue, "Developing a crash warning system for the bike lane area at intersections with connected vehicle technology," *Transportation Research Record: Journal of the Transportation Research Board*, vol. 2673, no. 4, pp. 47–58, 2019.
- [20] C. Oh, S. Park, and S. G. Ritchie, "A method for identifying rear-end collision risks using inductive loop detectors," *Accident Analysis & Prevention*, vol. 38, no. 2, pp. 295–301, 2006.
- [21] L. Yue, M. Abdel-Aty, Y. Wu, J. Yuan, and M. Morris, "Influence of pedestrian-to-vehicle technology on drivers' response and safety benefits considering pre-crash conditions," *Transportation Research Part F: Traffic Psychology and Behaviour*, vol. 73, pp. 50–65, 2020.
- [22] R. Wu, X. Zheng, Y. Xu et al., "Modified driving safety field based on trajectory prediction model for pedestrian-vehicle collision," *Sustainability*, vol. 11, no. 22, p. 6254, 2019.
- [23] M. Fallah Zavareh, A. R. Mamdoohi, and T. Nordfjærn, "The effects of indicating rear-end collision risk via variable message signs on traffic behaviour," *Transportation Research Part F: Traffic Psychology and Behaviour*, vol. 46, pp. 524–536, 2017.
- [24] T. M. Ruff and T. P. Holden, "Preventing collisions involving surface mining equipment: a GPS-based approach," *Journal of Safety Research*, vol. 34, no. 2, pp. 175–181, 2003.
- [25] J. Wu, H. Xu, Y. Zhang, and R. Sun, "An improved vehicle-pedestrian near-crash identification method with a roadside LiDAR sensor," *Journal of Safety Research*, vol. 73, pp. 211–224, 2020.
- [26] P. Chen, W. Zeng, G. Yu, and Y. Wang, "Surrogate safety analysis of pedestrian-vehicle conflict at intersections using unmanned aerial vehicle videos," *Journal of Advanced Transportation*, vol. 2017, Article ID 5202150, 12 pages, 2017.
- [27] J. Li, B. Dai, X. Li, X. Xu, and D. Liu, "A dynamic Bayesian network for vehicle maneuver prediction in highway driving scenarios: framework and verification," *Electronics*, vol. 8, no. 1, p. 40, 2019.
- [28] H. Araki, K. Yamada, Y. Hiroshima, and T. Ito, "Development of rear-end collision avoidance system," in *Proceedings of the Conference on Intelligent Vehicles*, pp. 224–229, IEEE, Tokyo, Japan, 1996.
- [29] L. García Cuenca, E. Puertas, J. Fernandez Andrés, and N. Aliane, "Autonomous driving in roundabout maneuvers using reinforcement learning with Q-learning," *Electronics*, vol. 8, no. 12, p. 1536, 2019.
- [30] M. Jannat, S. M. Roldan, S. A. Balk, and K. Timpone, "Assessing potential safety benefits of advanced pedestrian technologies through a pedestrian technology test bed," *Journal of Intelligent Transportation Systems*, vol. 25, no. 2, pp. 1–18, 2020.



- [31] R. Layton and K. Dixon, *Stopping Sight Distance*, Kiewit Center for Infrastructure and Transportation, Oregon Department of Transportation, Clackamas, OR, USA, 2012.
- [32] M. M. Minderhoud and P. H. L. Bovy, "Extended time-to-collision measures for road traffic safety assessment," *Accident Analysis & Prevention*, vol. 33, no. 1, pp. 89–97, 2001.
- [33] Y. Zhang, E. K. Antonsson, and K. Grote, "A new threat assessment measure for collision avoidance systems," in *Proceedings of the 2006 IEEE Intelligent Transportation Systems Conference*, pp. 968–975, IEEE, Toronto, Canada, 2006.
- [34] H. Kim, X. Wu, J. L. Gabbard, and N. F. Polys, "Exploring head-up augmented reality interfaces for crash warning systems," in *Proceedings of the 5th International Conference on Automotive User Interfaces and Interactive Vehicular Applications*, pp. 224–227, Eindhoven, Netherlands, 2013.
- [35] J. A. Hanley and B. J. Mcneil, "The meaning and use of the area under a receiver operating characteristic (ROC) curve," *Radiology*, vol. 143, no. 1, pp. 29–36, 1982.
- [36] R. A. Shaikh and V. Thayananthan, "Risk-based decision methods for vehicular networks," *Electronics*, vol. 8, no. 6, p. 627, 2019.
- [37] C. Wang, L. Ma, R. Li, T. S. Durrani, and H. Zhang, "Exploring trajectory prediction through machine learning methods," *IEEE Access*, vol. 7, pp. 101441–101452, 2019.
- [38] Z. Cheng, Y. Li, and B. Wu, "Early warning method and model of inland ship collision risk based on coordinated collision-avoidance actions," *Journal of Advanced Transportation*, vol. 2020, Article ID 5271794, 14 pages, 2020.
- [39] J. Raj, K. Raghuwaiya, and J. Vanualilai, "Collision avoidance of 3D rectangular planes by multiple cooperating autonomous agents," *Journal of Advanced Transportation*, vol. 2020, Article ID 4723687, 13 pages, 2020.
- [40] J. Li, H. Wang, W. Zhao, and Y. Xue, "Ship's trajectory planning based on improved multiobjective algorithm for collision avoidance," *Journal of Advanced Transportation*, vol. 2019, Article ID 4068783, 12 pages, 2019.

## Research Article

# Exploring the Potential of Using Privately-Owned, Self-Driving Autonomous Vehicles for Evacuation Assistance

Thomas Shirley <sup>1</sup>, Bhavya Padmanabha <sup>2</sup>, Pamela Murray-Tuite <sup>1</sup>, Nathan Huynh <sup>2</sup>,  
Gurcan Comert <sup>3</sup> and Jiayun Shen <sup>1</sup>

<sup>1</sup>Department of Civil Engineering, Clemson University, Clemson, SC 29634, USA

<sup>2</sup>Department of Civil and Environmental Engineering, University of South Carolina, Columbia, SC 29208, USA

<sup>3</sup>Department of Computer Science, Physics, and Engineering, Benedict College, Columbia, SC 29204, USA

Correspondence should be addressed to Pamela Murray-Tuite; pmmurra@clemson.edu

Received 6 May 2021; Revised 23 August 2021; Accepted 30 August 2021; Published 25 September 2021

Academic Editor: Peter Chen

Copyright © 2021 Thomas Shirley et al. This is an open access article distributed under the Creative Commons Attribution License, which permits unrestricted use, distribution, and reproduction in any medium, provided the original work is properly cited.

The potential use of privately-owned autonomous vehicles (AVs) for the evacuation of carless households threatened by hurricanes is underexplored. Based on 518 original survey responses from South Carolina (SC) residents, an ordered logistic model was developed to determine the willingness of individuals to temporarily share their AVs for evacuation without their presence. The model results indicated that respondents who (a) were unemployed, (b) had experience giving disaster relief assistance, (c) took regular religious trips and were more comfortable with AVs (d) delivering packages and (e) being purchased and shared for income in the next five years were more willing to share for evacuation. Respondents who (a) were aged 65 or older, (b) had income below per year, and (c) had less than two social media accounts were less willing to share. The model was applied to a state-wide synthetic population to simulate a disaster scenario in SC under different AV market penetration ( $p$ ) scenarios to determine the potential use of AVs for evacuation assistance. Monte Carlo simulation results indicated that the percentage of households that can be evacuated increased linearly with respect to  $p$ , by 5.5% for every 1% increase in  $p$  until  $p$  was nearly 20%. When  $p$  was 30% or higher, the number of shared AVs was sufficient to evacuate all households in need. Therefore, in SC, if privately-owned AVs are widely available, they could serve as a viable alternative or be used to supplement the traditional evacuation programs that rely on buses.

## 1. Introduction

In recent years, the southeastern U.S. has experienced strong hurricanes, from Hurricane Joaquin creating historic flood levels in Columbia, South Carolina in 2015 [1] to Hurricane Irma causing mass evacuations and hundreds of deaths [2] and Hurricane Florence causing record-setting flooding in the Carolinas [3]. The intensity and frequency of these storms are expected to increase [4]. The coastal population in the southeast is growing faster than any other region in the U.S. [5], indicating the potential for greater destruction from future storms. Combined with millennials having less desire to obtain a driver's license and own a vehicle, these factors point to the greater need for government-assisted evacuations in the future [6]. This study explores a potential future

government-assisted evacuation transportation system that relies on privately-owned, self-driving autonomous vehicles.

Hurricane Katrina (2005) highlighted deficiencies in the evacuation plans for vulnerable populations, including the carless [7]. Since then, the topic of evacuating the vulnerable population, specifically the carless, elderly, and special needs population, has grown in interest [8, 9]. Evacuation plans have evolved to address these segments of the population.

Currently, government-assisted evacuations for the carless and vulnerable populations typically rely on buses, which have high capacities to meet the potential demand for assistance. Across the country, transportation and emergency management agencies estimate an average of 6–10% of their population is classified as special needs and could use some form of assistance when ordered to evacuate for a

hurricane [10]. Those who could need assistance because of a lack of a readily-available vehicle represent approximately 8.7% of U.S. households, with this number expected to grow in the near future [11, 12]. South Carolina (SC) estimates that 5% of its population, or 49,000 residents, within evacuation zones would need assistance evacuating for a strengthening, category 5 storm. Currently, the State's plan primarily involves transporting these evacuees by school buses to local shelters [13].

Transit is not the only option available to households lacking a reliable personal vehicle. Carpooling with peers is one alternative. In a study of Hurricane Lili evacuees, Lindell et al. [14] found that 9% obtained rides from family or friends. Based on a study using surveys from New York City, the largest transit commuting city in the U.S., researchers found a near-even split in carpooling (8% and 14%) and transit evacuation (12% and 16%) [15].

Other forms of shared vehicles for evacuation assistance have been considered recently. In the past five years, Uber and Lyft have helped people evacuate by offering ride vouchers [16]. In 2020, Florida's Emergency Management Agency mentioned the use of Uber and Lyft to transport evacuees instead of mass transportation to minimize the spread of COVID-19 [17].

The potential future system envisioned in this paper goes beyond currently deployed technologies and is based on privately-owned autonomous vehicles (AVs). Upon a government official's announcement of receiving an official request for assistance from the public, some AV owners from around the state (or other geographic areas) would voluntarily and temporarily allow their vehicles to be used to assist with preimpact evacuation in designated evacuation zones, regardless of whether they would share their AVs for normal conditions. Thus, our use of the term "shared" (focusing on a temporary arrangement without the owner present) is slightly different from the mainstream interpretation of shared vehicles. The objective of this study is to explore the system's feasibility of using privately-owned AVs as a viable alternative or as a supplement to the traditional evacuation programs that rely on buses from the public's willingness to share perspective (for this potential AV ownership future) and an evacuee demand coverage perspective for a hurricane in SC. To this end, this paper presents an ordinal logit model developed from original survey responses from SC residents to (1) determine the public's willingness to let state and/or federal agencies use their AVs to assist others in evacuations and (2) identify factors that affect their willingness. The model is then applied to a synthetic SC population and used with simulation to determine what percentage of the critical transportation need (CTN) population can be evacuated, incorporating both the predicted level of the public's willingness to share their AVs and different AV market penetration levels.

The remainder of this paper is divided into six sections. Section 2 reviews selected research on assisting carless evacuees and future AV adoption projections. Section 3 provides an overview of the survey data used to develop the ordinal logit model. Section 4 describes the ordinal logit modeling process, synthetic household generation, and

simulation modeling background. Section 5 is the experimental design section, describing the factors tested during the simulation process. Section 6 discusses the results of the modeling process and experiments, including factors affecting willingness to share and the percentage of the CTN population that could be evacuated at different AV market penetration levels. Section 7 presents conclusions and future directions.

## 2. Literature Review

Many studies investigated the use of public transit vehicles and school buses to assist with mass evacuation. For example, Bish [18] developed an optimization model for regional evacuation planning as a variant of the vehicle routing problem. He assumed that the evacuees arrived at predetermined pickup locations at constant rates. Swamy et al. [19] implemented a simulation model which considered the dispatching of a given number of buses, stochastic arrivals of evacuees, queueing effects, and transport of evacuees to shelters. Naghawi and Wolshon [20] modeled and simulated transit-based evacuation strategies for the evacuation of the CTN population.

However, Renne et al. [7] stated that most cities do not have a sufficient number of buses to evacuate the entire CTN population. Moreover, buses cannot provide door-to-door services, which is an important consideration for those who cannot afford a ride to the pickup point. For these reasons, the recent work on mass evacuation of the CTN population has considered the use of ridesharing. Wong et al. [16] concluded that public agencies could leverage shared resources to assist with evacuation. Their study, which used survey responses from recent Hurricane Irma evacuees on a hypothetical future disaster, reported that 29.1% of evacuees would be willing to offer a ride to another evacuee before the evacuation process and 23.6% would be willing to offer a ride during the evacuation process. Li et al. [21] studied the utilization of shared vehicles for emergency evacuation under no-notice evacuation scenarios with limited time horizons. They performed numerical simulations to quantify the improvements in the total distance traveled and number of people evacuated. Naoum-Sawaya and Yu [22] addressed a problem in which individuals with vehicles are instructed to pick up others along their routes to evacuate the maximum number of individuals within a limited time. A mixed integer programming model was proposed to model the problem. Lu et al. [23] proposed a two-phase model that optimized trip planning and operations by integrating ridesharing processes for short-notice evacuation situations. Their model jointly optimized the driver-rider matching and transfer connections among shared vehicle trips. These studies assumed the active participation of the vehicle's driver/owner who was in the same area as the individuals needing assistance.

Many researchers consider AVs to be the next revolution in transportation. Bansal and Kockelman projected anywhere from 25% to 87% adoption of level 4 AVs, the lowest level AV able to drive without a human, by 2045 [24]. Another study projected that AVs would account for 20%–40% of the entire

vehicle fleet by the 2040s [25]. Yet another study projected anywhere from 15–90% adoption of AVs by 2050, depending on annual price reductions [26]. The most prominent cause for the slower adoption of AVs was considered to be the high cost [27]. The adoption increase with cost reduction was thoroughly discussed in [24]. AV adoption from a technology trust and ethics perspective was discussed in [28]. According to the study, human-machine interaction/integration needs significant investment to be able to achieve full trust in autonomous vehicles. Incidents in AVs or in other co-piloting systems indicated that sensor failures could lead to catastrophic events. However, there are additional factors to consider, such as increased risks in the case of incidents, complex nonuniform surroundings with ever-changing user behaviors, cyber vulnerabilities, and higher road construction costs [27, 29].

AV ownership was investigated by several researchers. AVs are expected to be expensive, and in the most optimistic scenario, only 35% of the survey respondents were willing to use shared AVs, while others prefer personal ownership [30, 31]. This is partly understandable, given the convenience of accessibility and being able to leave items in the vehicle. However, shared vehicles are predicted to be maintained better, to have higher security and to have less liability [27]. Regardless, Robinette et al. [31] showed that AV technology would reduce ownership by 1.1 vehicle but would result in a 13% increase in vehicle miles traveled (VMT) as unoccupied vehicles. This would also result as an increase in transportation energy usage and cause higher emissions. In [32], the authors discussed possible consequences of AV introduction with driving behavior and ownership changes. With personal AVs, the authors argued longer as well as unoccupied trips could be preferred by the owners. The authors also argued shared AVs can drive overall lower cost for vehicles. Redistribution of vehicles would also increase the number of trips per day. Many studies projected that AVs will be shared when implemented, similar to Uber and Lyft today [25, 33, 34]. These shared AVs could provide a transportation option that is significantly less expensive than taxi services and is convenient for citizens in urban areas [35]. However, to date, few studies have examined the potential use of self-driving AVs shared by the public to assist with mass evacuation and/or the potential of integrating shared-AVs into evacuation assistance systems.

AVs are expected to be widely adopted in the next 20–30 years indicating a need to examine their potential uses for evacuation. Though recent advances in technology point toward adoption in the near future, relatively little has been studied regarding their potential use in evacuation situations. However, for connected vehicles (CVs), Yin et al. designed an application that helps vulnerable households evacuate by providing pickup time and location options, optimizing route guidance to reduce congestion, and locating food and fuel along their route [36]. Our study explores the use of temporarily shared AVs to assist SC CTN households evacuate from a hurricane. The integration of shared AVs could aid in the service gap (e.g., door-to-door service) that public transit vehicles do not provide. Without the limitation of only picking up evacuees from a few

selected pickup points, shared AVs could provide more personalized pickups for the vulnerable population that has challenges reaching those pickup points.

This study addresses gaps in extant knowledge. First, it builds on the limited body of work addressing the potential use of AVs for evacuation by considering self-driving AVs rather than vehicles shared by driver-owners. This requires an examination of willingness to share a personally-owned vehicle without being physically present. Second, the potential of a self-driving AV assistance program to replace a bus-based system is examined, addressing issues associated with insufficient resources and last-mile issues as well as the established preference for using personal vehicles to evacuate rather than transit-based options (see for example [37]).

### 3. Survey Data Overview

To gauge the public's willingness to share their future, driverless AVs to help evacuate an area before a hurricane makes landfall, the research team developed a survey; the survey questions were formed and guided by three focus group sessions. This survey was implemented using Qualtrics Panels and distributed to SC residents across the state. A total of 1,050 responses were received, split evenly between two scenarios: evacuation (used in this manuscript) and disaster relief. The age and gender splits of the respondents were representative of SC demographics, according to the American Community Survey (ACS) [38]. However, the sample had an intentionally slightly higher number of individuals with income above the median and higher number of individuals with education above a high school degree. This slight oversampling was performed to adequately capture demographic categories more likely to be able to afford future AVs [25, 34, 39]. After data cleaning, the final dataset used for the ordered logit model had 518 responses.

The survey placed respondents in a scenario where they considered temporarily sharing a personally-owned, driverless AV for use in an evacuation, where their local area was not affected. The Likert-type question of how willing (extremely willing (15%), willing (21%), somewhat willing (23%), neither willing nor unwilling (10%), somewhat unwilling (7%), unwilling (10%), and extremely unwilling (14%)) respondents were to share in this context was used as the dependent variable in an ordinal logit model. The extremely willing/willing and extremely unwilling/unwilling categories were combined to condense the data to five ordered categories. However, this does not affect any ordered categories not involved in the category combination [40]. To determine factors associated with greater willingness to share, the survey also asked respondents about existing travel habits, current vehicle technology, general technology adoption, experience with the sharing economy, experience giving and volunteering, experience with natural disasters, comfort with autonomous vehicles, and demographic characteristics. Table 1 provides summary statistics of selected variables and the single-variable ordered logit models between the variable and willingness to share a personal vehicle for evacuation assistance.

TABLE 1: Summary statistics of selected variables and relationship with evacuation sharing variable

Variable	Total $n$	Min	Max	Mean	S. dev	Parameters	S. err
Dependent variable							
Willingness to share AV for evacuation	518	1	5	3.409	1.603	—	—
Independent variables							
Demographics							
Gender: womenfemale	518	0	1	0.494	0.500	0.038	0.158
High income (> \$100,000 per year)	518	0	1	0.288	0.453	-0.120	0.175
Household size	512	1	5	2.740	1.207	0.010	0.066
Educated with a 4-year degree or more	518	0	1	0.508	0.500	0.008	0.158
Age 65 or older	518	0	1	0.168	0.374	-0.754***	0.213
Income under \$15,000 per year	518	0	1	0.077	0.267	-0.504*	0.296
Unemployed	518	0	1	0.071	0.258	0.646**	0.320
Race: white/caucasian	518	0	1	0.689	0.463	0.011	0.171
Living in urban area	518	0	1	0.110	0.313	0.202	0.255
Technology							
Use of ride-hailing services 8+ times in past year	518	0	1	0.168	0.374	0.671**	0.219
0 or 1 social media accounts	518	0	1	0.214	0.411	-0.886***	0.195
High comfort in AV deliveries in 5 years	518	0	1	0.514	0.500	0.993***	0.163
High comfort in sharing AV for income in 5 years	518	0	1	0.108	0.311	1.144***	0.280
High number of technology features on newest vehicle	501	0	1	0.158	0.365	-0.279	0.220
Evacuation experience							
Household evacuation experience	518	0	1	0.322	0.468	0.105	0.170
Experience evacuating with friends/family	167	0	1	0.144	0.352	1.925***	0.498
Received evacuation assistance from friends/family	167	0	1	0.329	0.471	1.346***	0.321
Giving and volunteering							
Giving to charitable causes more than once per year	518	0	1	0.635	0.482	0.382**	0.165
Volunteering more than once per year	518	0	1	0.508	0.500	0.527**	0.160
Experience giving any disaster relief assistance	518	0	1	0.629	0.483	1.070***	0.168
Experience giving to assist friends/family in disaster relief efforts	518	0	1	0.259	0.438	0.514**	0.184
Takes religious trips during a typical week	518	0	1	0.334	0.472	0.458**	0.170
Commuting							
Commuting by single-occupancy vehicle	335	0	1	0.833	0.374	-0.281	0.267
Commute length	324	10	60	23.386	13.825	-0.005	0.007
Regular weekly commute schedule	335	0	1	0.684	0.466	-0.126	0.213

Note: \*\*\*  $p < 0.001$ , \*\*  $p < 0.05$ , and \*  $p < 0.1$ .

## 4. Methodology

The methodology consisted of two major components: estimating the availability of AVs to transport evacuees from SC coastal evacuation zones and determining the degree to which these AVs met the anticipated evacuee demand.

*4.1. Estimating AV Availability.* Estimating the AV availability involved two steps. First, an ordered logit model was developed from the survey data. Second, this model was applied to a synthetic population generated based on Census data. The dependent variable for this model was a five-point Likert-type question asking respondents to rate their willingness to share a personally-owned AV to help others evacuate from a hurricane. Ordered logit models containing multiple explanatory variables can be written as in the following equation:

$$\ln(\pi_j) = \alpha_j - (\beta_1 x_1 + \beta_2 x_2 + \dots + \beta_n x_n), \quad (1)$$

where  $x_1, x_2, \dots, x_n$  are the explanatory variables,  $\pi_j = p(\text{score} \leq j) / p(\text{score} > j)$ ,  $\alpha_j$  is the intercept of the logit

$j$ , and  $\beta_1, \beta_2, \dots, \beta_n$  are the regression coefficients of each explanatory variable [41]. The ordered logit model's proportional odds assumption was tested using the Parallel Line Test, which ensured that the slope coefficients were the same across all categories [42, 43]. The model was created using a manual forward stepwise process [44] with the variables' entering order based on the  $p$ -values arising from ordered logit models developed using each variable individually (see Table 1). Improvement to the model was determined by an increase in the McFadden Pseudo R-Square value as well as a 95% confidence level that the parameter estimates were significantly different from zero. This process was repeated until reaching the individual variable significance level of 0.25, as recommended for large sample sizes [45].

The ordered logit model (see Table 2) was then applied to a synthetic population of SC to obtain a spatially distributed number of AVs available for evacuation assistance. The population synthesis process expands a seed population sample to match the marginal distribution desired characteristics of the control. In this study, the seed population was obtained from the 2018 Public Use Microdata Sample (PUMS) [46] and the regional control was set to the number



TABLE 2: Ordinal logit regression model.

	Parameter estimate	Standard error	Significance
Age 65 or older	-0.531	0.228	0.020
Income under \$15,000 per year	-0.728	0.333	0.029
Unemployed	1.219	0.357	0.001
Takes religious trips during a typical week	0.374	0.178	0.035
0 or 1 social media accounts	-0.540	0.213	0.011
High comfort in AV deliveries in 5 years	0.747	0.172	0.000
High comfort in sharing AV for income in 5 years	0.604	0.296	0.042
Experience giving any disaster relief assistance	0.886	0.180	0.000
Number of responses		518	
McFadden Pseudo R-Square		0.072	
Adjusted McFadden Pseudo R-Square		0.067	
Parallel line test (0.549)		Pass	
Number of variables		8	

of people in each subcounty using ACS 2018. The PUMS data was contained in the Public Use Microdata Areas (PUMA), which are geographic units containing no fewer than 100,000 people each. The desired spatial resolution for this study was the subcounty area, which was smaller than the PUMA. The PopulationSim package in the Python environment bridged the gap between the two geographic levels and produced the synthetic population at the subcounty level [47]. The resulting synthetic population had 1,894,711 households which was the exact number from the 5-year estimates of households from 2014–2018 ACS data. Demographic variables age, income, and employment status, statistically significant in the ordered logit model, were also generated for each household during the population synthesis process. These variables were then recoded into binary indicator variables for model application. Other non-demographic variables needed for the model were generated using the observed distribution from the survey (see Table 1). Based on equation (1), the probability of each outcome was calculated using the following equation [40]:

$$p(\text{score} = j) = \pi_j - \pi_{j-1}. \quad (2)$$

*4.2. Estimating the Ability to Meet Evacuation Assistance Demand.* To determine how many critical transportation need households (CTNH) could be evacuated from the evacuation zones using AVs shared by the public, a Monte Carlo simulation model was developed. The simulation model required the following input data: percentage of SC citizens willing to share their AVs to assist with evacuation (output from the ordered logit model using a synthetic SC population), percentage of AV market penetration (see Table 3), total population in an evacuation zone [48], total population in a nonevacuation zone [49], percentage of the CTN population that needed to be evacuated [50], distribution of time for which an AV would be available (survey data from this study), average speed of AVs during evacuation [51], shelter locations [50], average number of people per household [52], a GIS map of SC at the subcounty level [53], and a GIS map of evacuation zones [48].

The model's primary output was the covered demand ratio (CDR), which was obtained by dividing the number of

TABLE 3: Covered demand ratio for different scenarios.

Year	Scenario 1*		Scenario 3*		Scenario 6*		Scenario 8*	
	$p$	CDR	$p$	CDR	$p$	CDR	$p$	CDR
2025	11.1	0.575	5.2	0.290	15.1	0.694	19.4	0.875
2030	19.7	0.891	10.3	0.540	27.2	0.999	33.8	1
2035	28.6	0.999	15	0.752	38.3	1	44.2	1
2040	37	1	19.2	0.888	45.7	1	74.7	1

\*as numbered in [24];  $p$  = % market penetration rate.

CTNH evacuated from the evacuation zones using AVs by the total number of CTNH. Figure 1 presents the logic implemented in the Monte Carlo simulation model which was implemented with the following assumptions:

- (1) AVs were only available in the nonevacuation region.
- (2) One household had only one AV.
- (3) One AV evacuated one CTNH in a single trip.
- (4) All AVs available in a subcounty started and ended their trips at the centroid of that subcounty.
- (5) All evacuees in an evacuation zone were picked up at the centroid of that evacuation zone.

As shown in Figure 1, in Step 1, the model read the input data mentioned above. Among the input data were the CTNH that need to be evacuated from an evacuation zone (shown in gray in Figure 2) and brought to a shelter located in the nonevacuation zone (shown in white in Figure 2). In this study, the evacuation zones considered were those defined by the South Carolina Emergency Management Division based on their vulnerability to hurricanes. In all, there were 20 zones in the evacuation region. Instead of using the exact home address of the CTNH as the pickup location, without loss of generality, this study used the centroid of the zone as the pickup location. The start and end location of each AV were also assumed to be at the centroid of the nonevacuation zone. The spatial scale chosen for the nonevacuation zone was the census county division level, referred to as "subcounties" hereafter. This was chosen to be consistent with the spatial scale used by the logit model. Subcounties consist of incorporated cities, boroughs, and towns. Geographically, a subcounty is larger than a census



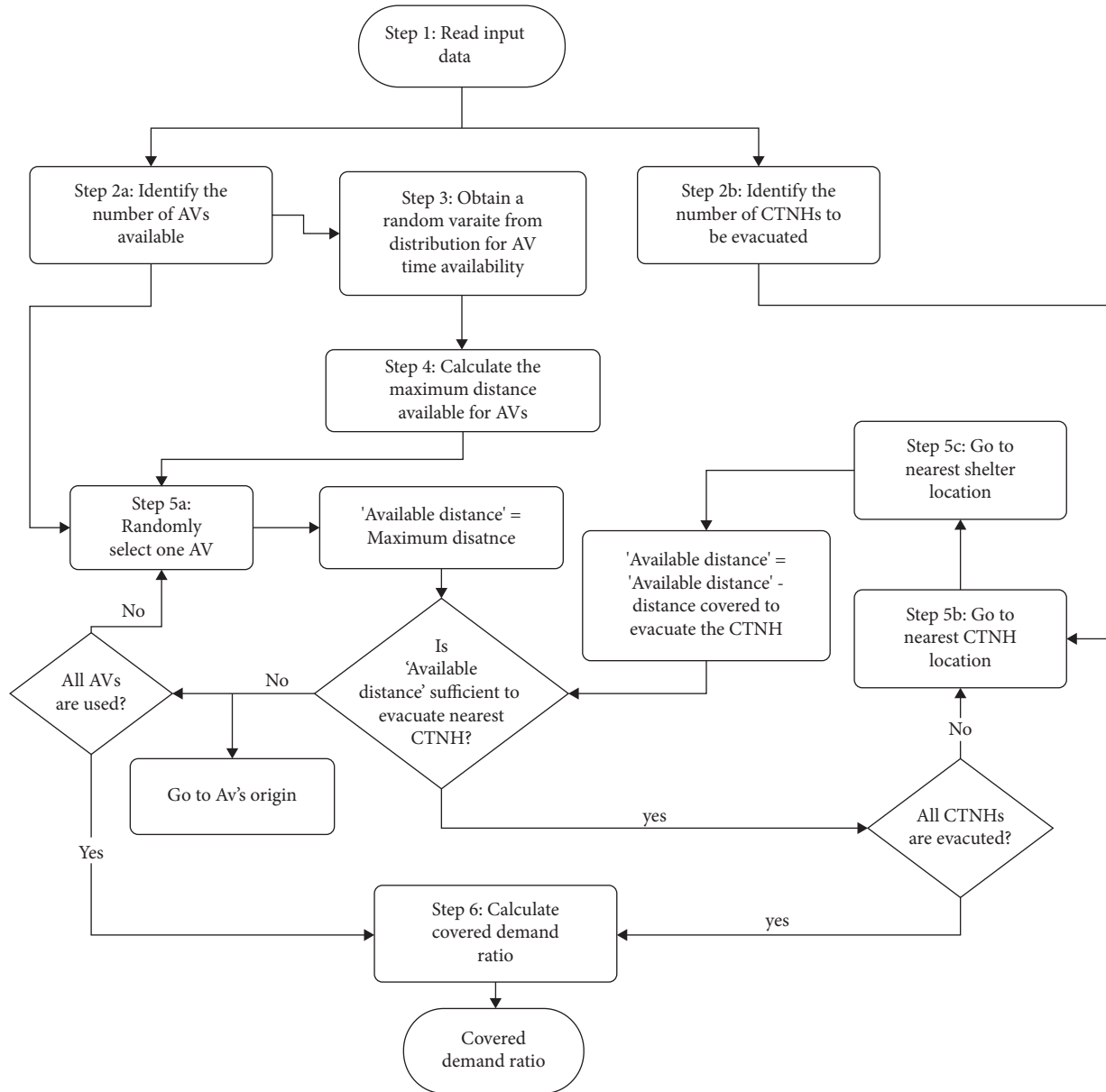


FIGURE 1: Logic of the Monte Carlo simulation model.

block but smaller than a county. In all, there were 265 zones in the nonevacuation region. The shelter locations were actual locations, not centroids of nonevacuation zones. In Step 2, the model calculated the number of AVs available in the nonevacuation region and the number of CTNH in the evacuation region requiring assistance. The number of AVs available in each subcounty was calculated using equation (3). The sum of this number for all subcounties in the nonevacuation region gave the total number of AVs available in SC for evacuation. The number of CTNH in each evacuation zone was calculated using equation (4). The sum of this number for all evacuation zones gave the total number of CTNH:

$$n = \left(\frac{p}{100}\right) \times \left(\frac{s}{100}\right) \times h, \quad (3)$$

where  $n$  = number of AVs available in a subcounty,  $p$  = percentage of AV market penetration,  $s$  = percentage of households willing to share their AVs for emergency evacuation, and  $h$  = number of households in a subcounty:

$$np = \left(\frac{pp}{hs}\right) \times \left(\frac{pc}{100}\right), \quad (4)$$

where  $np$  = number of CTNH in an evacuation zone,  $pp$  = total population in an evacuation zone,  $hs$  = average persons per household of the evacuation zone, and  $pc$  = percentage of CTN.

In Step 3, the time (i.e., duration) for which each AV was available was obtained from a discrete distribution; this distribution was generated from survey response data (see Figure 3). In Step 4, given the AV time availability, the

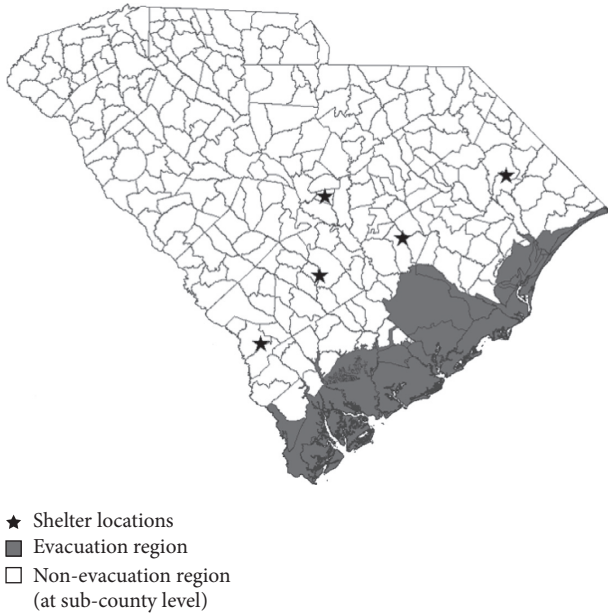


FIGURE 2: South Carolina evacuation region map layers' source [48, 53].

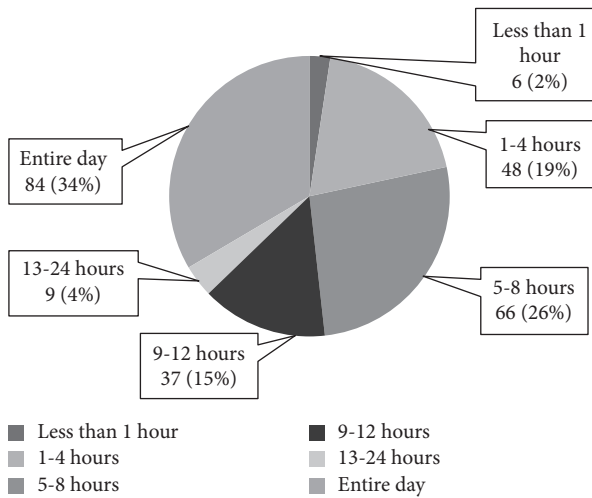


FIGURE 3: Discrete distribution of AV time availability ( $n = 250$ ).

maximum distance (in miles) for which an AV was available was calculated using the following equation:

$$d = t \times v. \tag{5}$$

In Step 5, an AV was randomly selected from the pool of available AVs. Available distance for the selected AV was the maximum distance calculated using equation (5). If the available distance was sufficient to evacuate the nearest CTNH, then the model simulated the AV going to the nearest CTNH and dropping the CTNH off at the nearest shelter. When the AV was at the shelter location, the model determined if the AV's remaining available distance was sufficient to evacuate another nearest CTNH. If not, it returned to its owner at its original location. If sufficient time/distance remained, the AV was assigned to the next nearest CTNH and dropped that CTNH off at the nearest

shelter. This process for the selected AV was repeated until its time/distance availability was exhausted. The model then selected another AV and repeated this process until either all CTNH were evacuated or no more AVs were available. In Step 6, the CDR was calculated using the following equation:

$$CDR = \frac{\text{Number of CTNH evacuated}}{\text{Total number of CTNH}}. \tag{6}$$

### 5. Simulation Scenarios

To determine what percentage of the CTNH could be evacuated (i.e., CDR) at the predicted public's willingness to share their AVs to assist with the evacuation, the developed Monte Carlo simulation was used. The model was run for four AV market penetration scenarios obtained from Bansal and Kockelman [24]. The AV market penetration for future years under each scenario is shown with the results in Table 3. Scenario 3 represented the most conservative estimate of AV market penetration whereas Scenario 8 represented the most optimistic. These scenarios were based on the projected annual increase in the willingness to pay (WTP), annual drops in technology price, and changes in government regulations. Scenario 1 was with constant WTP, 10% drop in the technology price, and no regulations. Scenario 3 was with 0% but no-zero WTP, 10% drop in the technology price, and no regulations; in this scenario, the tenth percentile WTP (among nonzero WTP individuals) for the individual's household-demographic cohort was used. Scenario 6 was with 5% annual increase in WTP, 10% drop in the technology price, and with regulations. Scenario 8 was with 10% annual increase in WTP, 10% drop in the technology price, and with regulations [24].

The experiments assumed a category 5 hurricane. As such, the percentage of CTN used was 5% based on findings from the State of South Carolina CTN Evacuation Operations Plan [13]. The SC population was assumed to be 5.1 million, and the number of occupied homes was assumed to be 2.3 million based on the most recent Census data [54]. The time for which an AV was available was randomly drawn from the developed discrete distribution shown in Figure 3. It was assumed that 70% of the evacuees evacuated during the day and 30% evacuated during the night [55]. The average speed for the AV during evacuation was assumed to be 20 mi/hr during the day and 40 mi/hr during the night based on archived speeds along SC highways during the past six hurricanes [50].

### 6. Results and Discussion

6.1. *Ordered Logit Model Results.* The final ordered logit model contained 518 observations and had an adjusted McFadden Pseudo R-Square of 0.067, within the 0.012 to 0.138 range found in previous studies [56]. In this model, negative coefficients signified a lower willingness to share [40]. The model shown in Table 2 had eight statistically significant variables with age 65 or older, income under \$15,000 per year, and 0 or 1 social media accounts being negatively associated with willingness to share, meaning that

individuals with these characteristics were less likely to share their AVs to assist with evacuation. Being unemployed, taking regular religious trips, having high comfort in AV deliveries in five years, having high comfort in sharing an AV for income in 5 years, and having any experience giving for disaster relief were positively associated with willingness to share.

The model in Table 2 was then applied to the synthetic population. The probability of selecting a 5, which represented the maximum willingness to share an AV, was recorded for each household in SC. This probability was then aggregated based on each subcounty. The overall probability of selecting a 5 for all subcounties had a mean of 32.02% and standard deviation of 0.6%.

**6.2. Simulation Modeling Results.** The results of the simulation experiments, averaged over 15 runs, are shown in Table 3. At the projected AV penetration level in 2025, 29% (scenario 3) to 87.5% (scenario 8) of the CTNH could be evacuated. By 2040, 88.8% could be evacuated in the most pessimistic scenario and 100% in the most optimistic scenario. It should be noted that these projections were done in 2017 [24]. At the present time, year 2020, it is clear that the deployment of level 4 AVs is still many years away from becoming a reality.

Figure 4 shows the relationship between the covered demand ratio (CDR) and AV market penetration ( $p$ ). These results indicated that the CDR increased linearly with respect to AV market penetration, up to about 20%, beyond which the relationship resembled a concave function. For scenarios 1, 3, and 8, CDR was approximately 0.9 at 20% AV market penetration. That meant 90% of the CNTH could be evacuated if the AV market penetration was 20%. For scenario 6, at 20% market penetration, approximately 85% of the CNTH could be evacuated. At 30% AV market penetration and beyond, the number of shared AVs was sufficient to evacuate all the required CTNH. These results were in agreement with the Pareto principle [57]: 80% of CTNH could be evacuated with 20% AV market penetration.

Figure 5 provides four alternative models that could be used to determine what market penetration level would be needed to be able to cover a certain evacuation demand: polynomial, logistic, exponential, and hyperbolic tangent. Based on the root mean squared errors (RMSE), the logistic and polynomial regression models performed equally well and were superior to the exponential and hyperbolic tangent. The logistic regression model had a more complex form compared to the polynomial model, but its advantage was that it could be used for any  $0 \leq p \leq 100\%$ . The polynomial regression model can only be used when  $p \leq 28\%$ . The logistic regression model can be used to derive important insight. Specifically, for each additional 1% increase in AV market penetration, there was a 5.5% increase in CDR. The CDR increased linearly with respect to AV market penetration up to about 20%. Beyond 20%, AV market penetration had less effect on the covered demand ratio:

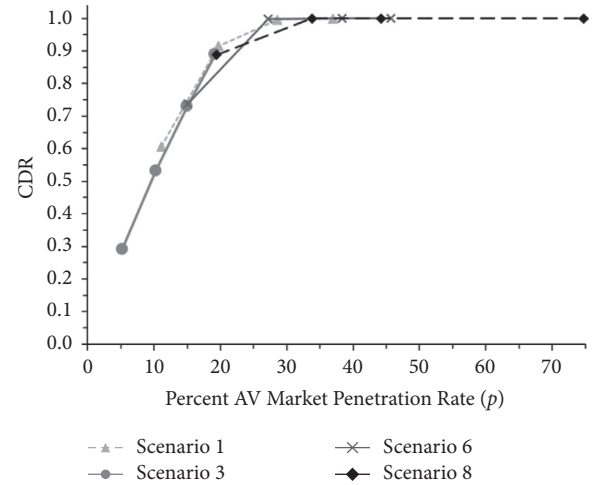


FIGURE 4: Effect of AV market penetration on CDR.

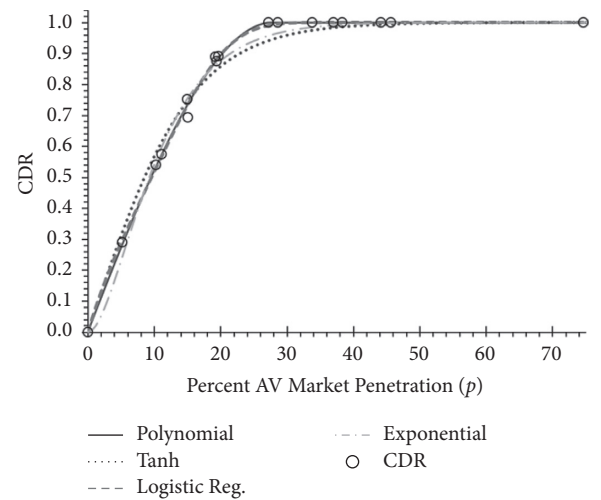


FIGURE 5: AV market penetration versus CDR models.

$$\text{CDR} = \begin{cases} -19.89p^3 - 1.59p^2 + 5.58p, & p \leq 28\% \\ 1.0, & \text{o.w.} \end{cases} \quad (7)$$

A 3<sup>rd</sup> order polynomial model was given in equation (7) which was able to express the CDR within 1.2% RMSE.

$$\text{CDR} = \frac{e^{6.43p} - e^{-6.43p}}{e^{6.43p} + e^{-6.43p}}, \quad 0 \leq p \leq 100\%. \quad (8)$$

The hyperbolic tangent (tanh) model in equation (8) can estimate CDR within 3.2% RMSE.

$$\text{CDR} = 1 - \frac{9.96}{1 + 4.33^{0.73+0.08p-0.00234p^2+0.00021p^3}}, \quad 0 \leq p \leq 100\%. \quad (9)$$

The logistic regression model in equation (9) can estimate CDR within 1.2% RMSE.

$$\text{CDR} = 1 - e^{-18.01p} - 18.01pe^{-18.01p}, \quad 0 \leq p \leq 100\%. \quad (10)$$

The exponential model in equation (10) can estimate CDR within 2.6% RMSE.

## 7. Conclusions

This manuscript explored voluntarily, temporarily shared, privately-owned, and driverless autonomous vehicles for assistance with hurricane evacuations. Using original survey data from South Carolina residents, an ordered logit model was developed to determine the willingness to share privately-owned autonomous vehicles and factors affecting this willingness to share. The model's significant variables indicated that respondents aged 65 or older, respondents with income under \$15,000 per year, and respondents with 0 or 1 social media accounts were less likely to share their AVs to assist with evacuation. On the contrary, being unemployed, taking regular religious trips, having high comfort in AV deliveries in five years, having high comfort in sharing an AV for income in five years, and having any experience giving for disaster relief were positively associated with willingness to share.

When the ordered logit model was applied to the synthetic SC population, approximately 32% of households were willing to share their AVs to assist with hurricane evacuation. Based on this estimate, a Monte Carlo simulation model was used to determine the ability of the AV sharing system to meet CTNH needs for evacuations. When the AV market penetration was 30% or higher, the model indicated that the number of shared AVs would be sufficient to evacuate all households in need, given the potential AV ownership future examined in this study.

This study suggests that such a future evacuation assistance system has the potential to be successful, although many details will have to be considered in the future and initial trials would have to be run in conjunction with current methods of transporting vulnerable populations. It is important to note the potential limitations on the use of this paper's results. First, AVs are not widely owned yet, necessitating that the survey be stated preference for a novel topic; thus, there was the potential for overenthusiasm in volunteering to share personally owned, driverless AVs as well as possible complications in fully understanding the survey topics. Second, multiple possible AV ownership futures exist, some of which include a shift from personally owned vehicles to subscription service, which would impact the availability of AVs for evacuation assistance. To manage the length of the paper, this study addressed only one potential future here, but future efforts will explore the subscription service as well with the public's tolerance for service delays. Third, current populations and demographics were used, which may or may not conform with those corresponding to the future AV market penetration rates. Fourth, the details of how evacuation travel assistance could be requested were not part of this study; this would have to be determined in the next step of more rigorously identifying the demand side of the issue and the matching of demand with the available supply. Fifth, the evacuation speeds were assumed to be 20 mi/hr during the day and 40 mi/hr during the night. Sixth, it was assumed that one AV can evacuate an

entire household. Seventh, for simplicity, the centroid of the evacuation zone was assumed to be the CTNH pickup location, and the centroid of the nonevacuation zone was assumed to be the starting and ending locations of AVs.

In addition to those mentioned above, a number of research areas could be pursued in the future. First, the survey could be applied to other states or hurricane-prone counties to determine the feasibility of this type of the system in other disaster-prone areas. Also, future surveys of this type could delve into potential limitations on sharing such as compensation desires as well as comfort levels of those potentially needing this evacuation assistance. Future studies could also examine different potential AV ownership scenarios and incorporate the system into larger evacuation simulations.

## Data Availability

The survey data used to support the findings of this study are available from the corresponding author upon request. The data used in the simulation are available from both the corresponding author and C2M2.

## Disclosure

The authors are solely responsible for the content of this paper.

## Conflicts of Interest

The authors declare that there are no conflicts of interest regarding the publication of this paper.

## Acknowledgments

The authors are grateful for the support from C2M2. This study was based upon a project funded by the US Department of Transportation (USDOT) Center for Connected Multimodal Mobility (C2M2) (Tier 1 University Transportation Center) headquartered at Clemson University, Clemson, South Carolina, USA, Grant 69A3551747117.

## References

- [1] J. Murphy, *The Historic South Carolina Floods of October 1–5, 2015*, US Department of Commerce, National Oceanic and Atmospheric Administration, National Weather Service, Silver Spring, MD, USA, 2015.
- [2] A. Issa, K. Ramadugu, P. Mulay et al., "Deaths related to hurricane Irma-Florida, Georgia, and North Carolina, September 4–October 10, 2017," *MMWR. Morbidity and Mortality Weekly Report*, vol. 67, no. 30, pp. 829–832, 2018.
- [3] S. Stewart and R. Berg, "National hurricane center tropical cyclone report: hurricane florence (al062018)," *National Hurricane Center*, vol. 30, p. 98, 2019.
- [4] A. J. Broccoli and S. Manabe, "Can existing climate models be used to study anthropogenic changes in tropical cyclone climate?" *Geophysical Research Letters*, vol. 17, no. 11, pp. 1917–1920, 1990.



- [5] K. M. Crosset, *Population Trends along the Coastal United States: 1980–2008*, Government Printing Office, Washington, DC, USA, 2005.
- [6] T. Dutzik and P. Baxandall, *A New Direction: Our Changing Relationship with Driving and the Implications for America's Future*, U.S. PIRG Education Fund Frontier Group, Boston, MA, USA, 2013.
- [7] J. L. Renne, T. W. Sanchez, and R. C. Peterson, *National Study on Carless and Special Needs Evacuation Planning: Case Studies*, University of New Orleans, New Orleans, LA, USA, 2008.
- [8] J. L. Renne, T. W. Sanchez, and T. Litman, "Carless and special needs evacuation planning," *Journal of Planning Literature*, vol. 26, no. 4, pp. 420–431, 2011.
- [9] J. L. Renne, "Emergency evacuation planning policy for carless and vulnerable populations in the United States and United Kingdom," *International Journal of Disaster Risk Reduction*, vol. 31, pp. 1254–1261, 2018.
- [10] P. Murray-Tuite and B. Wolshon, "Evacuation transportation modeling: an overview of research, development, and practice," *Transportation Research Part C: Emerging Technologies*, vol. 27, pp. 25–45, 2013.
- [11] US Census Bureau, "2014–2018 American community survey 5-year estimates," Technical Report, U.S. Census Bureau, Suitland, MD, USA, 2019.
- [12] T. Dutzik, J. Inglis, and P. Baxandall, *Millennials in Motion: Changing Travel Habits of Young Americans and the Implications for Public Policy*, U.S. PIRG Education Fund Frontier Group, Boston, MA, USA, 2014.
- [13] South Carolina Emergency Management Division, "State of South Carolina critical transportation need evacuation operations plan," 2019, <http://www.scemd.org/media/1331/annex-b-critical-transportation-need-evacuation-operations-plan.pdf> Technical Report.
- [14] M. K. Lindell, J. E. Kang, and C. S. Prater, "The logistics of household hurricane evacuation," *Natural Hazards*, vol. 58, no. 3, pp. 1093–1109, 2011.
- [15] R. Bian, C. G. Wilmot, R. Gudishala, and E. J. Baker, "Modeling household-level hurricane evacuation mode and destination type joint choice using data from multiple post-storm behavioral surveys," *Transportation Research Part C: Emerging Technologies*, vol. 99, pp. 130–143, 2019.
- [16] S. D. Wong, J. L. Walker, and S. A. Shaheen, "Bridging the gap between evacuations and the sharing economy," *Transportation*, vol. 48, pp. 1–50, 2020.
- [17] K. Miller, "Coronavirus could change Florida's hurricane planning: hotels, lyft, uber all in play," 2020, <https://www.usatoday.com/story/travel/news/2020/05/02/coronavirus-florida-considers-using-hotels-lyft-during-hurricanes/3074108001/>.
- [18] D. R. Bish, "Planning for a bus-based evacuation," *Spectrum*, vol. 33, no. 3, pp. 629–654, 2011.
- [19] R. Swamy, J. E. Kang, R. Batta, and Y. Chung, "Hurricane evacuation planning using public transportation," *Socio-Economic Planning Sciences*, vol. 59, pp. 43–55, 2017.
- [20] H. Naghawi and B. Wolshon, "Transit-based emergency evacuation simulation modeling," *Journal of Transportation Safety & Security*, vol. 2, no. 2, pp. 184–201, 2010.
- [21] M. Li, J. Xu, X. Liu, C. Sun, and Z. Duan, "Use of shared-mobility services to accomplish emergency evacuation in urban areas via reduction in intermediate trips-case study in Xi'an, China," *Sustainability*, vol. 10, no. 12, p. 4862, 2018.
- [22] J. Naoum-Sawaya and J. Y. Yu, "Ridesharing for emergency evacuation," *INFOR: Information Systems and Operational Research*, vol. 55, no. 4, pp. 339–358, 2017.
- [23] W. Lu, L. Liu, F. Wang, X. Zhou, and G. Hu, "Two-phase optimization model for ride-sharing with transfers in short-notice evacuations," *Transportation Research Part C: Emerging Technologies*, vol. 114, pp. 272–296, 2020.
- [24] P. Bansal and K. M. Kockelman, "Forecasting Americans' long-term adoption of connected and autonomous vehicle technologies," *Transportation Research Part A: Policy and Practice*, vol. 95, pp. 49–63, 2017.
- [25] T. Litman, *Autonomous Vehicle Implementation Predictions*, Victoria Transport Policy Institute, Victoria, Canada, 2017.
- [26] A. Talebian and S. Mishra, "Predicting the adoption of connected autonomous vehicles: a new approach based on the theory of diffusion of innovations," *Transportation Research Part C: Emerging Technologies*, vol. 95, pp. 363–380, 2018.
- [27] T. Litman, "Autonomous vehicle implementation predictions: implications for transport planning," 2020, <https://www.vtpi.org/avip.pdf>.
- [28] A. R. Wagner, J. Borenstein, and A. Howard, "Overtrust in the robotic age," *Communications of the ACM*, vol. 61, no. 9, pp. 22–24, 2018.
- [29] A. Faisal, M. Kamruzzaman, T. Yigitcanlar, and G. Currie, "Understanding autonomous vehicles," *Journal of transport and land use*, vol. 12, no. 1, pp. 45–72, 2019.
- [30] P. Bansal, K. M. Kockelman, and A. Singh, "Assessing public opinions of and interest in new vehicle technologies: an austin perspective," *Transportation Research Part C: Emerging Technologies*, vol. 67, pp. 1–14, 2016.
- [31] P. Robinette, A. R. Wagner, and A. M. Howard, "Investigating human-robot trust in emergency scenarios: methodological lessons learned," in *Robust Intelligence and Trust in Autonomous Systems*, pp. 143–166, Springer, Berlin, Germany, 2016.
- [32] W. Gruel and J. M. Stanford, "Assessing the long-term effects of autonomous vehicles: a speculative approach," *Transportation research procedia*, vol. 13, pp. 18–29, 2016.
- [33] D. J. Fagnant and K. Kockelman, "Preparing a nation for autonomous vehicles: opportunities, barriers and policy recommendations," *Transportation Research Part A: Policy and Practice*, vol. 77, pp. 167–181, 2015.
- [34] J. Piao, M. McDonald, N. Hounsell, M. Graindorge, T. Graindorge, and N. Malhene, "Public views towards implementation of automated vehicles in urban areas," *Transportation research procedia*, vol. 14, pp. 2168–2177, 2016.
- [35] K. M. Gurusurthy, K. M. Kockelman, and B. J. Loeb, "Sharing vehicles and sharing rides in real-time: opportunities for self-driving fleets," in *The Sharing Economy and The Relevance for Transport*, vol. 4, pp. 59–85, Elsevier, Amsterdam, Netherlands, 2019.
- [36] W. Yin, G. Cordahi, D. Roden, and B. Wolshon, "Risk reduction impact of connected vehicle technology on regional hurricane evacuations: a simulation study," *International journal of disaster risk reduction*, vol. 31, pp. 1245–1253, 2018.
- [37] H.-C. Wu, M. K. Lindell, and C. S. Prater, "Logistics of hurricane evacuation in hurricanes katrina and rita," *Transportation Research Part F: Traffic Psychology and Behaviour*, vol. 15, no. 4, pp. 445–461, 2012.
- [38] US Census Bureau, American Community Survey 1-Year Estimates, <https://data.census.gov/cedsci/>.
- [39] C. J. Haboucha, R. Ishaq, and Y. Shiftan, "User preferences regarding autonomous vehicles," *Transportation Research Part C: Emerging Technologies*, vol. 78, pp. 37–49, 2017.
- [40] M. Norusis, *SPSS 14.0 Statistical Procedures Companion*, Prentice-Hall, Inc., Hoboken, NJ, USA, 2005.
- [41] H. Chen, Q. Chen, L. Chen, and G. Zhang, "Analysis of risk factors affecting driver injury and crash injury with drivers

- under the influence of alcohol (dui) and non-dui,” *Traffic Injury Prevention*, vol. 17, no. 8, pp. 796–802, 2016.
- [42] R. Williams, “Generalized ordered logit/partial proportional odds models for ordinal dependent variables,” *STATA Journal: Promoting communications on statistics and Stata*, vol. 6, no. 1, pp. 58–82, 2006.
- [43] Statistical Consulting Group, Ordered Logistic Regression SPSS Annotated Output, 2020, <https://stats.idre.ucla.edu/spss/output/ordered-logistic-regression/>.
- [44] G. Heinze, C. Wallisch, and D. Dunkler, “Variable selection-a review and recommendations for the practicing statistician,” *Biometrical Journal*, vol. 60, no. 3, pp. 431–449, 2018.
- [45] R. B. Bendel and A. A. Afifi, “Comparison of stopping rules in forward “stepwise” regression,” *Journal of the American Statistical Association*, vol. 72, no. 357, pp. 46–53, 1977.
- [46] US Census Bureau, Pums Data, 2020, <https://www.census.gov/programs-surveys/acs/data/pums.html>.
- [47] B. M. Paul, J. Doyle, B. Stabler, J. Freedman, and A. Bettinardi, “Multi-level population synthesis using entropy maximization-based simultaneous list balancing,” in *Proceedings of the Transportation Research Board 97th Annual Meeting*, Washington, DC, USA, 2018.
- [48] SCDOT, SC Hurricane Evacuation Zones, 2018, <https://uscgeography.maps.arcgis.com/home/item.html?id=e59a4ef74f3a43d08b0c635b4136c8de>.
- [49] US Census Bureau, Census Data, 2020, <https://data.census.gov/cedsci/>.
- [50] South Carolina Department of Transportation, Scdot Data, 2020, <http://dbw.scdot.org/Poll5WebAppPublic/wfrm/wfrmHomePage.aspx>.
- [51] South Carolina Department of Transportation, Scdot Gis Data, 2020, <http://info2.scdot.org/GISMapping/Pages/GIS.aspx>.
- [52] US Census Bureau, Census Data, 2020, [https://data.census.gov/cedsci/advanced?g=0100000US.330000\\_0400000US45.060000&t=Housing\%3APopulations\and\People&tid=ACSDT5Y2018.B05010&vintage=2018](https://data.census.gov/cedsci/advanced?g=0100000US.330000_0400000US45.060000&t=Housing\%3APopulations\and\People&tid=ACSDT5Y2018.B05010&vintage=2018).
- [53] US Census Bureau, Census Data, 2020, <https://www.census.gov/cgi-bin/geo/shapefiles/index.php?year=2018&layergroup=County+Subdivisions>.
- [54] US Census Bureau, Census Data, 2020, <https://data.census.gov/cedsci/>.
- [55] S. Wong, S. Shaheen, and J. Walker, *Understanding Evacuee Behavior: A Case Study of Hurricane Irma*, Institute of Transportation Studies at UC Berkeley, Berkeley, CA, USA, 2018.
- [56] S. Hotle, P. Murray-Tuite, and K. Singh, “Influenza risk perception and travel-related health protection behavior in the us: insights for the aftermath of the COVID-19 outbreak,” *Transportation Research Interdisciplinary Perspectives*, vol. 5, Article ID 100127, 2020.
- [57] J. C. Wood and M. C. Wood, *J. M. Juran: Critical Evaluations in Business and Management*, Psychology Press, Hove, UK, 2005.



## Research Article

# Multi-Depot Pickup and Delivery Problem with Resource Sharing

Yong Wang <sup>1</sup>, Lingyu Ran <sup>1</sup>, Xiangyang Guan <sup>2</sup>, and Yajie Zou <sup>3</sup>

<sup>1</sup>School of Economics and Management, Chongqing Jiaotong University, Chongqing 400074, China

<sup>2</sup>Department of Civil and Environmental Engineering, University of Washington, Seattle, WA 98195, USA

<sup>3</sup>Key Laboratory of Road and Traffic Engineering of Ministry of Education, Tongji University, Shanghai 201804, China

Correspondence should be addressed to Yajie Zou; [zouyajie@tongji.edu.cn](mailto:zouyajie@tongji.edu.cn)

Received 10 April 2021; Revised 28 April 2021; Accepted 15 May 2021; Published 2 June 2021

Academic Editor: Xiaoyue Liu

Copyright © 2021 Yong Wang et al. This is an open access article distributed under the Creative Commons Attribution License, which permits unrestricted use, distribution, and reproduction in any medium, provided the original work is properly cited.

Resource sharing (RS) integrated into the optimization of multi-depot pickup and delivery problem (MDPDP) can greatly reduce the logistics operating cost and required transportation resources by reconfiguring the logistics network. This study formulates and solves an MDPDP with RS (MDPDPRS). First, a bi-objective mathematical programming model that minimizes the logistics cost and the number of vehicles is constructed, in which vehicles are allowed to be used multiple times by one or multiple logistics facilities. Second, a two-stage hybrid algorithm composed of a  $k$ -means clustering algorithm, a Clark-Wright (CW) algorithm, and a nondominated sorting genetic algorithm II (NSGA-II) is designed. The  $k$ -means algorithm is adopted in the first stage to reallocate customers to logistics facilities according to the Manhattan distance between them, by which the computational complexity of solving the MDPDPRS is reduced. In the second stage, CW and NSGA-II are adopted jointly to optimize the vehicle routes and find the Pareto optimal solutions. CW algorithm is used to select the initial solution, which can increase the speed of finding the optimal solution during NSGA-II. Fast nondominated sorting operator and elite strategy selection operator are utilized to maintain the diversity of solutions in NSGA-II. Third, benchmark tests are conducted to verify the performance and effectiveness of the proposed two-stage hybrid algorithm, and numerical results prove that the proposed methodology outperforms the standard NSGA-II and multi-objective particle swarm optimization algorithm. Finally, optimization results of a real-world logistics network from Chongqing confirm the applicability of the mathematical model and the designed solution algorithm. Solving the MDPDPRS provides a management tool for logistics enterprises to improve resource configuration and optimize logistics operation efficiency.

## 1. Introduction

With the advancement of information technology and Internet of Things, the logistics industry is playing an increasingly important role in the development of modern businesses [1, 2]. However, national and local governments worldwide are focusing on the environmental impacts of logistics and the efficient use of resources [3, 4]. In a logistics network, customers send out a series of requests for delivery and pickup services, and logistics service providers (LSPs) design service plans and arrange vehicles for these requests to deliver or pickup goods [5, 6]. Efficient logistics service plan can improve the operation efficiency of LSPs and resource utilization [7, 8]. Therefore, making an effective logistics service plan with resource sharing (RS) is essential,

which not only helps to reduce the operating cost for logistics facilities but also promotes the development of green logistics and provides better logistics services for consumers [9, 10].

In this study, a multi-depot pickup and delivery problem with RS (MDPDPRS) combines components from three subproblems: multi-depot vehicle routing problem (MDVRP) with pickups and deliveries (MDVRPPD), MDVRP with pickups and deliveries and time windows (MDVRPPDTW), and RS [11–13]. However, one of the difficult challenges in solving this problem is how to handle pickup and delivery activities among multiple depots through RS [14, 15]. In the traditional MDVRPPD, each vehicle performs only one type of activity in the service route, which may be delivering or picking up goods [16–18].

In addition, the traditional MDVRPPDTW and single-depot vehicle routing problem with pickups and deliveries mostly only consider the optimization of logistics operational costs [19, 20]. Therefore, MDPDPRS focuses on how to support and achieve the efficient utilization of transportation resources with RS strategy, and optimizes the logistics network.

With regard to RS, it is often jointly adopted with collaboration or cooperation between LSPs to optimize the logistics networks with multiple depots [21, 22]. RS strategy supports the sharing of customer information and transport resources to improve the resource configuration among logistics facilities to optimize the logistics network [23, 24]. Here, the sharing of customer information is often enabled by customer clustering, whereas the sharing of transportation resources is related to the use of shared transportation equipment [25, 26].

As for MDVRPPD, it is a crucial logistics issue with extensive applications, especially in reverse logistics [27]. Three basic types of vehicle routing problems exist in reverse logistics [28]. The first type is the vehicle routing problem with mixed deliveries and pickups, which involves customers with delivery demands, pickup demands, and delivery and pickup demands [29]. Vehicle routing problem with simultaneous delivery and pickup is the second type, which requires all customers to have both delivery and pickup demands [30]. The third type is the common MDVRPPD, which includes delivery and pickup customers in the logistics network [19, 31–33]. In this study, the consideration of customer service time windows makes MDVRPPD realistic.

In this study, the MDPDPRS can be formulated into a bi-objective mathematical model to minimize the total logistics operating cost and number of vehicles [32, 34]. On the basis of the multi-depot and RS properties of MDPDPRS, a two-stage hybrid algorithm is proposed to find the Pareto optimal solution. In the first stage, a  $k$ -means algorithm is adopted to reconfigure resources through customer clustering; thus, the MDVRPPDTW is simplified for solving [35]. The second stage focuses on finding the Pareto optimal solution for the bi-objective optimization problem [23, 36]. The Clarke-Wright (CW) algorithm, which is good at constructing the initial solution of vehicle routes, and the nondominated sorting genetic algorithm (NSGA-II), which is known for its capability of finding the Pareto solution, are adopted to optimize the vehicle routing in the second stage [33, 37, 38].

The remainder of this study is arranged as follows. Section 2 reviews the relevant literature. Section 3 elaborates the specifics of the MDPDPRS. Section 4 explains the bi-objective mathematical model for the MDPDPRS. Section 5 presents the designed methodology for solving the MDPDPRS. Section 6 analyzes the performance and application of the proposed model formulation and solution algorithm in a real-world case study compatible to the MDPDPRS. Finally, Section 7 summarizes the conclusions and discusses potential future research.

## 2. Literature Review

MDPDPRS is mainly related to the MDVRPPD, MDVRPPDTW, and RS strategy [18, 36]. MDVRPPD and

MDVRPPDTW are the extension problems of MDVRP and MDVRPTW with respect to the logistics service type of customer demands, respectively [39, 40]. In the widely studied MDVRP and MDVRPTW, the service types of customers are either deliveries or pickups [16, 33, 41]. However, in a real-world logistics network with multiple depots, customers with distribution and pickup demands often exist simultaneously and the service time windows are the additional characteristics of customers; this issue is abbreviated by scholars as MDVRPPD [11, 13]. Therefore, MDVRPPD and MDVRPPDTW have begun to attract the attention of scholars, and the difference between the two issues is mainly whether customers' service time window feature is considered [42, 43]. In the MDVRPPDTW, the optimization of vehicle routes focuses on the confirmation of customers' service time windows and the integration of vehicles' delivery and pickup activities, which are suitable with the factors that LSPs must consider if optimizing vehicle routes [44, 45]. The adoption of RS into the optimization of logistics network is also a current trend [12]. Thus, the MDPDPRS in this study integrates vehicles' distribution and pickup arrangement with the RS strategy to optimize the MDVRPPDW.

In contrast to the MDVRP, the MDVRPPD studies customers with delivery and pickup demands [35, 42]. The MDVRPPDTW is an extension of MDVRPPD, which considers the characteristics of customer service time windows [46, 47]. Many scholars have studied MDVRPPD and MDVRPPDTW considering diverse aspects and proposed different mathematical models and algorithms [30, 48]. In terms of models, many of the proposed mathematical models reflect the characteristics of their problem studied by different constraints, including capacity, time windows, and priority constraints [29, 49]. Ropke et al.[50] established a standard three-index model based on the characteristics of customer time window and designed an accurate algorithm to solve it. Gribkovskaia et al.[19] studied the vehicle routing problem with deliveries and pickups considering the number of times a customer has been visited and proposed a mixed integer linear programming model. Chen et al.[31] established a comprehensive mathematical model to minimize the transportation costs for unpaired vehicle routing problem with deliveries and pickups in a multi-factory production network. Conversely, hybrid heuristics algorithms (e.g., genetic algorithm and adaptive large neighborhood search algorithm) and exact algorithms based on column generation are commonly designed to solve MDVRPPD and MDVRPPDTW [50–52]. The proposed model and solution methodology in the above studies provide abundant reference for solving the basic MDVRPPD and MDVRPPDTW. However, few studies have optimized MDVRPPDTW with RS strategy [32, 34].

Customer clustering analysis is a research aspect that groups customers based on their characteristics (e.g., location and time window), and common clustering algorithms include  $k$ -means clustering, parallel clustering, and fuzzy-based customer clustering [53–56]. In comparison with other customer clustering algorithms,  $k$ -means clustering is widely adopted to solve vehicle routing problems [57, 58].

Xu et al.[59] proposed an enhanced ant colony algorithm based on  $k$ -means clustering to solve dynamic vehicle routing problems and achieved good optimization results. Hakim et al.[60] designed a cluster-based method to solve a vehicle routing problem with limited vehicle capacity, and their calculation results proved the effectiveness of that method. Mourelo Ferrandez et al.[61] reduced the calculation difficulty of truck-drone in tandem delivery network by  $k$ -means clustering algorithm. Wang et al.[35] proposed a hybrid heuristic algorithm based on three-dimensional  $k$ -means clustering and improved reference point NSGA-II to solve the multi-objective optimization model. Therefore, cluster analysis can simplify the difficulty of solving vehicle routing problem [62, 63].

At present, the construction of multi-objective optimization model and multi-objective optimization algorithm is the research hotspot of finding the Pareto solution of vehicle routing problems, and scholars have designed different algorithms [38, 64]. NSGA-II and multi-objective particle swarm optimization (MOPSO) algorithm are two common multi-objective algorithms [65, 66]. NSGA-II adopts a reference point strategy to maintain population diversity [67]. Srivastava et al. [68] proposed a NSGA-II to solve the multi-objective optimization model for MDVRPTW and verified that the method is superior to the latest method of that problem through a real-world case study. Maadanpour Safari et al.[69] adopted NSGA-II, multi-objective simulated annealing (MOSA), and MOPSO to optimize the proposed three-objective mathematical function and concluded that NSGA-II was superior to MOSA according to the results of their examples. Shafiei Nikabadi et al. [70] formed a multi-objective model for the route selection of freight fleet, optimized it with NSGA-II and MOPSO, and considered that MOPSO was superior to NSGA-II. Therefore, NSGA-II and MOPSO are two commonly typical multi-objective optimization algorithms that can find Pareto solutions [71].

Many scholars have adopted the cooperation and RS strategy to optimize the multicenter logistics network [11, 17, 24]. Zhang et al. [15] believed that in the collaborative e-commerce truck carrier, participants can share transportation resources and customer demands to maximize the total profit of the whole alliance and improve vehicle utilization. Wang et al. [14] adopted the cooperation strategy to optimize the MDVRPPDTW with minimization of the operating cost of the transportation network and the total number of vehicles. Deng et al. [21] allowed the capabilities of the logistics facility, the vehicle resources, and the customer information to be shared through RS strategies, and they proved that this strategy can improve the utilization of logistics resources. In the study of Nourinejad et al. [72], vehicles can be used multiple times to reduce fleet size by extending vehicle reservation time. Li et al. [73] adopted the resource-sharing strategy to significantly optimize the logistics network and maximized the utilization of resources. Therefore, the adoption of RS strategy not only helps optimize the logistics costs but also improves the utilization of resources to protect the environment [22, 74].

In summary, the existing literature has provided rich reference materials about MDVRPPD, MDVRPPDTW, and

RS, including model formulations and solution algorithms. However, the existing literature related to MDPDPRS has the following limitations. (1) Few studies on MDPDPRS have considered RS, MDVRPPD, and MDVRPPDTW. (2) The fact that a vehicle can be used multiple times on a working day is insufficiently considered in the proposed mathematical models. (3) Most of the proposed solution algorithms in the existing literature only address how to solve MDVRP, MDVRPPD, and MDVRPPDTW, and RS has not been incorporated into the designed algorithms. (4) Most of the existing literature focuses on raising problems and designing algorithms but neglects testing the proposed methods with practical cases.

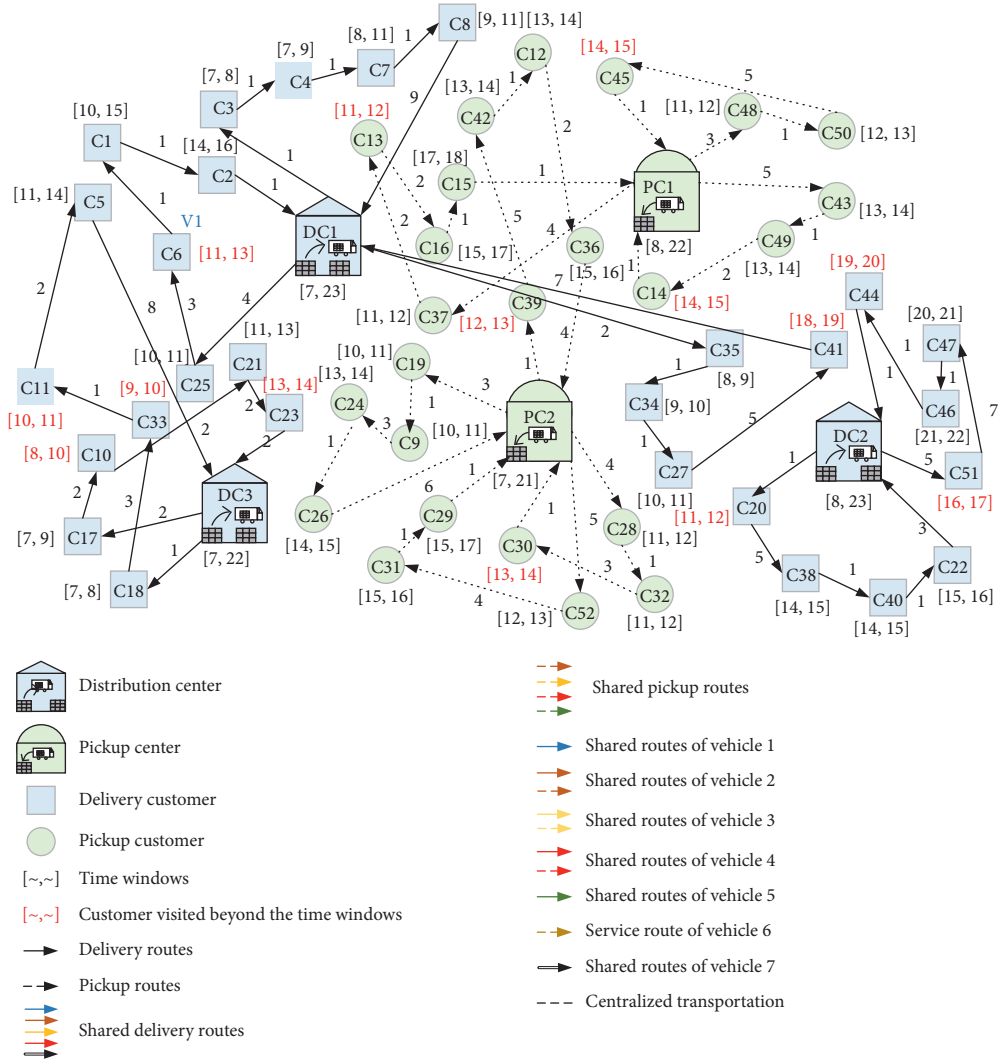
In consideration of the aforementioned shortcomings, the main contributions of this study to MDPDPRS are as follows: (1) Characteristics of RS, MDVRPPD, and MDVRPPDTW are comprehensively incorporated to enrich the research on MDPDPRS. (2) On the basis of RS, this study proposes and tests that vehicles can be used multiple times and that customer information can be shared to save the transportation resources of logistics networks, which are considered in the proposed mathematical model. (3) A two-stage algorithm is designed to combine RS with vehicle routing optimization to optimize the logistics network. (4) Benchmark and real-world cases are utilized to test and verify the performance and applicability of the proposed model and solution algorithm in this study.

### 3. Problem Statement

RS is an effective strategy that can optimize logistics operation costs and resource allocation in a multicenter logistics network with pickups and deliveries [21, 35]. In this study, the logistics network consists of multiple distribution centers (DCs), multiple pickup centers (PCs), and multiple customers. The logistics network before and after optimization with RS, which is composed of DC1, DC2, DC3, PC1, PC2, and 52 customers (marked C1, C2, ..., C52), is shown in Figure 1. The numerical number near the line represents the time distance between two elements (including facilities and customers).

In Figure 1(a), the unreasonable arrangement of vehicle routes and the nonsharing of resources are the main reasons for the higher operating costs of the logistics network. First, staggered driving and long-distance service are the two most significant unreasonable arrangements, and they cause additional travel costs. Second, vehicles that violate customers' time windows often occur. Arriving early and arriving late are generating penalty costs. Finally, the nonsharing of resources between facilities results in the capacity of facilities and transportation resources being left unused. For example, the vehicle no longer works after returning from C2 to DC1 in the service route DC1  $\rightarrow$  C25  $\rightarrow$  C6  $\rightarrow$  C1  $\rightarrow$  C2  $\rightarrow$  DC1.

In Figure 1(b), the logistics network is optimized through the sharing of customers and transportation resources among facilities. First, the reallocation of customers between facilities facilitates the rearrangement of vehicles, which can avoid staggering and long-distance service.



(a)

FIGURE 1: Continued.

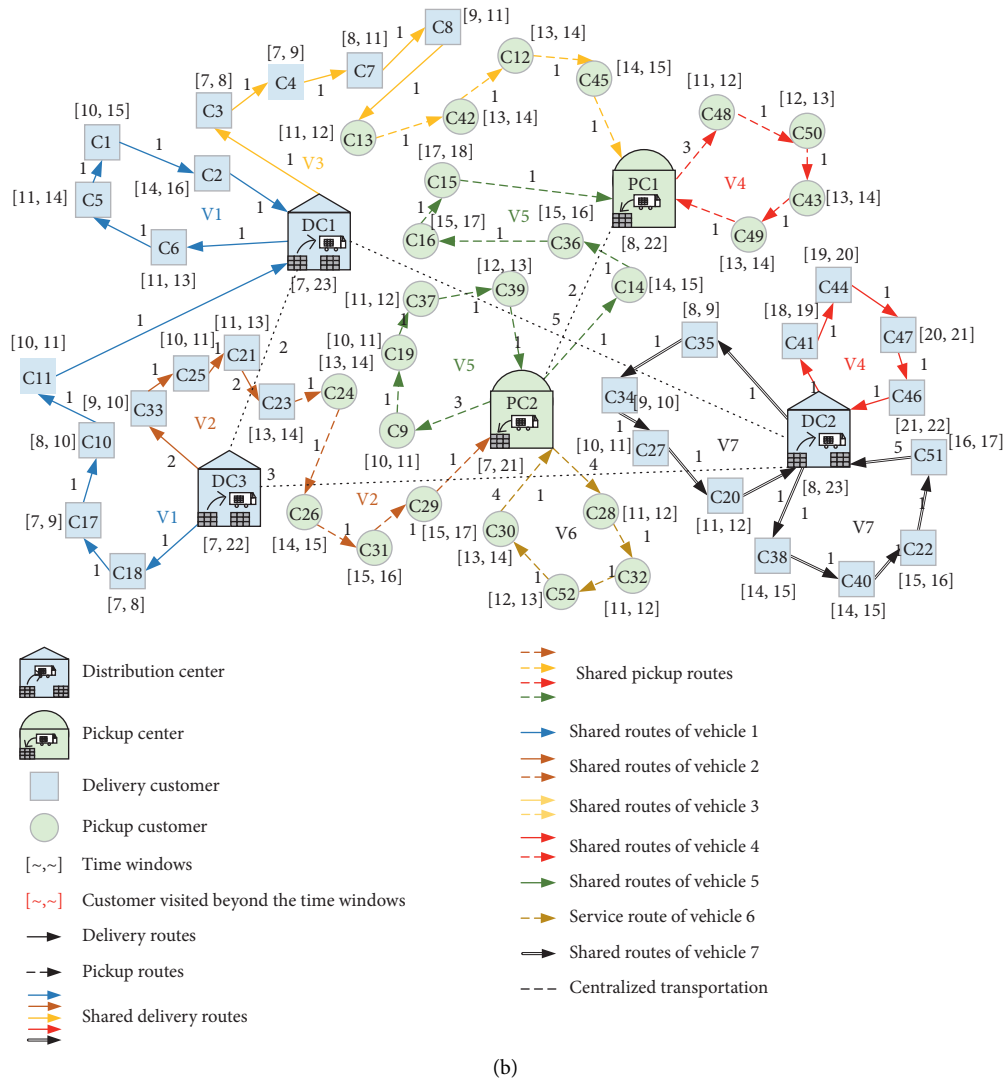


FIGURE 1: Logistics network optimization diagram of MDPDPRS. (a) Initial logistics network before resource sharing. (b) Optimized logistics network with resource sharing.

Second, vehicle resources can be better configured through sharing among multiple facilities. For example, V1 is used by DC3 and DC1. V2 and V3 have also implemented distribution and pickup services. The repeated use of vehicles prevents resources from being idle. Finally, the situation of vehicle violating the customers' time window is avoided.

To clearly demonstrate the discounts that RS brings to logistics network optimization, six indicators are counted, namely, total travel cost (TTC), total penalty cost (TPC), total maintenance cost (TMC), total fixed cost (TFC), number of vehicles (NV), and total operating cost (TOC), which are listed in Table 1. The unit time travel cost using a vehicle can be set to \$10/h, and the unit time penalty cost for waiting or late can be set to \$20/h, and the maintenance cost using a vehicle in a working period can be defined as \$100, and the fixed cost of a facility being used in a working period can be set to \$200.

In Table 1, the gap of TOC and NV in the initial and optimized logistics network is \$1880 and 7, respectively,

which are highly significant. Before optimization, TTC (\$1500), TPC (\$440), and TMC (\$1400) are the main elements that cause additional logistics costs. In the optimized logistics network, the penalty costs are avoided, and the reduction in the number of vehicles also reduces the maintenance costs with RS. In addition, the travel costs of vehicles are also greatly reduced. Therefore, RS is an effective strategy for optimizing the logistics network of the MDPDPRS.

#### 4. Mathematical Model for MDPDPRS

4.1. Assumptions and Notations. Some necessary assumptions can ensure the usability of the mathematical model [75] and those assumptions are listed as follows [14, 30, 36, 42, 49, 50].

Assumption 1. In a working period, the demand and coordination of customers are stable and known.

*Assumption 2.* Centralized transportation among logistics facilities is performed by trucks.

*Assumption 3.* The vehicles can be used multiple times by the same or different logistics facilities.

The relevant notations and their descriptions are listed in Table 2.

**4.2. Mathematical Model.** A bi-objective mathematical model that minimizes the logistics operational costs (Equation (1)) and the number of vehicles (Equation (2)) is formed to solve the MDPDPRS. In Equation (1), the logistics operation cost is composed of four parts, which are marked by the TTC (Equation (3)), TPC (Equation (4)), TMC (Equation (5)), and TFC (Equation (6)). In Equation (2),  $\sum_{c \in S_F} \sum_{h \in C_U} x_{vch}$  represents the shared times of vehicle  $v$ .

$$\text{Min TOC} = \text{TTC} + \text{TPC} + \text{TMC} + \text{TFC}, \quad (1)$$

$$\text{Min TNV} = \sum_{v \in V} \min \left\{ \sum_{c \in S_F} \sum_{h \in C_U} x_{vch}, 1 \right\}, \quad (2)$$

$$\begin{aligned} \text{TTC} = & T \times \sum_{v \in V} \sum_{c \in C_U \cup S_F} \sum_{h \in \widehat{C_U} \cup S_F} x_{vch} \times d_{ch} \times f_v \times P_v \\ & + T \times \sum_{b \in B} \sum_{o \in S_F} \sum_{w \in S_F} \sum_{f \in S_F} x_{bowf} \times d_{wf} \times f_b \times P_b, \end{aligned} \quad (3)$$

$$\begin{aligned} \text{TPC} = & T \times \sum_{v \in V} \sum_{c \in C_U} \sum_{f \in S_F} \sum_{k \in R_v} x_{vcfk} \\ & \times (P_E \times \max\{E_c - A_{vck}, 0\} + P_L \times \max\{A_{vck} - L_c, 0\}), \end{aligned} \quad (4)$$

$$\text{TMC} = \sum_{v \in V} \frac{M_v}{W} \min\{R_v, 1\} + \sum_{b \in B} \sum_{o \in S_F} \sum_{w=0} \sum_{f \in S_F} \frac{M_b}{W} \times x_{bowf}, \quad (5)$$

$$\text{TFC} = \sum_{f \in S_F} \frac{z_f \times I_f}{W}. \quad (6)$$

Subject to

$$\sum_{v \in V} \sum_{f \in S_F} \sum_{k \in R_v} x_{vcfk} = 1, \quad \forall c \in C_U, \quad (7)$$

$$R_v = \sum_{c \in S_F} \sum_{h \in C_U} x_{vch}, \quad \forall v \in V, \quad (8)$$

$$\sum_{f \in S_F} x_{vcfk} = 1, \quad \forall v \in V, k \in R_v, c \in C_U, \quad (9)$$

$$\sum_{h \in C_U} x_{vch} - \sum_{h \in C_U} x_{vhc} = 0, \quad \forall v \in V, c \in C_U, \quad (10)$$

$$\sum_{c \in S_F} \sum_{h \in C_U} x_{vch} = \sum_{h \in C_U} \sum_{n \in S_F} x_{vhn}, \quad \forall v \in V, \quad (11)$$

$$\sum_{w=0, f \in S_F \setminus \{0\}} x_{bowf} = \sum_{w=0, f \in S_F \setminus \{0\}} x_{bowf}, \quad \forall b \in B, o \in S_F, \quad (12)$$

$$\sum_{w \in S_F} x_{bowf} - \sum_{w \in S_F} x_{bowf} = 0, \quad \forall b \in B, o, f \in S_F, \quad (13)$$

$$\sum_{c \in C_D} x_{vcfk} \times Q_c^D \leq C_V, \quad \forall v \in V, f \in S_F, k \in R_v, \quad (14)$$

$$\sum_{c \in C_P} x_{vcfk} \times Q_c^P \leq C_V, \quad \forall v \in V, f \in S_F, k \in R_v, \quad (15)$$

$$\sum_{f \in S_F} x_{bof} \cdot Q_{of} \leq C_b, \quad \forall b \in B, o \in S_F, \quad (16)$$

$$Q_{of} = \sum_{c \in C_D} x_{cof} \times Q_c^D, \quad \forall o, f \in D, \quad (17)$$

$$Q_{of} = \sum_{c \in C_P} x_{cfo} \times Q_c^P, \quad \forall o, f \in P, \quad (18)$$

$$\sum_{v \in V} \sum_{c \in C_D} \sum_{k \in R_v} x_{vcfk} \times Q_c^D \leq C_f, \quad \forall f \in S_D, \quad (19)$$

$$\sum_{v \in V} \sum_{c \in C_P} \sum_{k \in R_v} x_{vcfk} \times Q_c^P \leq C_f, \quad \forall f \in S_P, \quad (20)$$

$$E_f \leq G_{vfk} \leq L_f, \quad \forall v \in V, c \in S_F, k \in R_v, \quad (21)$$

$$A_{vck} + t_{cf} \leq G_{vf(k+1)}, \quad \forall v \in V, c, f \in S_F, k \in R_v, \quad (22)$$

$$E_c \leq A_{vck} \leq L_c, \quad \forall v \in V, c \in S_F \cup C_U, k \in R_v, \quad (23)$$

$$\begin{aligned} E_h \times x_{vch} \leq & (A_{vck} + t_{ch}) \times x_{vch} \leq L_h \times x_{vch}, \\ \forall v \in V, & c \in C_U, h \in C_U \cup S_F, k \in R_v, \end{aligned} \quad (24)$$

$$\sum_{c, h \in S_F \cup C_U} x_{vch} \times t_{ch} \leq T_v, \quad \forall v \in V, \quad (25)$$

$$\begin{aligned} \sum_{c, h \in C_U, r \neq h} x_{vcfk} \times x_{vch} = & \sum_{c \in C_U} x_{vcfk} - 1, \\ \forall v \in V, & f \in S_F, k \in R_v, \end{aligned} \quad (26)$$

$$\sum_{f, w \in S_D \setminus \{0\}} x_{bowf} \leq \sum_{f \in S_D \setminus \{0\}} x_{bof} - 1, \quad \forall b \in B, o \in S_D, \quad (27)$$

$$\sum_{f, w \in S_P \setminus \{0\}} x_{bowf} \leq \sum_{f \in S_P \setminus \{0\}} x_{bof} - 1, \quad \forall b \in B, o \in S_P, \quad (28)$$

$$x_{vcfk} = \{0, 1\}, \quad \forall v \in V, c \in C_U, f \in S_F, k \in R_v, \quad (29)$$



TABLE 1: Comparison of MDPDRS before and after optimization.

	TTC (\$)	TPC (\$)	TMC (\$)	TFC (\$)	NV	TOC (\$)	NV	Gap TOC (\$)
Initial	1500	440	1400	1000	14	4340		
Optimized	760	0	700	1000	7	2460	7	1880

TABLE 2: Notations and description.

Set	Description
$S_D$	Set of DCs, the total number of DCs is $N_D$
$S_P$	Set of PCs, the total number of PCs is $N_P$
$S_F$	Set of DCs and PCs, $S_F = S_D \cup S_P$
$C_D$	Set of delivery customers
$C_P$	Set of pickup customers
$C_U$	Set of all customers, $U = C_D \cup C_P$
$V$	Set of vehicles, the total number of vehicles is $N_V$
$B$	Set of trucks, the total number of trucks is $N_B$
<b>Parameters</b>	
$Q_c^D$	Delivery demand of customer $c$ , $c \in C_D$
$Q_c^P$	Pickup demand of customer $c$ , $c \in C_P$
$[E_o, L_c]$	Service time window of customer or logistics facility $c$ , $c \in C_U \cup S_F$
$d_{ch}$	Travel distance between customer or facility $c$ and customer $h$ , $c, h \in C_U \cup S_F$
$t_{ch}$	Travel time of a vehicle driving from customer or facility $c$ to customer $h$ , $c, h \in C_U \cup S_F$
$P_E$	Waiting penalty coefficient of arriving earliness (unit: dollars/unit time)
$P_L$	Tardiness penalty coefficient of arriving delay (unit: dollars/unit time)
$W$	Number of working periods in a year
$T$	Number of working days in a working period
$T_v$	Maximum travel time of vehicle $v$ , $v \in V$
$T_b$	Maximum travel time of truck $b$ , $b \in B$
$f_v$	Fuel consumption rate of vehicle $v$ per km (unit: gallon/miles)
$f_b$	Fuel consumption rate of truck $b$ per km (unit: gallon/miles)
$P_v$	Gasoline price (unit: dollars/gallon)
$P_b$	Gasoline price (unit: dollars/gallon)
$C_v$	Capacity of vehicle $v$ , $v \in V$
$C_b$	Capacity of truck $b$ , $b \in B$
$C_f$	Capacity of facility $f$ , $f \in S_F$
$M_v$	Annual maintenance cost of vehicle $v$ , $v \in V$
$M_b$	Annual maintenance cost of truck $b$ , $b \in B$
$I_f$	Annual fixed cost of facility $f$ , $f \in S_F$
$R_v$	The total service route number of vehicle $v$ , $v \in V$
$G_{vfk}$	The departure time of vehicle $v$ from facility $f$ in the $k$ th service route, $v \in V$ , $f \in S_F$ , $k \in R_v$
$A_{vck}$	The arriving time of vehicle $v$ at customer or facility $c$ in the $k$ th service route, $v \in V$ , $c \in C_U \cup S_F$ , $k \in R_v$
$Q_{of}$	The number of transported goods from facility $o$ to $f$ , $o, f \in S_F$
<b>Variables</b>	
$x_{vcfk}$	$x_{vcfk} = 1$ if customer $c$ is served by vehicle $v$ departing from DC or PC $f$ in the $k$ th service route of vehicle $v$ ; otherwise, $x_{vcfk} = 0$ , $v \in V$ , $c \in C_U$ , $f \in S_F$ , $k \in v$
$x_{cof}$	$x_{cod} = 1$ if the facility providing logistics service for customer $c$ is changed from facility $o$ to $f$ ; otherwise, $x_{cod} = 0$ , $c \in C_U$ , $o, f \in S_F$
$x_{vch}$	$x_{vch} = 1$ if vehicle $v$ travels directly from facility or customer $c$ to $h$ ; otherwise, $x_{vch} = 0$ , $v \in V$ , $c, h \in S_F \cup C_U$
$x_{bof}$	$x_{bof} = 1$ , if the goods transported from facility $o$ to $f$ is carried by truck $k$ ; otherwise, $x_{bof} = 0$ , $b \in B$ , $o, f \in S_F$
$x_{bowf}$	$x_{bowf} = 1$ , if truck $k$ departs from facility $o$ and travels directly from facility $w$ to $f$ ; otherwise, $x_{bowf} = 0$ , $b \in B$ , $o, w, f \in S_F$
$z_f$	$z_f = 1$ if facility $f$ agrees to share resource, otherwise, $z_f = 0$ , $f \in S_F$ .

$$x_{cof} = \{0, 1\}, \quad \forall c \in C_U, o, f \in S_F, \quad (30)$$

$$z_f = \{0, 1\}, \quad \forall f \in S_F. \quad (34)$$

$$x_{vch} = \{0, 1\}, \quad \forall v \in V, c, h \in C_U \cup S_F, \quad (31)$$

$$x_{bof} = \{0, 1\}, \quad \forall b \in B, o, f \in S_F, \quad (32)$$

$$x_{bowf} = \{0, 1\}, \quad \forall b \in B, o, w, f \in S_F, \quad (33)$$

Constraint (7) ensures that each customer is served once. Constraint (8) counts the shared times of vehicle  $v$ . Constraints (9)–(11) ensure that flow conservation is achieved on each customer. Constraints (12) and (13) are the flow balance constraints of the truck. Constraints (14)–(16) ensure that the loading quantity of each vehicle and each truck cannot

exceed their capabilities. Constraints (17) and (18) count the quantity of transshipment goods between logistics facilities. Constraints (19) and (20) guarantee that the total service quantity of each facility does not exceed its capacity. Constraints (21) and (22) require that the departure time and return time of each vehicle must meet the service time window of its served facility. Constraints (23) and (24) ensure that each vehicle must provide services for customers within the customers' service time window. Constraint (25) requires that the total working time of each vehicle does not exceed its maximum working time. Constraints (26)–(28) are used to eliminate the sub-tours of each vehicle and truck. The constraints of relevant binary variables are listed in Constraints (29)–(34).

## 5. Solution Methodology for MDPDPRS

MDVRPTW and MDVRPPDTW are typical NP-hard problems [12, 18, 41]. Multi-objective optimization algorithm and two-stage algorithm are often designed in combination to solve MDVRPPDTW [14, 23, 36]. Here, a two-stage algorithm with customer clustering first and then vehicle routing optimization is designed to solve MDPDPRS. This two-stage hybrid algorithm is composed of  $k$ -means, CW, and NSGA-II algorithms, and named KCW-NSGA-II. In the first stage of KCW-NSGA-II, customers and resources are reconstructed by the  $k$ -means clustering algorithm [57, 58]. The main purpose of the second stage is to optimize vehicle routes and find the Pareto optimal solution. The CW algorithm is adopted to construct the initial solution for NSGA-II [33, 37, 64, 65, 67].

The designed algorithm flow is illustrated in Figure 2. Here,  $Gen$  is the current number of iterations;  $MaxGen$  is the maximum number of iterations;  $r$  is the number of iterations of the current internal re-optimization mechanism, which is between clustering and vehicle routing optimization; and  $MaxR$  is its maximum number of iterations.

In Figure 2, the two-stage characteristics of customer clustering first and vehicle routing optimization later are clearly demonstrated. First, a  $k$ -means customer clustering mechanism based on Manhattan distance is designed. The clustering results are checked, updated, and saved after finishing the reallocation of all customers. Second, the CW algorithm is adopted to design the initial population and initial feasible solution, which accelerates the speed and possibility of NSGA-II algorithm to find the Pareto optimal solution. Third, the elite strategy and genetic operation of NSGA-II are used to iteratively optimize the generated initial solution to find the Pareto optimal solution, which is mainly embodied in the change of  $Gen$ . Fourth, a regulatory re-optimization mechanism between customer clustering and vehicle routing optimization is set up to maintain gene stability during genetic operation, and this mechanism is implemented by the re-updating of  $r$ . Finally, if  $Gen$  is updated to  $MaxGen$ , then the iterative optimization of the algorithm is finished and the found Pareto optimal solution is outputted.

**5.1.  $K$ -Means Clustering Algorithm.** Customer clustering is an important measure to reduce the complexity of solving MDVRPPDTW [36].  $K$ -means algorithm is widely used to

solve MDVRPTW due to its simplicity and efficiency [14, 21]. The  $k$ -means clustering pseudocode based on Manhattan distance is listed in Algorithm 1.

**5.2. CW Algorithm.** A common and effective way to construct the initial solution of VRP is the CW savings algorithm, which is actually a greedy heuristic algorithm [33, 37, 76]. The service time windows of customers and the capacity of vehicles are the main constraints to construct the initial solution [77, 78]. The pseudocode of the CW algorithm designed in this study is listed in Algorithm 2.

**5.3. NSGA-II.** NSGA-II is a multi-objective optimization algorithm based on GA, which searches the Pareto optimal solution for multi-objective optimization [38, 64, 68]. Fast nondominated sorting operator, individual crowding distance operator, and elite strategy selection operator are the three key designs of NSGA-II [33, 65]. Here, we suppose that the population is  $P$  and  $n$  individuals exist, and the individual objective function value of individual  $i$  is  $x_i$ .

**5.3.1. Fast Nondominated Sorting Operator.** The key design of NSGA-II is to find the Pareto optimal solution. To enhance the possibility of finding the Pareto solution, the fast nondominated sorting operator stratifies the population  $P$  according to the quality of individual solutions [33, 64, 65, 67]. This method is a cyclic process of grading based on population fitness. Here, the nondominated solution set and the rank value assigned to the individual are the two indicators for fast nondominated sorting. Assume that  $F_r$  represents the nondominated solution set, and  $i_r$  represents the rank value of individual  $i$ . Then, the pseudocode of the fast nondominated sort operator is shown in Algorithm 3.

**5.3.2. Crowding Distance and Its Comparison Principle.** The crowding distance is designed to drive the population to converge to the Pareto optimal solution and maintain the diversity of the population, which is mainly for individuals in the same nondominant layer [38, 64, 68]. We assume that  $n$  individuals exist in the nondominant level of  $S_F$ , and the objective function value of individual  $i$  is  $x_i$ . Then, the crowding distance is calculated as

$$L(i) = \begin{cases} \infty, & i = 1 \text{ or } i = n, \\ |x_{i-1} - x_{i+1}|, & i = 2, 3, \dots, n-1. \end{cases} \quad (35)$$

In Equation (35),  $|x_{i-1} - x_{i+1}|$  represents the sum of the distance between individuals  $i-1$  and  $i+1$  in each direction of the objective function. Here, the objective function values of individuals need to be sorted before calculating the crowding distance. If the rank values of individuals  $i$  and  $j$  are  $i_r$  and  $j_r$ , then the crowding distance is  $L(i)$  and  $L(j)$ , respectively. The individual crowding comparison strategy based on crowding distance and nondominated ranking results is as follows.

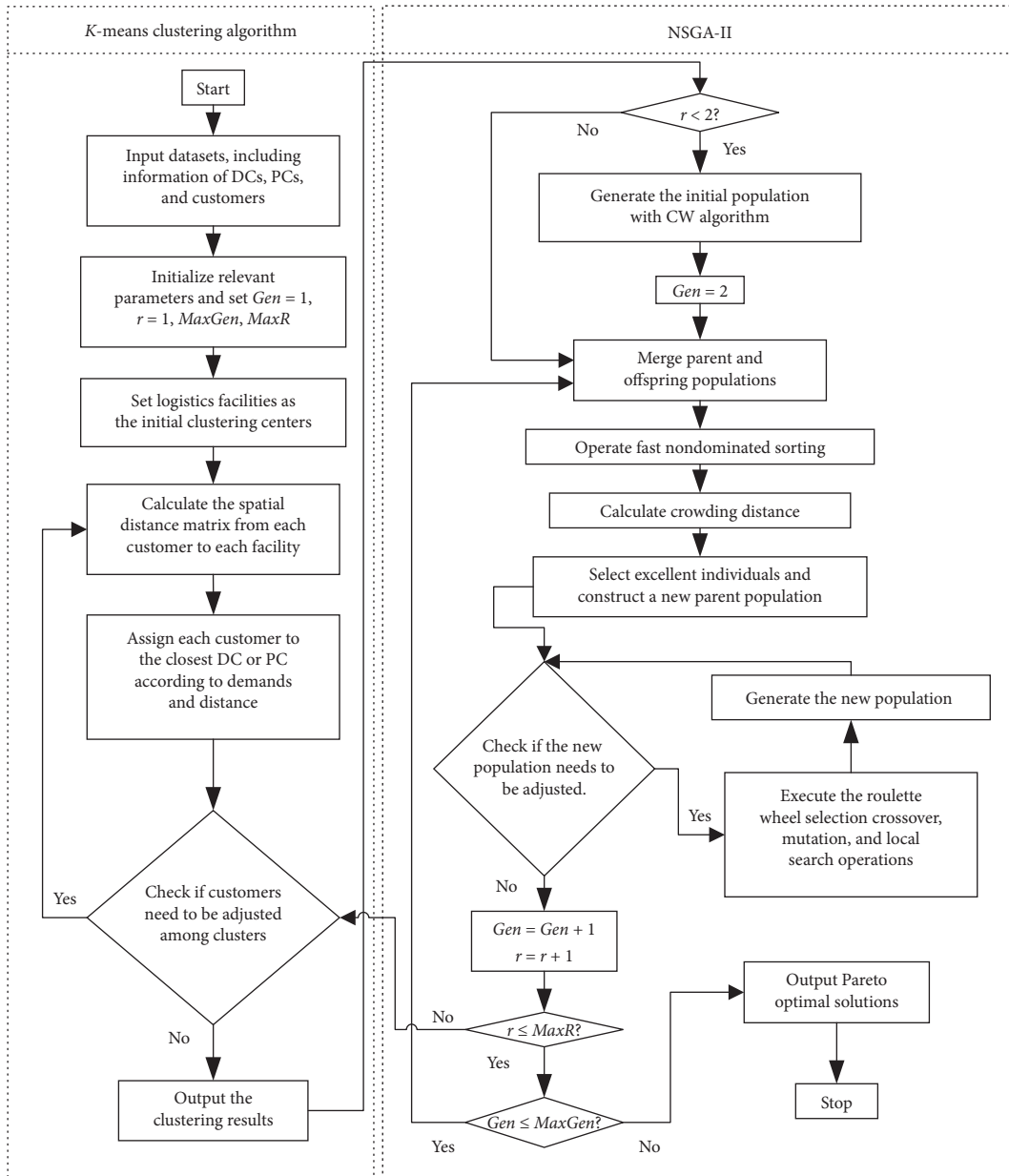


FIGURE 2: Algorithm flowchart of MDPDPRS.

**Input:** The datasets, including logistics facility and customer information, such as the coordination, time windows, and demands  
**Output:** The clustering results  
 (1) **Step 1:** Select  $k$  objects as the initial clustering center  
 (2) **Step 2:** Calculate the Manhattan distance between each customer and each clustering center  
 (3) **Step 3:** (Re-)Assign each customer to their closest clustering center  
 (4) **Step 4:** If some customers need to be adjusted among the clustering results, then enter **Step 3**; otherwise, go to **Step 5**  
 (5) **Step 5:** Update the clustering centers  
 (6) **Step 6:** Output the clustering results

ALGORITHM 1: Procedure of  $k$ -means algorithm.

- (1) If  $i_r > j_r$ , then individual  $i$  is the best one. If  $i_r < j_r$ , then individual  $j$  is the best one.
- (2) If  $i_r = j_r$ , then the individual with the most crowded distance is the better one.

**5.3.3. Elite Strategy Selection Operator.** To prevent the Pareto optimal solution from being lost in the iteration process, an elite strategy selection operator is designed, which selects the optimal solution by nondominated sorting and crowding distance between the parent and offspring populations. Suppose that the current iteration is  $t$  and the parent population is  $P_t$ , the offspring population is  $Q_t$ , and  $R_t$  is composed by  $P_t$  and  $Q_t$ . First, a fast nondominated sorting is performed for  $R_t$ , and the crowding distance is then calculated. On the basis of the crowding distance and the nondominated layer,  $N$  individuals with high-quality solution is selected to form a new population  $P_{t+1}$ .

## 6. Empirical Analyses

**6.1. Algorithm Comparison.** The standard NSGA-II, GA-PSO, and MOPSO are adopted for comparison to verify the applicability and effectiveness of the proposed KCW-NSGA-II algorithm in solving MDPDPRS [38, 64–66, 68, 79]. The benchmark dataset C-mdvrptw (consisting of instances of 20 groups) is utilized for the test, which is mainly obtained from the website. Networking and emerging optimization and their related characteristics are listed in Table 3. To meet the characteristics of the research object in this study, depots are regarded as logistics facilities, and customers are divided into two types, that is, those with distribution demands and those with pickup demands.

In Table 3, the number of customers and logistics facilities in each instance is different. The first instance comprises four facilities and 48 customers, whereas Instance 10 includes six facilities and 288 customers. In addition, the loading capacity of vehicle used in each instance is differentiated.

Relevant parameters are properly unified to mitigate their effects on algorithm performance. These parameters are set as follows [38, 64–66, 68, 79]: (1) parameters about GA: population size  $popsiz = 200$ , selection possibility  $sp = 0.6$ , crossover possibility  $cp = 0.9$ , mutation possibility  $mp = 0.2$ ; (2) parameters about PSO:  $popsiz = 200$ , inertia weight  $iw = 0.85$ , the personal learning confidences  $pc = 2$ , and social learning confidence  $gc = 3$ ; and (3) other relevant parameters: maximum number of generation  $genmax = 1200$  and velocity of vehicle  $v = 5$ . The costs, number of vehicles (NV), and computation time (CT) are calculated to verify the performance of the algorithms and the numerical results are listed in Table 4.

The numerical results shown in Table 4 demonstrate that the proposed algorithm KCW-NSGA-II performs better than the other three algorithms. First, the average cost of the four algorithms is \$2584, \$2944, \$2746, and \$3025, respectively. By contrast, the costs and the number of vehicles optimized by KCW-NSGA-II are the most economical

solution compared with the other three algorithms in each instance. Second, the value of  $t$ -test also shows that the KCW-NSGA-II is significantly different from the other three algorithms. In addition, the proposed algorithm can obtain the optimal solution quickly. Therefore, the proposed algorithm KCW-NSGA-II outperforms the other three algorithms. Moreover, this algorithm can be adjusted to address problems such as VRPMDP, VRPSDP, and PVRP.

**6.2. Data Source and Relevant Parameter Setting.** As an inland international logistics hub and an open highland, Chongqing is a new first-tier city in China. Therefore, as our numerical experiments, the logistics network adopted from Chongqing is appropriate to verify the applicability of this study. Six logistics facilities (i.e., DC1, DC2, DC3, PC1, PC2, and PC3) and 220 customers are the main elements of this real-world logistics network. The information and characteristics of these elements are listed in Table 5, and the spatial allocation information is plotted in Figure 3.

In Table 5, the number of customers served by the six logistics facilities is 27, 36, 39, 46, 31, and 41, respectively. In Figure 3, an obvious feature is that the customer allocation of each facility is relatively dispersed. The service area edge of each facility is not a clear division. In Table 6, the initial vehicle routes for the logistics network are shown, including the specific information of each service route.

In Table 6, the total number of vehicles used in the initial logistics network is 33, and the number of vehicles used at each facility is 5, 6, 6, 6, 4, and 6, respectively. In addition, some vehicles return to their origin early, such as V9, V10, V17, and V18, indicating that these vehicle resources are underutilized. The service vehicle routes of DC1 and the 27 customers it serves in the logistics network are shown in Figure 4.

In Figure 4, the service routes of V3, V4, and V5 are relatively complex. V5 performs delivery services for customers C23, C22, C6, C16, C2, and C5. However, these customers may be closer to DC3 on the basis of the perspective of spatial distribution. Therefore, optimizing this logistics network is necessary. The values of the relevant parameters used in this real-world case study are shown in Table 7 [38, 64, 65, 68].

**6.3. Optimization Results.** Clustering customers to optimize resource allocation is the first step in optimizing the logistics network. The customer clustering results of this logistics network by  $k$ -means algorithm are shown in Figure 5.

In Figure 5, the service relationship between customers and facilities is optimized by clustering. Each customer is covered by the logistics facility that is located close to that customer. On the whole, the service area of each logistics facility has been obviously allocated. For example, C23, C22, C6, C16, and C2 are served by DC1 before clustering; however, they are also served by DC3. Statistical analysis of customers whose service relationship has changed like those five customers is the key to handle centralized transportation. The details of the amount of goods transferred among facilities are shown in Figure 6.

**Input:** The datasets of customer and facility information including location, time window, demand, and other relevant parameters  
**Output:** The initial feasible solution

- (1) **Step 1:** Mark the initial distance saving values with numbers 1, 2, 3, . . . , (n-1)
- (2) **Step 2:** Assign vehicles to each customer
- (3) **Step 3:** Calculate the distance savings of new vehicle routes, which are formed by any two routes
- (4) **Step 4:** Sort the distance savings in descending order
- (5) **Step 5:** If new vehicle routes meet the time window and capacity constraints, then go directly to **Step 6**; otherwise set  $n=n+1$  and return to **Step 5**
- (6) **Step 6:** Generate a new vehicle route with two vehicle routes whose distance savings are maximum
- (7) **Step 7:** Update the distance savings value through the fusion of vehicle routes
- (8) **Step 8:** Generate new vehicle route with two vehicle routes whose distance savings are maximum
- (9) **Step 9:**  $n = 1$
- (10) **Step 10:** If new vehicle routes meet the time window and capacity constraints, then go directly to **Step 11**; otherwise, return to **Step 7**
- (11) **Step 11:**  $n = n+1$
- (12) **Step 12:** Generate new vehicle route with two vehicle routes whose distance savings are maximum
- (13) **Step 13:** If there exists a route that serves only one, then go back to **Step 7**; otherwise enter **Step 14**
- (14) **Step 14:** Output the service route of each vehicle

ALGORITHM 2: Procedure of CW algorithm.

**Input:** Initial population  $P$   
**Output:** The nondominated sorting results of population  $P$

- (1) **Step 1:** Setting  $PP=P$ ,  $rank=1$ ,  $F=1$
- (2) **Step 2:** for  $F=1:n$
- (3) **Step 3:** for  $i=1:n$
- (4) **Step 4:** for  $j=1:n$  &  $j \neq i$
- (5) **Step 5:** Compare the solution quality of  $x_i$  and  $x_j$ , and determine the dominant and nondominant relationships of  $i$  and  $j$ .  
End
- (6) **Step 6:** If  $x_i$  is superior to all  $x_j$ , then the individual  $i$  is considered to be a nondominant individual, and the nondominant ranking value of  $i$  is  $rank$   
End
- (7) **Step 7:** The nondominant individuals found in the above steps constitute set  $S_F$ , which is regarded as the  $F$ -level nondominant layer of the population  $P$
- (8) **Step 8:**  $PP=PP \setminus S_F$ ,  $i_r=i_r+1$
- (9) **Step 9:** If  $PP$  is an empty set, then enter **Step 10**, otherwise continuous this cycle
- (10) **Step 10:** Stratify population  $P$
- (11) **Step 11:** End

ALGORITHM 3: Procedure of the fast nondominated sorting operator.

In Figure 6, the amount of goods shipped from DC1 to DC2 is zero; thus, the initial customers of DC1 are not allocated to DC2 with clustering. The amount of goods transported from DC2 to DC1 is 170, which indicates that the service relationship of some customers has changed from DC2 to DC1. Here, the spatial distance between DC1 and DC2 is 33.07 km. The centralized transportation service routes of the truck are listed in Table 8.

In Table 8, T1 and T2 serve three routes. At the end of each service route, the trucks should return to their origin. The activity of T1 occurs early on each workday, and that of T2 occurs late on each workday. Table 9 shows the optimized vehicle service routes.

In Table 9, the number of vehicles used jointly by the six logistics facilities is 12. Some of the vehicles are used multiple times within and between the facilities. For example, V1 performs the route DC1  $\rightarrow$  C86  $\rightarrow$  C13

$\rightarrow$  C20  $\rightarrow$  C11  $\rightarrow$  C4  $\rightarrow$  C12  $\rightarrow$  C7  $\rightarrow$  C5  $\rightarrow$  C1  $\rightarrow$  C25  $\rightarrow$  C3  $\rightarrow$  C8  $\rightarrow$  DC1 and the route DC3  $\rightarrow$  C73  $\rightarrow$  C97  $\rightarrow$  C42  $\rightarrow$  C2  $\rightarrow$  C82  $\rightarrow$  C29  $\rightarrow$  C16  $\rightarrow$  C40  $\rightarrow$  DC3, which occur in DC1 and DC3, respectively. V10 provides service for PC2 and PC3 successively. V2, V4, and V6 are shared in DC1, DC2, and DC3, respectively.

To clarify the effect of the proposed model and algorithm, the gap of the cost and the number of vehicles in the initial and optimized logistics network are counted and listed in Table 10. Here, the TOC of the logistics facility includes the TTC, TFC, TPC, and TMC. Centralized transportation is a special project generated by the sharing of customer information and transportation resources among facilities. Therefore, the costs of centralized transportation should be jointly borne by all the facilities participating in the sharing. Similarly, given that



TABLE 3: Characteristics of benchmark datasets.

Instance	Datasets	Maximum loading capacity	Number of depots		Number of customers	
			DCs	PCs	Delivery demands	Pickup demands
1	C-mdvrptw-pr01	200	2	2	24	24
2	C-mdvrptw-pr02	195	2	2	48	48
3	C-mdvrptw-pr03	190	2	2	72	72
4	C-mdvrptw-pr04	185	2	2	96	96
5	C-mdvrptw-pr05	180	2	2	120	120
6	C-mdvrptw-pr06	175	2	2	144	144
7	C-mdvrptw-pr07	200	3	3	36	36
8	C-mdvrptw-pr08	190	3	3	72	72
9	C-mdvrptw-pr09	180	3	3	108	108
10	C-mdvrptw-pr10	170	3	3	144	144
11	C-mdvrptw-pr11	200	2	2	24	24
12	C-mdvrptw-pr12	195	2	2	48	48
13	C-mdvrptw-pr13	190	2	2	72	72
14	C-mdvrptw-pr14	185	2	2	96	96
15	C-mdvrptw-pr15	180	2	2	120	120
16	C-mdvrptw-pr16	175	2	2	144	144
17	C-mdvrptw-pr17	200	3	3	36	36
18	C-mdvrptw-pr18	190	3	3	72	72
19	C-mdvrptw-pr19	180	3	3	108	108
20	C-mdvrptw-pr20	170	3	3	144	144

TABLE 4: Comparison results of the four algorithms.







Instance	KCW-NSGA-II			NSGA-II			GA-PSO			MOPSO		
	Cost	NV	CT	Cost	NV	CT	Cost	NV	CT	Cost	NV	CT
1	1033	4	71	1178	4	77	1298	5	82	1593	5	98
2	1787	8	72	1724	9	91	2172	10	93	2115	8	119
3	2742	17	110	3121	18	133	2879	18	103	3309	18	127
4	3216	20	129	4027	21	146	3371	21	171	3579	21	184
5	3693	18	181	3827	22	239	3835	22	217	4121	30	264
6	3569	15	306	3671	23	290	4008	24	301	4577	33	298
7	1687	7	85	2386	9	83	1767	8	97	2044	14	79
8	2093	12	95	2394	13	141	2181	12	114	2361	12	147
9	2614	19	218	4010	22	210	2653	20	203	3167	30	240
10	3123	24	258	3355	24	311	3277	25	277	3459	29	325
11	1118	4	77	1405	5	74	1190	6	85	1754	11	101
12	2068	10	94	2692	11	96	2394	11	88	2135	11	114
13	2570	18	97	2655	18	103	2690	22	119	3282	28	99
14	3028	21	162	3564	24	186	3108	23	162	3620	25	172
15	3709	22	209	4117	26	240	3812	27	241	4272	33	248
16	3993	25	262	4072	25	305	4154	28	301	4366	34	339
17	1578	7	69	1763	7	87	1665	7	65	1652	7	126
18	2324	12	66	2428	12	110	2430	14	109	2635	19	166
19	2440	20	212	2790	21	206	2493	22	202	3029	22	241
20	3295	23	186	3692	25	316	3546	25	213	3421	26	309
Average	2584	15	148	2944	17	172	2746	18	162	3025	21	190
<i>t</i> -test				-13.95	-3.73	-3.29	-6.44	-4.76	-3.41	-8.60	-4.84	-5.31
<i>p</i> -value				9.8E-12	7.2E-04	1.9E-03	1.8E-06	6.8E-05	1.5E-03	2.8E-08	5.7E-05	2.0E-05

the vehicle is shared and some vehicles are used multiple times, the maintenance of the vehicles should be co-paid by all facilities.

In Table 10, the fixed costs of each facility are stable, which are \$315, \$427, \$533, \$578, \$612, and \$590, respectively. Reducing the travel, penalty, and maintenance costs is the main objective of optimizing the logistics operating cost. The TOC of

the initial logistics network is \$25473, whereas the optimized TOC is \$16614, which indicates that the logistics network is significantly improved. Transportation resources are greatly saved, as the number of vehicles before and after optimization is 33 and 14, respectively. The gap of TTC before and after optimization is shown in Figure 7, which can directly prove the optimization effect of vehicle routes.

TABLE 5: Characteristics of the logistics network.

Symbol	Description	Number of served customers	Mark of customers
	DC1 and its customers	27	C1 - C27
	DC2 and its customers	36	C28 - C63
	DC3 and its customers	39	C64 - C102
	PC1 and its customers	46	C103 - C148
	PC2 and its customers	31	C149 - C179
	PC3 and its customers	41	C180 - C220

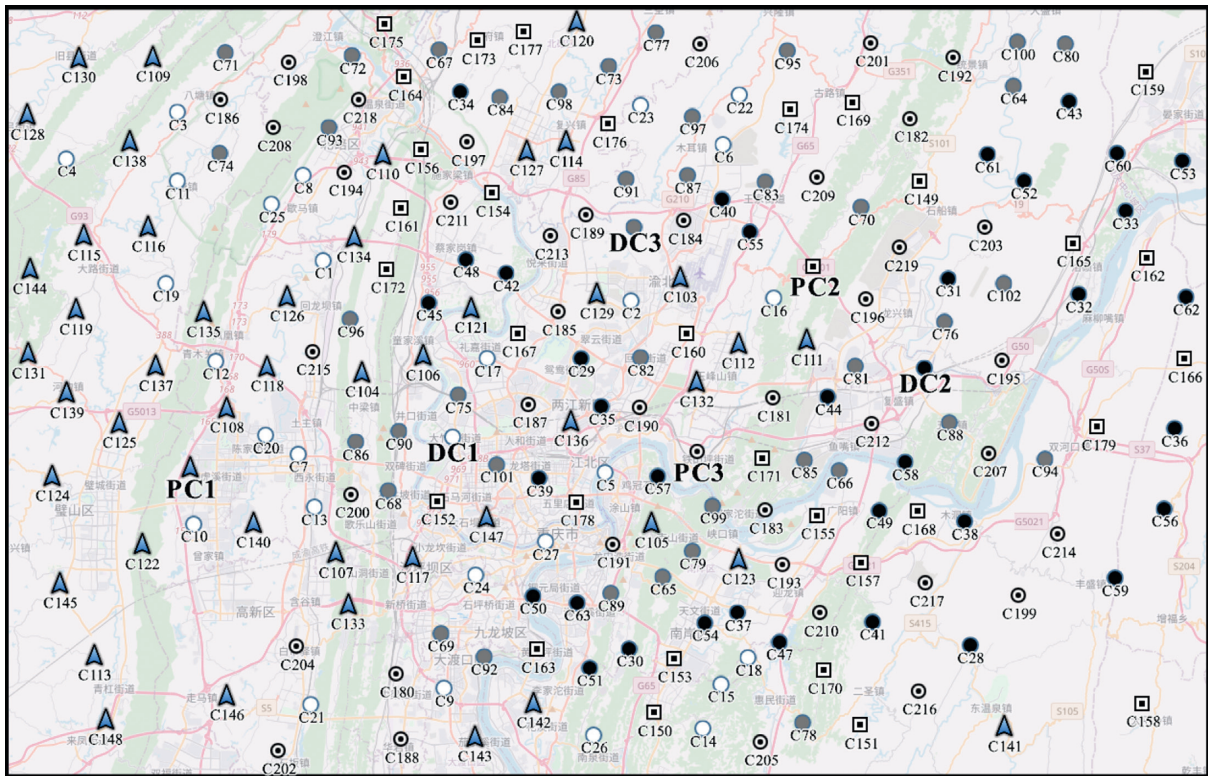


FIGURE 3: Spatial distribution of DCs, PCs, and their customers.

TABLE 6: Distribution routes of DCs and pickup routes of PCs in the initial logistics network.

Facility	Vehicle	Departure time	Arriving time	Route
DC1	V1	162	689	DC1→C19→C1→C17→DC1
	V2	0	906	DC1→C13→C7→C20→C12→DC1
	V3	159	619	DC1→C8→C25→C11→C3→C4→C10→DC1
	V4	33	730	DC1→C27→C24→C21→C9→C26→C14→C15→C18→DC1
	V5	0	924	DC1→C23→C22→C6→C16→C2→C5→DC1
DC2	V6	0	1037	DC2→C42→C45→C48→C34→C35→C50→C54→DC2
	V7	30	1016	DC2→C58→C39→C41→C47→C37→C30→C43→C40→DC2
	V8	0	1014	DC2→C46→C61→C28→C59→C36→C32→C62→C52→C60→DC2
	V9	0	319	DC2→C63→C51→C49→DC2
	V10	35	823	DC2→C56→C55→C38→C53→DC2
	V11	10	1196	DC2→C31→C33→C44→C29→C57→DC2

TABLE 6: Continued.

Facility	Vehicle	Departure time	Arriving time	Route
DC3	V12	121	1002	DC3→C83→C98→C95→C77→C73→C93→C75→DC3
	V13	92	831	DC3→C79→C89→C92→C69→C101→C90→C68→DC3
	V14	109	1176	DC3→C86→C99→C78→C82→C100→C64→DC3
	V15	0	865	DC3→C102→C81→C85→C76→C70→C80→C97→C88→DC3
	V16	0	936	DC3→C74→C67→C84→C87→C71→C72→C91→C65→C96→DC3
	V17	0	295	DC3→C94→C66→DC3
PC1	V18	0	353	PC1→C114→C145→C119→PC1
	V19	19	891	PC1→C117→C125→C121→C120→C130→C113→C128→C111→C118→PC1
	V20	4	992	PC1→C115→C144→C116→C123→C140→C122→C106→C139→C124→PC1
	V21	95	1103	PC1→C135→C104→C136→C103→C147→C142→C141→C143→C112→PC1
	V22	138	951	PC1→C148→C133→C146→C107→C131→C137→C138→PC1
	V23	0	1055	PC1→C134→C132→C105→C127→C129→C126→C110→C109→C108→PC1
PC2	V24	0	883	PC2→C165→C162→C153→C151→C170→C168→C158→PC2
	V25	37	1067	PC2→C149→C179→C174→C176→C169→C166→C159→0
	V26	0	1115	PC2→C156→C172→C167→C157→C155→C152→C163→C150→PC2
	V27	18	819	PC2→C171→C178→C160→C161→C164→C177→C154→C173→C175→PC2
PC3	V28	202	1031	PC3→C192→C201→C182→C184→PC3
	V29	127	918	PC3→C220→C183→C193→C214→C207→C217→C205→C202→C180→PC3
	V30	0	720	PC3→C206→C211→C209→C212→C200→C215→C196→PC3
	V31	23	1121	PC3→C191→C185→C187→C188→C216→C199→PC3
	V32	217	674	PC3→C181→C213→C219→C203→C195→C210→PC3
	V33	66	918	PC3→C204→C198→C194→C197→C186→C208→C218→C190→C189→PC3

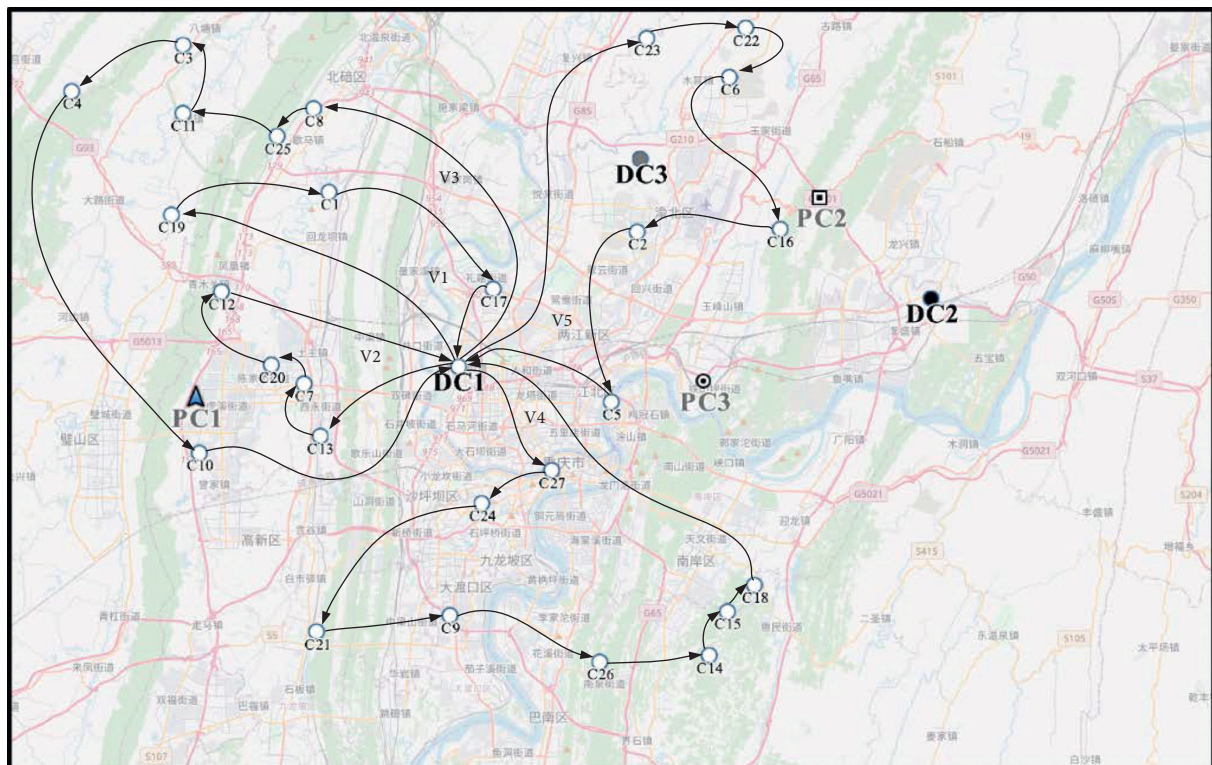


FIGURE 4: Initial vehicle service routes of DC1.

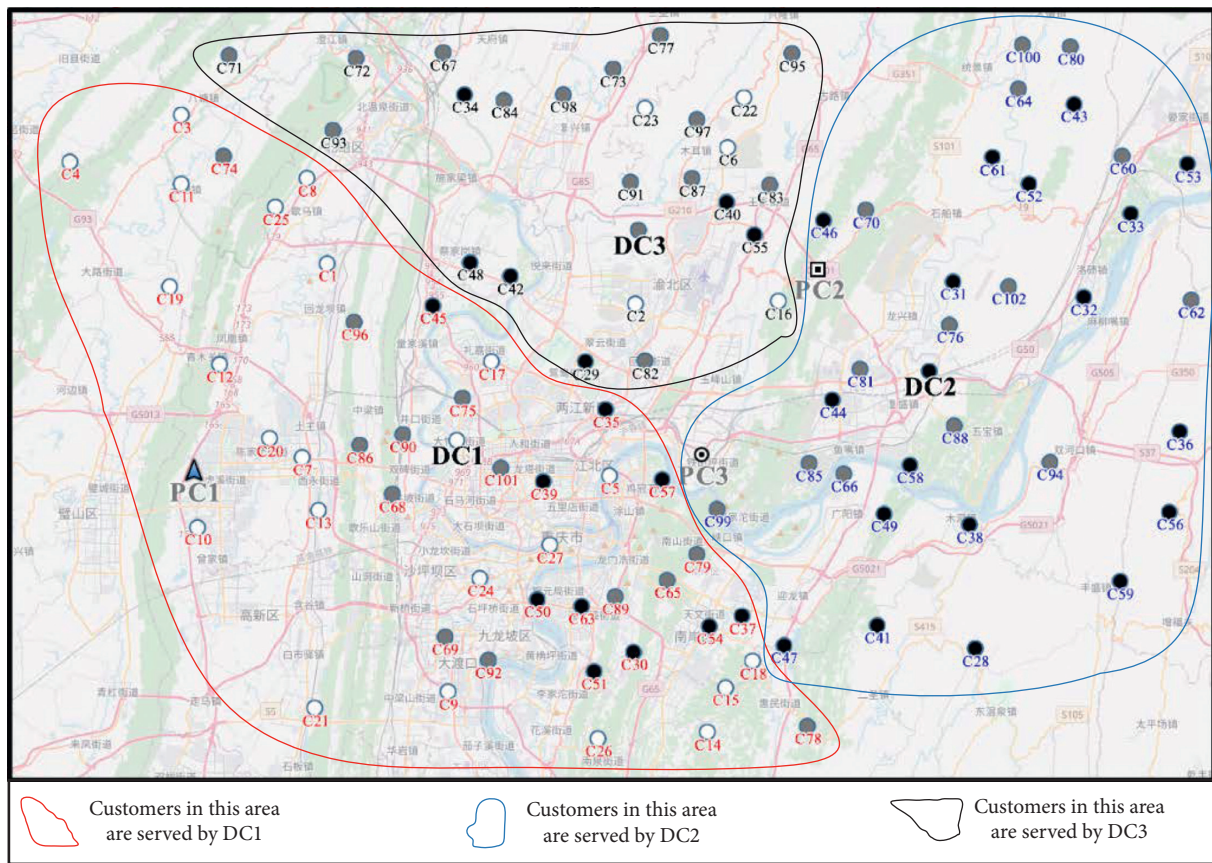
In Figure 7, the initial TTC of DC1, DC2, DC3, PC1, PC2, and PC3 is \$2210, \$3581, \$3730, \$4900, \$3067, and \$3506, respectively. The optimized TTC of each facility is \$2047, \$1738, \$1134, \$2064, \$2025, and \$2361, respectively. The

difference of TTC before and after optimization is relatively obvious. Although the transportation cost generated by the centralized transportation is \$1651, the logistics network is still significantly optimized on the whole.



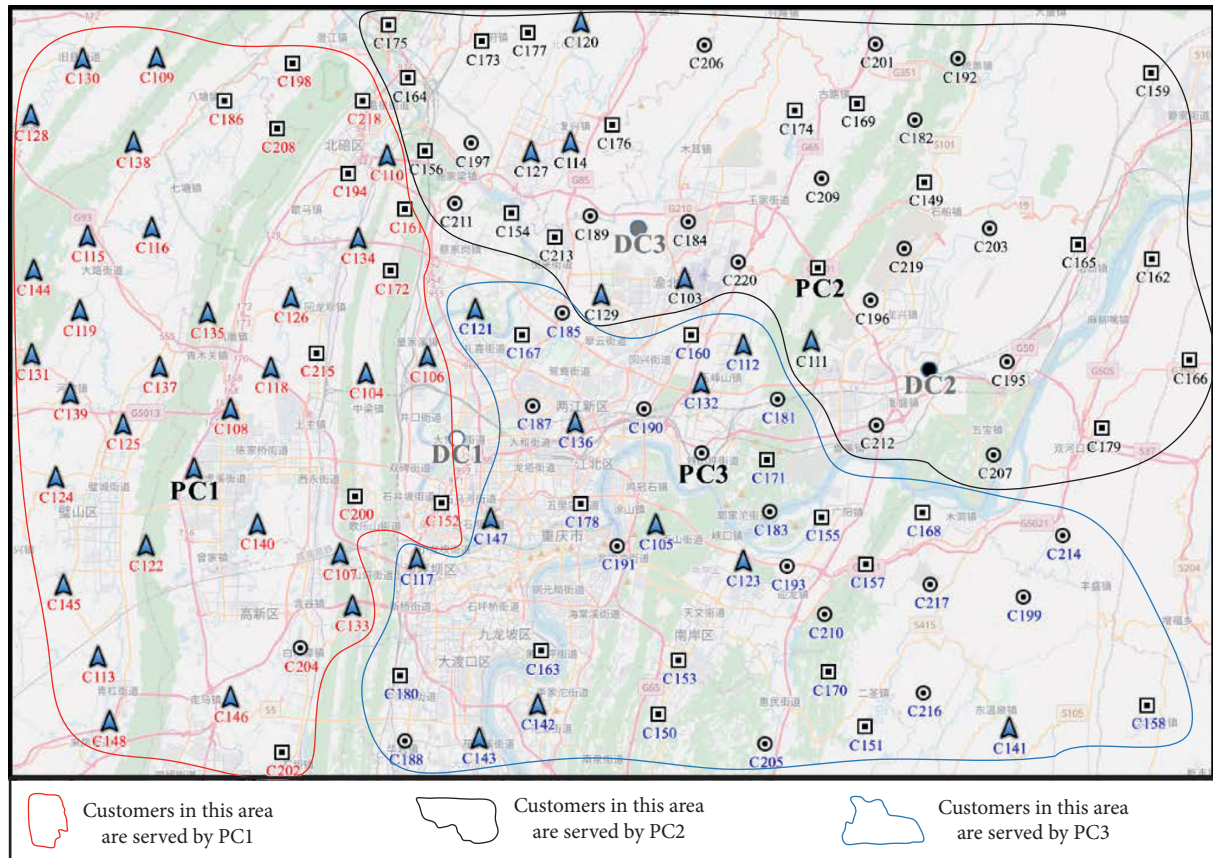
TABLE 7: Relevant parameter setting.

Parameter	Numerical value	Parameter	Numerical value
$P_E$	\$35 per hour	$C_b$	1000
$P_L$	\$35 per hour	$C_f$	2000
$W$	52	$M_v$	\$13000
$T$	7	$M_b$	\$20000
$T_v$	10 hour	$[I_{DC1}, I_{DC2}, I_{DC3}, I_{PC1}, I_{PC2}, I_{PC3}]$	[\$315, \$427, \$533, \$578, \$612, \$590]
$T_b$	15 hour	Population size	300
$f_v$	0.363 gallon per miles	Maximum generations	1000
$f_b$	0.566 gallon per miles	Crossover probability	0.8
$P_v$	\$6.18 per gallon	Mutation probability	0.2
$P_b$	\$6.18 per gallon	Travel speed of vehicle	40
$C_v$	200	Travel speed of truck	60



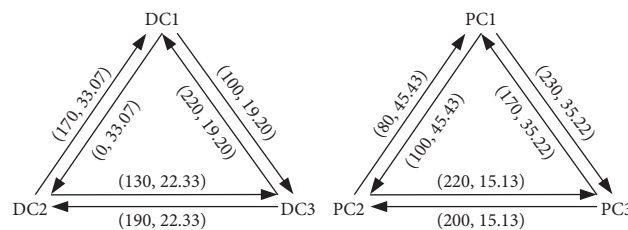
(a)

FIGURE 5: Continued.



(b)

FIGURE 5: Customer clustering results with k-means algorithm. (a) Customer clustering results with DCs as cluster centers. (b) Customer clustering results with PCs as cluster centers.



(\* , #): \* is the number of transported goods, # is the distance between facilities

FIGURE 6: Description of transmissions and distances among facilities.

TABLE 8: Optimized truck routes of centralized transportation.

Truck	Service routes
T1	DC1 → DC2 → DC1
	DC2 → DC3 → DC1 → DC2
	DC3 → DC2 → DC1 → DC3
T2	PC1 → PC2 → PC3 → PC1
	PC2 → PC3 → PC1 → PC2
	PC3 → PC2 → PC1 → PC3

6.4. Analysis and Discussion. The optimization of the logistics network is divided into four cases based on the RS strategy to analyze the influence of RS on the optimization

of the logistics network. In Case 1, customer information and transportation resources are privately owned by each logistics facility. In Case 2, RS is adopted by DCs (i.e., DC1, DC2, and DC3). Correspondingly, in Case 3, the members participating in RS are PCs (i.e., PC1, PC2, and PC3). In Case 4, all six facilities receive the RS strategy. Transportation resources can be used jointly by DCs and PCs in Case 4. Table 11 and Figure 8 show the numerical optimization results of the logistics network in the four scenarios.

In Table 11 and Figure 8, Case 4 outperforms Cases 2 and 3 in most aspects. First, the TOC of Cases 2 and 3 is \$17038 and \$16977, respectively, which are larger than

TABLE 9: Vehicle distribution and pickup sharing routes in the optimized logistics network.

Vehicle	Facility	Departure time	Arriving time	Origin	Destination	Vehicle distribution and pickup sharing routes
V1		200	602	DC1	DC3	C86→C13→C20→C11→C4→C12→C7→C5→C1→C25→C3→C8
V2		107	427	DC1	DC1	C24→C79→C39→C27→C89→C74→C51→C14→C9→C92
V2	DC1	577	1102	DC1	DC1	C17→C90→C101→C78→C30→C18→C65→C35→C96→C75→C50→C54→C57
V3		0	773	DC1	DC1	C63→C21→C45→C19→C26→C69→C37→C15→C10→C68
V4		0	420	DC2	DC2	C46→C31→C102→C61→C33→C56→C85→C66→C81→C76→C32
V4		491	1007	DC2	DC2	C62→C52→C80→C70→C99→C88→C53→C100→C43→C64→C60
V5	DC2	65	526	DC2	DC2	C49→C58→C94→C28→C36→C59→C41→C47→C38→C44
V1		672	938	DC3	DC3	C73→C97→C42→C2→C82→C29→C16→C40
V6		121	433	DC3	DC3	C83→C22→C6→C84→C67→C48→C87→C55→C23
V6		450	712	DC3	DC3	C98→C95→C77→C34→C71→C72→C93→C91
V7		69	556	PC1	PC1	C119→C115→C198→C130→C194→C161→C186→C128→C116
V7		640	1089	PC1	PC1	C122→C134→C140→C131→C139→C137→C118→C138→C109→C218→C110→C108→C124
V8		91	351	PC1	PC1	C145→C135→C104→C172→C126→C144→C204→C125
V8	PC1	393	906	PC1	PC1	C113→C148→C146→C133→C152→C107→C200→C215→C208→C106→C202
V9		37	571	PC2	PC2	C219→C220→C103→C213→C206→C174→C192→C169→C173→C175→C184
V9		592	1104	PC2	PC2	C149→C165→C162→C179→C196→C207→C212→C195→C189→C203→C201→C182→C166→C159
V10		0	630	PC2	PC3	C114→C211→C156→C120→C176→C209→C197→C177→C164→C154→C127→C129→C111
V10	PC2	692	997	PC3	PC3	C141→C188→C143→C163→C150→C216→C190→C112
V11		24	306	PC3	PC3	C117→C191→C180→C132→C160→C171→C183→C155
V11		355	843	PC3	PC3	C167→C136→C153→C142→C147→C187→C185→C123→C205→C170
V12	PC3	49	170	PC3	PC3	C121→C105→C178→C217
V12		192	928	PC3	PC3	C181→C157→C193→C151→C214→C210→C168→C158→C199



TABLE 10: Comparison before and after optimization.

Facility	Initial TOC				NV	Optimized TOC				Gap		
	TTC	TFC	TPC	TMC		TTC	TFC	TPC	TMC	NV	TOC	NV
DC1	2210	315	27	179	5	2047	315	0				
DC2	3581	427	55	214	6	1738	427	0				
DC3	3730	533	44	214	6	1134	533	0	429	12	8859	19
PC1	4900	578	65	214	6	2064	578	0				
PC2	3067	612	22	143	4	2025	612	0				
PC3	3506	590	33	214	6	2361	590	0				
Centralized transportation	-	-	-	-	-	1651	-	0	110	2		
Total			25473		33			16614		14	-	-

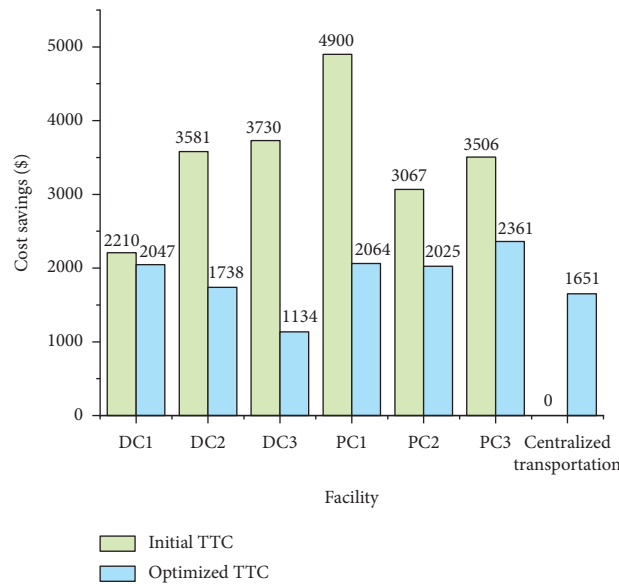


FIGURE 7: Comparison results of TTC before and after optimization.

TABLE 11: Comparison results of the four cases.

Cases	TTC (\$)	TPC (\$)	TFC (\$)	NV	TMC (\$)	TOC (\$)	NV	Gap	
								TTC (\$)	TOC (\$)
Case 1	20994	246	3055	33	1178	25473			
Case 2	17038	120	3055	23	841	21053	10	3956	4420
Case 3	16977	126	3055	24	876	21034	9	4017	4439
Case 4	13020	0	3055	14	539	16614	19	7974	8859

\$13020 in Case 4. Second, the number of vehicles and the TMCs of Scenario 4 is 14 and \$539, respectively, which indicates that Case 4 is more conducive to saving resources. Finally, the gap of TOC between Cases 4 and 1 is \$8859. Therefore, if the six logistics facilities adopt RS simultaneously, then the logistics costs can be optimized better and the transportation resources can be saved considerably.

6.5. *Management Insights.* In this study, the RS strategy optimizes the logistics network significantly by reallocating customers, including the logistics operation costs and the

number of vehicles. Therefore, the management insights obtained in this study are as follows:

- (1) In a multi-depot, large-scale logistics network with pickups and deliveries, customer information, facility capacity, and transportation resources can be shared to amplify resource utilization by introducing RS strategies. RS is not only conducive to the operation of logistics facilities, including the use of logistics costs and transport resources, but also conducive for providing customers with more convenient logistics services. In a logistics network with vehicle sharing, vehicles are used multiple times within and between facilities to avoid idle

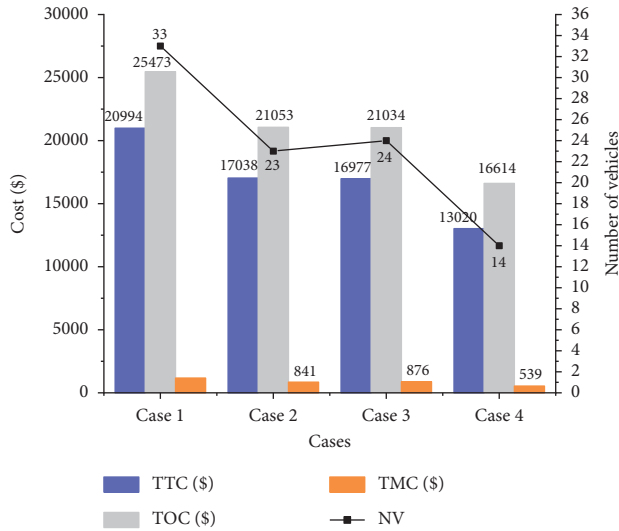


FIGURE 8: Comparison results of TTC, TC, TMC, and NV in the four cases.

vehicle resources. In addition, the sharing of customer information helps facilities provide logistics services to customers with higher quality. Therefore, participating actively in RS is remarkably necessary for LSPs.

- (2) From the perspective of local traffic management departments and environmental departments, the optimization of the logistics network through RS not only reduces transportation resources but also relieves the local traffic pressure. In addition, the efficient use of resources promotes the development of green environment. Therefore, local government departments can actively support and give incentive policies to promote RS among local logistics facilities to optimize the logistics network and ease the traffic environment. Moreover, the effective sharing mechanism in the multicenter logistics network with pickups and deliveries can enhance the efficient operation of the logistics system and promote the green and sustainable development of the local intelligent logistics system. Therefore, the introduction of RS can promote the construction and development of local smart and green urban logistics with the incentive of departments and the active participation of facilities.

## 7. Conclusions

This study handles the MDPDPRS, which optimizes the logistics network by sharing customer and transportation resources. The reconfiguration of resources and customers improve the operating efficiency of the logistics network. The main contributions of this study include the following aspects. First, the MDPDPRS is modeled as a bi-objective mathematical model to optimize the total logistics operating cost and number of vehicles. Second, a two-stage hybrid algorithm is designed to solve the MDPDPRS, which

contains the  $k$ -means, CW, and NSGA-II algorithms. Third, the application of the proposed mathematical model and methodology are improved by the numerical result of a real-world case study and benchmark.

In view of the shared transportation resources and customers' information, a two-stage algorithm is designed, which initially clusters customers to reconfigure the resources and then optimizes the vehicle routes. On the one hand,  $k$ -means algorithm, which clusters customers based on Manhattan distance, helps reduce the difficulty of solving MDPDPRS and enables vehicle resources to be used in a centralized manner multiple times. On the other hand, the combination of CW and NSGA-II algorithms improves the global searching capability and the speed of the algorithm in finding the Pareto optimal solutions.

The numerical results of a real-world case study, which is obtained in Chongqing, China, is discussed and analyzed to improve the application and performance of the designed mathematical model and methodology in solving practical problems similar to the MDPDPRS. The gap of the logistics operating costs and number of vehicles before and after the optimization are \$8859 and 19, respectively, which verify the effectiveness of the model and methodology proposed in this study. In addition, the algorithm comparison results of benchmarks (from C-mdvrptw datasets) verify that the proposed KCW-NSGA-II algorithm is superior to the standard NSGA-II, GA-PSO, and MOPSO. The results of numerical discussion on the four cases in which different RS strategies are adopted prove that RS is helpful to optimize logistics costs and save transportation resources.

In this study, the bi-objective mathematical model and methodology of MDPDPRS are designed, which provide references for the reconfiguration of resources and the optimization of logistics operation costs. In view of the limitations of the current study and the dynamic development of the logistics industry, further research can be considered from the following aspects. (1) The dynamic change in customer demands and customer satisfaction are the two aspects that the realistic LSPs focus on, and these aspects can be added into the study of MDPDPRS. (2) Constructing a dynamic mathematical programming model and designing an exact algorithm to find the exact solution of MDPDPRS are worthy of research. (3) Exploring the approaches to realize RS in a large logistics network and the means to reduce the effect of logistics transportation on the environment can be considered in the study of MDPDPRS. (4) Considering the cost sharing mechanism under the RS mechanism to promote the formation of collaboration and maintain its stability can enrich the study of MDPDPRS.

## Data Availability

The data used to support the findings of this study are included within the article.

## Conflicts of Interest

The authors declare that they do not have any conflicts of interest.

## Acknowledgments

This research was supported by National Natural Science Foundation of China (Project Nos. 71871035 and 41977337), the Fundamental Research Funds for the Central Universities (grant no. 22120210009), Humanity and Social Science Youth Foundation of Ministry of Education of China (18YJC630189), Key Science and Technology Research Project of Chongqing Municipal Education Commission (KJZD-K202000702), Key Project of Human Social Science of Chongqing Municipal Education Commission (No. 20SKGH079), Social Science Foundation of Chongqing of China (2019YBGL054), and Chongqing Graduate Tutor Team Construction Project (No. JDDSTD2019008). This research was also supported by 2018 Chongqing Liuchuang Plan Innovation Project (cx2018111).

## References

- [1] C. K. M. Lee, Y. Lv, K. K. H. Ng, W. Ho, and K. L. Choy, "Design and application of Internet of things-based warehouse management system for smart logistics," *International Journal of Production Research*, vol. 56, no. 8, pp. 2753–2768, 2017.
- [2] S. Liu, Y. Zhang, Y. Liu, L. Wang, and X. V. Wang, "An "Internet of Things" enabled dynamic optimization method for smart vehicles and logistics tasks," *Journal of Cleaner Production*, vol. 215, pp. 806–820, 2019.
- [3] S. A. R. Khan, C. Jian, Y. Zhang, H. Golpira, A. Kumar, and A. Sharif, "Environmental, social and economic growth indicators spur logistics performance: from the perspective of South Asian Association for Regional Cooperation countries," *Journal of Cleaner Production*, vol. 214, pp. 1011–1023, 2019.
- [4] O. Seroka-Stolka, "The development of green logistics for implementation sustainable development strategy in companies," *Procedia - Social and Behavioral Sciences*, vol. 151, pp. 302–309, 2014.
- [5] G. Ann E, K. Uday S, and S. Abraham, "Design and operation of an order-consolidation warehouse: models and application," *European Journal of Operational Research*, vol. 58, no. 1, pp. 14–36, 1992.
- [6] T. C. Poon, K. L. Choy, H. K. H. Chow, H. C. W. Lau, F. T. S. Chan, and K. C. Ho, "A RFID case-based logistics resource management system for managing order-picking operations in warehouses," *Expert Systems with Applications*, vol. 36, no. 4, pp. 8277–8301, 2009.
- [7] R. Dekker, J. Bloemhof, and I. Mallidis, "Operations Research for green logistics - an overview of aspects, issues, contributions and challenges," *European Journal of Operational Research*, vol. 219, no. 3, pp. 671–679, 2012.
- [8] Y. Yu, C. Yu, G. Xu, R. Y. Zhong, and G. Q. Huang, "An operation synchronization model for distribution center in E-commerce logistics service," *Advanced Engineering Informatics*, vol. 43, 2020.
- [9] S. A. R. Khan, "The nexus between carbon emissions, poverty, economic growth, and logistics operations-empirical evidence from southeast Asian countries," *Environmental Science and Pollution Research*, vol. 26, no. 13, pp. 13210–13220, 2019.
- [10] W. Zhang, M. Zhang, W. Zhang, Q. Zhou, and X. Zhang, "What influences the effectiveness of green logistics policies? A grounded theory analysis," *Science of the Total Environment*, vol. 714, Article ID 136731, 2020.
- [11] M. Gansterer and R. F. Hartl, "Shared resources in collaborative vehicle routing," *Top*, vol. 28, no. 1, pp. 1–20, 2020.
- [12] M. Mirabi, S. M. T. Fatemi Ghomi, and F. Jolai, "Efficient stochastic hybrid heuristics for the multi-depot vehicle routing problem," *Robotics and Computer-Integrated Manufacturing*, vol. 26, no. 6, pp. 564–569, 2010.
- [13] M. D. A. Serna, C. A. S. Uran, J. A. Z. Cortes, and A. F. A. Benitez, "Vehicle routing to multiple warehouses using a memetic algorithm," *Procedia - Social and Behavioral Sciences*, vol. 160, pp. 587–596, 2014.
- [14] Y. Wang, J. Zhang, K. Assogba, Y. Liu, M. Xu, and Y. Wang, "Collaboration and transportation resource sharing in multiple centers vehicle routing optimization with delivery and pickup," *Knowledge-Based Systems*, vol. 160, pp. 296–310, 2018.
- [15] M. Zhang, S. Pratap, G. Q. Huang, and Z. Zhao, "Optimal collaborative transportation service trading in B2B e-commerce logistics," *International Journal of Production Research*, vol. 55, no. 18, pp. 5485–5501, 2017.
- [16] W. Ho, G. T. S. Ho, P. Ji, and H. C. W. Lau, "A hybrid genetic algorithm for the multi-depot vehicle routing problem," *Engineering Applications of Artificial Intelligence*, vol. 21, no. 4, pp. 548–557, 2008.
- [17] Y. Wang, X. Ma, Z. Li, Y. Liu, M. Xu, and Y. Wang, "Profit distribution in collaborative multiple centers vehicle routing problem," *Journal of Cleaner Production*, vol. 144, pp. 203–219, 2017.
- [18] D. Chen and Z. Yang, "Multiple depots vehicle routing problem in the context of total urban traffic equilibrium," *Journal of Advanced Transportation*, vol. 2017, Article ID 8524960, 14 pages, 2017.
- [19] I. Gribkovskaia, Ø. Halskau, G. Laporte, and M. Vlček, "General solutions to the single vehicle routing problem with pickups and deliveries," *European Journal of Operational Research*, vol. 180, no. 2, pp. 568–584, 2007.
- [20] J. Luo and M.-R. Chen, "Multi-phase modified shuffled frog leaping algorithm with extremal optimization for the MDVRP and the MDVRPTW," *Computers & Industrial Engineering*, vol. 72, pp. 84–97, 2014.
- [21] S. Deng, Y. Yuan, Y. Wang, H. Wang, and C. Koll, "Collaborative multicenter logistics delivery network optimization with resource sharing," *PLoS One*, vol. 15, no. 11, Article ID e0242555, 2020.
- [22] A. Angelopoulos, D. Gavalas, C. Konstantopoulos, D. Kyriadis, and G. Pantziou, "Incentivized vehicle relocation in vehicle sharing systems," *Transportation Research Part C: Emerging Technologies*, vol. 97, pp. 175–193, 2018.
- [23] Y. Wang, Y. Yuan, X. Guan et al., "Collaborative two-echelon multicenter vehicle routing optimization based on state-space-time network representation," *Journal of Cleaner Production*, vol. 258, 2020.
- [24] L. Verdonck, A. Caris, K. Ramaekers, and G. K. Janssens, "Collaborative logistics from the perspective of road transportation companies," *Transport Reviews*, vol. 33, no. 6, pp. 700–719, 2013.
- [25] C. Defryn and K. Sörensen, "A fast two-level variable neighborhood search for the clustered vehicle routing problem," *Computers & Operations Research*, vol. 83, pp. 78–94, 2017.
- [26] R. J. Kuo, C. H. Mei, F. E. Zulvia, and C. Y. Tsai, "An application of a metaheuristic algorithm-based clustering ensemble method to APP customer segmentation," *Neurocomputing*, vol. 205, pp. 116–129, 2016.

- [27] S. Yang, L. Ning, P. Shang, and L. Tong, "Augmented Lagrangian relaxation approach for logistics vehicle routing problem with mixed backhauls and time windows," *Transportation Research Part E: Logistics and Transportation Review*, vol. 135, 2020.
- [28] N. A. Wassan, G. Nagy, and S. Ahmadi, "A heuristic method for the vehicle routing problem with mixed deliveries and pickups," *Journal of Scheduling*, vol. 11, no. 2, pp. 149–161, 2008.
- [29] N. Wassan and G. Nagy, "Vehicle routing problem with deliveries and pickups: modelling issues and meta-heuristics solution approaches," *International Journal of Transportation*, vol. 2, no. 1, pp. 95–110, 2014.
- [30] R. Liu, X. Xie, V. Augusto, and C. Rodriguez, "Heuristic algorithms for a vehicle routing problem with simultaneous delivery and pickup and time windows in home health care," *European Journal of Operational Research*, vol. 230, no. 3, pp. 475–486, 2013.
- [31] Q. Chen, K. Li, and Z. Liu, "Model and algorithm for an unpaired pickup and delivery vehicle routing problem with split loads," *Transportation Research Part E: Logistics and Transportation Review*, vol. 69, pp. 218–235, 2014.
- [32] S. Vaziri, F. Etebari, and B. Vahdani, "Development and optimization of a horizontal carrier collaboration vehicle routing model with multi-commodity request allocation," *Journal of Cleaner Production*, vol. 224, pp. 492–505, 2019.
- [33] Y. Wang, S. Peng, X. Zhou, M. Mahmoudi, and L. Zhen, "Green logistics location-routing problem with eco-packages," *Transportation Research Part E: Logistics and Transportation Review*, vol. 143, 2020.
- [34] E. Benavent, M. Landete, E. Mota, and G. Tirado, "The multiple vehicle pickup and delivery problem with LIFO constraints," *European Journal of Operational Research*, vol. 243, no. 3, pp. 752–762, 2015.
- [35] Y. Wang, Q. Li, X. Guan, M. Xu, Y. Liu, and H. Wang, "Two-echelon collaborative multi-depot multi-period vehicle routing problem," *Expert Systems with Applications*, vol. 167, 2021.
- [36] Y. Wang, S. Peng, C. Xu et al., "Two-echelon logistics delivery and pickup network optimization based on integrated co-operation and transportation fleet sharing," *Expert Systems with Applications*, vol. 113, pp. 44–65, 2018.
- [37] T. Pichpibul and R. Kawtummachai, "An improved Clarke and Wright savings algorithm for the capacitated vehicle routing problem," *ScienceAsia*, vol. 38, no. 3, 2012.
- [38] A. Martínez-Puras and J. Pacheco, "MOAMP-Tabu search and NSGA-II for a real Bi-objective scheduling-routing problem," *Knowledge-Based Systems*, vol. 112, pp. 92–104, 2016.
- [39] J. Luo and M.-R. Chen, "Improved Shuffled Frog Leaping Algorithm and its multi-phase model for multi-depot vehicle routing problem," *Expert Systems with Applications*, vol. 41, no. 5, pp. 2535–2545, 2014.
- [40] S. N. Parragh, K. F. Doerner, and R. F. Hartl, "A survey on pickup and delivery problems," *Journal für Betriebswirtschaft*, vol. 58, no. 2, pp. 81–117, 2008.
- [41] C. Ting and C. H. Chen, "Combination of multiple ant colony system and simulated annealing for the multidepot vehicle-routing problem with time windows transportation research record," *Journal of the Transportation Research Board*, vol. 2089, no. 1, pp. 85–92, 2008.
- [42] S. Yanik, B. Bozkaya, and R. deKervenoael, "A new VRPPD model and a hybrid heuristic solution approach for e-tailing," *European Journal of Operational Research*, vol. 236, no. 3, pp. 879–890, 2014.
- [43] M. Alzaqebah, S. Jawarneh, S. Jawarneh, H. M. Sarim, and S. Abdullah, "Bees algorithm for vehicle routing problems with time windows," *International Journal of Machine Learning and Computing*, vol. 8, no. 3, pp. 236–240, 2018.
- [44] M. Oberscheider, J. Zazgornik, M. Gronalt, and P. Hirsch, "An exact approach to minimize the greenhouse gas emissions in timber transport," *Journal of Applied Operational Research*, vol. 7, no. 2, pp. 43–59, 2015.
- [45] M. Oberscheider, J. Zazgornik, C. B. Henriksen, M. Gronalt, and P. Hirsch, "Minimizing driving times and greenhouse gas emissions in timber transport with a near-exact solution approach," *Scandinavian Journal of Forest Research*, vol. 28, no. 5, pp. 493–506, 2013.
- [46] A. Bettinelli, A. Ceselli, and G. Righini, "A branch-and-price algorithm for the multi-depot heterogeneous-fleet pickup and delivery problem with soft time windows," *Mathematical Programming Computation*, vol. 6, no. 2, pp. 171–197, 2014.
- [47] S. Irnich, "A multi-depot pickup and delivery problem with a single hub and heterogeneous vehicles," *European Journal of Operational Research*, vol. 122, no. 2, pp. 310–328, 2000.
- [48] E. Queiroga, Y. Frota, R. Sadykov, A. Subramanian, E. Uchoa, and T. Vidal, "On the exact solution of vehicle routing problems with backhauls," *European Journal of Operational Research*, vol. 287, no. 1, pp. 76–89, 2020.
- [49] T. Leelertkij, P. Parthanadee, J. Buddhakulsomsiri, and A. Lambert, "Vehicle routing problem with transshipment: mathematical model and algorithm," *Journal of Advanced Transportation*, vol. 2021, Article ID 8886572, 15 pages, 2021.
- [50] S. Ropke and J.-F. Cordeau, "Branch and cut and price for the pickup and delivery problem with time windows," *Transportation Science*, vol. 43, no. 3, pp. 267–286, 2009.
- [51] V. Kachitvichyanukul, P. Sombuntham, and S. Kunnapapdeelert, "Two solution representations for solving multi-depot vehicle routing problem with multiple pickup and delivery requests via PSO," *Computers & Industrial Engineering*, vol. 89, pp. 125–136, 2015.
- [52] A. Soriano, M. Gansterer, and R. F. Hartl, "The two-region multi-depot pickup and delivery problem," *OR Spectrum*, vol. 40, no. 4, pp. 1077–1108, 2018.
- [53] Y. Wang, X. Ma, Y. Lao, and Y. Wang, "A fuzzy-based customer clustering approach with hierarchical structure for logistics network optimization," *Expert Systems with Applications*, vol. 41, no. 2, pp. 521–534, 2014.
- [54] S. Barreto, C. Ferreira, J. Paixão, and B. S. Santos, "Using clustering analysis in a capacitated location-routing problem," *European Journal of Operational Research*, vol. 179, no. 3, pp. 968–977, 2007.
- [55] S. Mitra, "A parallel clustering technique for the vehicle routing problem with split deliveries and pickups," *Journal of the Operational Research Society*, vol. 59, no. 11, pp. 1532–1546, 2017.
- [56] M. Assari, J. Delaram, and O. Fatahi Valilai, "Mutual manufacturing service selection and routing problem considering customer clustering in Cloud manufacturing," *Production & Manufacturing Research*, vol. 6, no. 1, pp. 345–363, 2018.
- [57] P. Singanamala, D. Reddy, and P. Venkataramaiah, "Solution to a multi depot vehicle routing problem using K-means algorithm, clarke and wright algorithm and ant colony optimization," *International Journal of Applied Engineering Research*, vol. 13, no. 21, pp. 15236–15246, 2018.

- [58] R. Nallusamy, K. Duraiswamy, R. Dhanalaksmi, and Parthiban, "Optimization of multiple vehicle routing problems using approximation algorithms," 2010, <https://arxiv.org/ftp/arxiv/papers/1001/1001.4197.pdf>.
- [59] H. Xu, P. Pu, and F. Duan, "Dynamic vehicle routing problems with enhanced ant colony optimization," *Discrete Dynamics in Nature and Society*, vol. 2018, Article ID 1295485, 13 pages, 2018.
- [60] M. W. A. Hakim, S. R. Dewi, Y. Windiatmoko, and U. A. Aziz, "Optimizing planning service territories by dividing into compact several sub-areas using binary K-means clustering according vehicle constraints, 2010.
- [61] S. Mourelo Ferrandez, T. Harbison, T. Weber, R. Sturges, and R. Rich, "Optimization of a truck-drone in tandem delivery network using k-means and genetic algorithm," *Journal of Industrial Engineering and Management*, vol. 9, no. 2, 2016.
- [62] M. Elango, S. Nachiappan, and M. K. Tiwari, "Balancing task allocation in multi-robot systems using K -means clustering and auction based mechanisms," *Expert Systems with Applications*, vol. 38, no. 6, pp. 6486–6491, 2011.
- [63] Y. Li, B. Qian, R. Hu, L.-P. Wu, and B. Liu, "Two-stage algorithm for solving multi-depot green vehicle routing problem with time window," *Intelligent Computing Theories and Application*, vol. 12, pp. 665–675, 2019.
- [64] N. Alikar, S. M. Mousavi, R. A. Raja Ghazilla, M. Tavana, and E. U. Olugu, "Application of the NSGA-II algorithm to a multi-period inventory-redundancy allocation problem in a series-parallel system," *Reliability Engineering & System Safety*, vol. 160, pp. 1–10, 2017.
- [65] V. Babaveisi, M. M. Paydar, and A. S. Safaei, "Optimizing a multi-product closed-loop supply chain using NSGA-II, MOSA, and MOPSO meta-heuristic algorithms," *Journal of Industrial Engineering International*, vol. 14, no. 2, pp. 305–326, 2017.
- [66] O. Kaiwartya, S. Kumar, D. K. Lobiyal, P. K. Tiwari, A. H. Abdullah, and A. N. Hassan, "Multiobjective dynamic vehicle routing problem and time seed based solution using particle swarm optimization," *Journal of Sensors*, vol. 2015, Article ID 189832, 14 pages, 2015.
- [67] Z. Cui, Y. Chang, J. Zhang, X. Cai, and W. Zhang, "Improved NSGA-III with selection-and-elimination operator," *Swarm and Evolutionary Computation*, vol. 49, pp. 23–33, 2019.
- [68] G. Srivastava, A. Singh, and R. Mallipeddi, "NSGA-II with objective-specific variation operators for multiobjective vehicle routing problem with time windows," *Expert Systems with Applications*, vol. 176, Article ID 114779, 2021.
- [69] F. Maadanpour Safari, F. Etebari, and A. Pourghader Chobar, "Modelling and optimization of a tri-objective Transportation-Location-Routing Problem considering route reliability: using MOGWO, MOPSO, MOWCA and NSGA-II," *Journal of Optimization in Industrial Engineering*, vol. 14, no. 2, pp. 99–114, 2021.
- [70] M. Shafiei Nikabadi, E. Molayi, and M. Akhavan Rad, "Optimization of vehicle routing problem under uncertainty with emphasis on green-lean practices and customer satisfaction," *Journal of Transportation Research*, vol. 18, no. 1, pp. 113–134, 2021.
- [71] M. Rabbani, N. Oladzaad-Abbasabady, and N. Akbarian-Saravi, "Ambulance routing in disaster response considering variable patient condition: NSGA-II and MOPSO algorithms," *Journal of Industrial Management Optimization*, vol. 13, no. 5, 2017.
- [72] M. Nourinejad and M. J. Roorda, "A dynamic carsharing decision support system," *Transportation Research Part E: Logistics and Transportation Review*, vol. 66, pp. 36–50, 2014.
- [73] J. Li, R. Wang, T. Li, Z. Lu, and P. M. Pardalos, "Benefit analysis of shared depot resources for multi-depot vehicle routing problem with fuel consumption," *Transportation Research Part D: Transport and Environment*, vol. 59, pp. 417–432, 2018.
- [74] R. Nair and E. Miller-Hooks, "Fleet management for vehicle sharing operations," *Transportation Science*, vol. 45, no. 4, pp. 524–540, 2011.
- [75] Y. Zou, B. Lin, X. Yang, L. Wu, M. Muneeb Abid, and J. Tang, "Application of the bayesian model averaging in analyzing freeway traffic incident clearance time for emergency management," *Journal of Advanced Transportation*, vol. 2021, Article ID 6671983, 9 pages, 2021.
- [76] T. Pichpibul and R. Kawtummachai, "A heuristic approach based on Clarke-Wright algorithm for open vehicle routing problem," *The Scientific World Journal*, vol. 2013, Article ID 874349, 11 pages, 2013.
- [77] H. Mei, Y. Jingshuai, M. Teng, L. Xiuli, and W. Ting, "The modeling of milk-run vehicle routing problem based on improved C-W algorithm that joined time window," *Transportation Research Procedia*, vol. 25, pp. 716–728, 2017.
- [78] İ. K. Altınel and T. Öncan, "A new enhancement of the Clarke and Wright savings heuristic for the capacitated vehicle routing problem," *Journal of the Operational Research Society*, vol. 56, no. 8, pp. 954–961, 2017.
- [79] B. Vahdani, F. Mansour, M. Soltani, and D. Veysmoradi, "Bi-objective optimization for integrating quay crane and internal truck assignment with challenges of trucks sharing," *Knowledge-Based Systems*, vol. 163, pp. 675–692, 2019.